Geotechnical and Structural Field Observations from Christchurch, February 2011 Earthquake, in New Zealand

Research Report

Panagiota Tasiopoulou

Eleni Smyrou

İhsan Engin Bal

George Gazetas

Elizabeth Vintzileou

September 2011

National Technical University of Athens, Greece

Contents

ACKNOWLEDGEMENTS

The authors would like specially thank Dr. Umut Akgüzel, Research Assistant, Canterbury University, for his critical help and Scott Shadbolt and Nick Reid, firefighters from Christchurch rescue team, for their everyday presence, willingness, smart tips and sense of humour, without which our visit would not be that fruitful and pleasant.

Special thanks also to:

John Berrill *Professor, University of Canterbury*

Brendon Bradley *Lecturer, University of Canterbury*

Misko Cubrinovski *Associate Professor, University of Canterbury*

Neil McLennan *Engineering Manager, Lyttelton Port Company*

Kirsti Murahidy *Geotechnical Engineer in Tonkin & Taylor Ltd.*

Stefano Pampanin *Associate Professor, University of Canterbury*

Guy Quaife *Engineer in HEB Construction Ltd*

for providing data and assisting the authors during their reconnaissance visit in Christchurch in April 2011.

The financial support for the expedition to the earthquake–stricken area and the work outlined in this paper has been provided under the research project “DARE”, funded through the “IDEAS” Programme of the European Research Council (ERC), under contract number ERC-2-9-AdG228254-DARE.

Chapter 1:

INTRODUCTION

1.1. GENERAL INFORMATION

The M_w = 6.3 earthquake of February 22 was the strongest seismic event in a series of damaging aftershocks in and around Christchurch after the Darfield earthquake on 4th of September in 2010. The source of the Darfield earthquake was in a sparsely populated area and thus it caused no life losses. Serious damage was mainly due to extensive liquefaction. By contrast, the Christchurch earthquake was generated on a fault in close proximity to the city, culminating in a death toll of 181 people.

The Canterbury Plains are covered with river gravels hiding any evidence of past fault activity in this region. The newly revealed Greendale fault was therefore completely unknown. Only a portion of it was revealed in the ground surface during the Darfield earthquake. Clearly the second fault (of February 2011) appears as a continuation of the first, although no fault structure directly connecting the faults has been recognized.

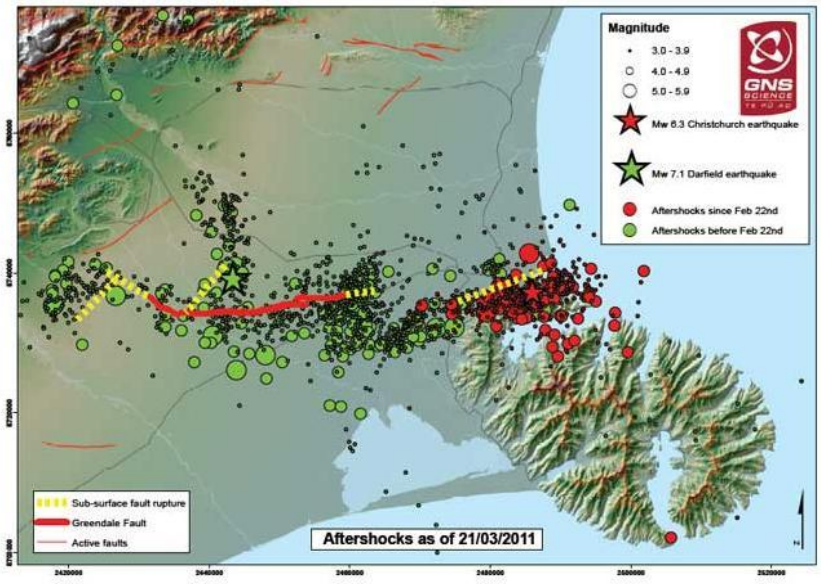

Figure 1.1.Map of the Canterbury regions showing epicenters of the Darfield and Christchurch earthquake sequences. Map axes show N. Zealand Map Grid coordinates in meters .Subsurface rupture segments are based on geodetic and strong motion modeling, with the top edges of the rupture mapped (Graphic by Rob Langridge and William Ries, GNS Science).

Due to its magnitude, shallow depth and proximity the February earthquake proved particularly destructive for the Central Business District (CBD) of Christchurch, the buildings of which suffered extensive damage. Thanks to a dense network of strong ground motion stations a large number of records have been obtained, providing valuable information on the event, and offering the possibility to relate damage versus ground shaking. Figure 1.2 presents the spatial distribution of the peak ground acceleration (PGA) values as characteristic indicator of the intensity of the Darfield and Christchurch earthquakes.

Apart from the southern part of the city on the hills and the Lyttelton port area, the city is built on deep estuarine soil, which has been shaped in the last thousands of years with the ever changing riverbed. Fine sands that are the dominant soil type and the high ground water level have contributed to widespread liquefaction in each one or both events. Often accompanied by 'lateral spreading', liquefaction amplified the level of damage, resulting in failure of structures in CBD and surrounding areas as will be explained in the sequel.

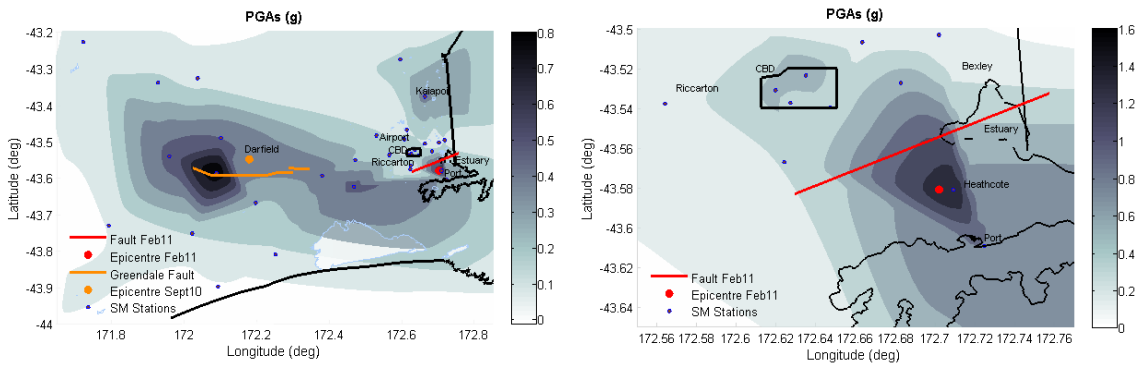

Figure 1.2. Approximate spatial distribution of the peak ground accelerations from the Darfield (left) and Christchurch (right) earthquakes.

The older buildings in the city centre, many of which are made of unreinforced masonry with timber floors, were mostly built late 19th and early in the 20th century, following the English architectural style and construction practice, with no consideration of the high seismicity of the region. However, some of these buildings had been retrofitted in recent years. On the contrary, many of the modern buildings in CBD were designed in accordance with recent seismic codes, although their foundation system was not always suitable for the adverse effects stemming from liquefaction. Thus, despite the fact that liquefied layers beneath CBD restricted somewhat

the amplitude of already significantly high accelerations, the increased velocities and displacements due to soil softening magnified the demands on long-period structures. Both structural and geotechnical aspects are investigated here in an effort to broadly explain and quantify the observed damage.

1.2. RECONNAISSANCE TRIP

Our five-member team, consisting of

- PanagiotaTasiopoulou, Phd candidate,
- EleniSmyrou, PhD researcher,
- IhsanEnginBal, PhD researcher,
- George Gazetas, Professor, and
- Elizabeth Vintzileou, Professor,

visited Christchurch between 3rd and 10th of April 2011, approximately one month after the destructive earthquake of 22nd February that severely hit Christchurch causing loss of life and extensive damage. Our team, escorted for obvious reasons of safety by the two firefighters Nick Reid and Scott Shadbolt, accessed CBD where most structural damage was concentrated, while we paid visits to areas in the wider region of Christchurch in order to collect data, make observations, witness the consequences of the earthquake event. Being a multi-disciplinary team, consisting of both structural and geotechnical engineers, our interest focused on several aspects of the earthquake related to structural damage, ground motion characteristics, liquefaction and lateral spreading phenomena etc.

During our seven-day stay, our team:

- entered CBD and several damaged buildings,
- inspected most bridges along Avon and Heathcote rivers,
- visited Kaiapoi, Bexley, Port Hills and Sumner, environs of Christchurch that severe liquefaction or rock falls occurred,
- arranged meeting with the manager engineer of Lyttelton Port and visited its damaged facilities,
- travelled Heathcote valley where the epicenter of the earthquake was,
- accessed a significant number of seismic stations in the proximity of Christchurch,
- had contacts with local engineers and academic staff of University of Canterbury.

Most of the information gathered is included in the present report in an attempt to summarize the most important observations made during our reconnaissance visit. Some preliminary

analyses have been conducted, the results of which have been presented in the following conference proceedings:

Smyrou, E., Tasiopoulou, P., Bal, I.E., Gazetas, G. and Vintzileou, E. (2011) "Structural and Geotechnical Aspects of the Christchurch and Darfield Earthquakes in N. Zealand", 7th National Turkish Conference on Earthquake Engineering (7UDMK), Istanbul, Turkey.

More sold results after further detailed analysis on structural and geotechnical aspects of the February earthquake are published in the following journal paper:

Smyrou, E., Tasiopoulou, P., Bal, I.E., Gazetas, G. and Vintzileou, E. (2011) "Ground Motions Versus Geotechnical and Structural Damage in the Christchurch February 2011 Earthquake," Seismological Research Letters, **82**(6).

However, this work is still in progress, hoping in having more interesting findings in the immediate future.

Chapter 2:

GROUND MOTION CHARACTERISTICS

2.1. INTRODUCTION

The Christchurch urban area, extending from Riccarton in the west to Bexley in the east and reaching Heathcote valley and the Port Hills in the south, is located on Canterbury Plains and its dominant geomorphic feature is the river floodplains. In particular, the rivers of Avon primarily and Heathcote (secondarily), originating from various springs in western Christchurch, form endless meanders through the city and the eastern suburbs, as they head to the estuary near the sea.

The subsoil in CBD (Central Business District) systematically comprises profiles with random variations in layering in the upper 15-25 m (Cubrinovsky *et. al*, 2010; Toshinawa *et al.*, 1997). The volcanic bedrock is located at an approximate depth of 400 m and emerges on the surface at the southern border of Canterbury Plains, forming the Port Hills of Banks Peninsula. Thick layers of gravel formations overlay the bedrock (Brown and Weeber, 1992), as depicted in Figure 2.1. The surficial sediments have an average thickness of about 25 m (Christchurch formation) and consist of alternating layers of alluvial sand, silt and gravel. They have been deposited by overbank flooding (Eidinger *et al.*, 2010) — hence, their loose disposition. In CBD, in particular, sand and non-plastic silt with low content of fines are the dominant soil types (Rees, 2010). The latter feature combined with the high ground water level (from 0 to 3 m) below the center of the city, explains the sensitivity to liquefaction.

There is significant variability of soil deposits within short distances that can differentiate the ground motion characteristics. For example, Toshinawa *et al*. (1997) describe the soil profiles of two characteristic sites 1.2 km distant, illustrated in Figure 2.2, one consisting of only sandy gravels and sand close to CBGS seismic station (Figure 2.3), and the other comprising silt and peat deposits to a depth of 7 m close to REHS seismic station. According to the aforementioned paper, during a 1994 distant earthquake greater amplification was observed at the second site, close to REHS, in agreement with the records of February 2011. However, both sites belong to the same broader classification of soft soils (class D) for structural design purposes in the New Zealand design standards (NZS 1170.5, 2004). This seems quite reasonable in cases of strong earthquakes, where the response of such type of soft mostly sandy soils is expected to be dominated by the effects of severe liquefaction.

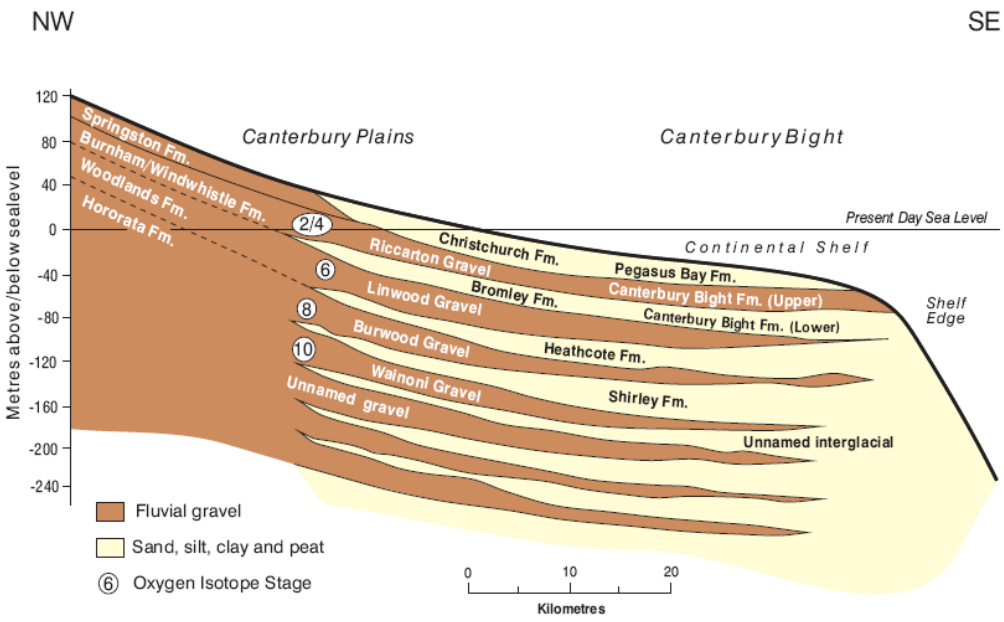

Figure 2.1. Cross section of deposits underlying Christchurch (Brown and Weeber, 1992).

In the eastern suburbs of Christchurch, the soil layering tends to be more distinct, without intense local variations. The thickness of the superficial deposits (Christchurch formation) increases towards the east, reaching 40-45m at South New Brighton. Moreover, there is greater homogeneity within the layers, comprising mainly sand, as illustrated in the map of Figure 2.2. Thus, liquefaction susceptibility is higher and no more localized compared to the CBD soil conditions.

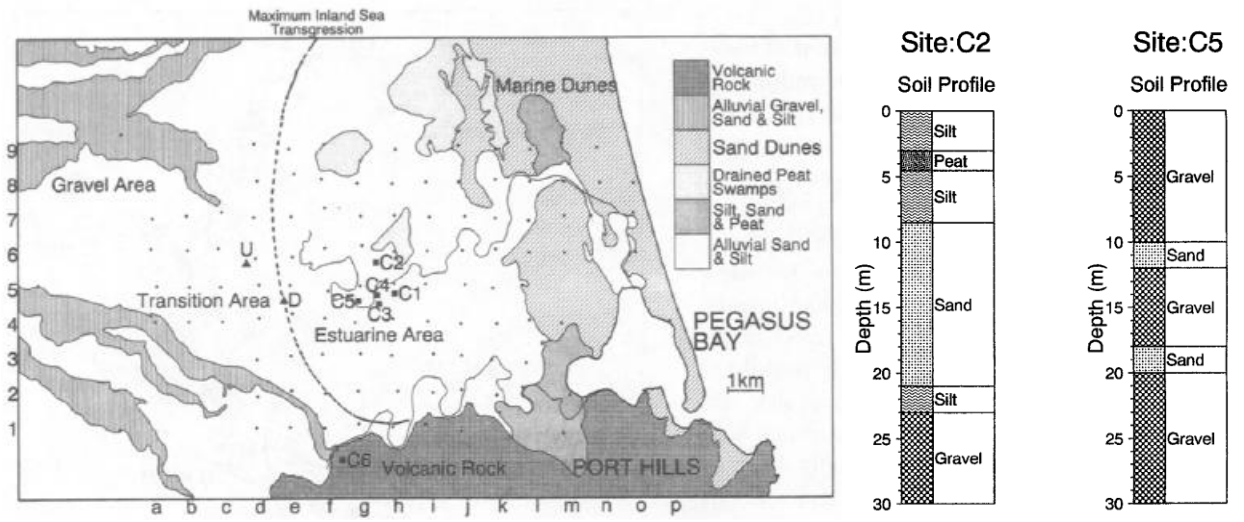

Figure 2.2. Surface geological map (left) of Christchurch (Brown and Weeber, 1992) and soil profiles of the top 30 m of the characteristic sites, C2 and C5 (Elder et al., 1991 and Berrill et al., 1993).

2.2. RECONNAISSANCE OF THE SEISMIC STATIONS SITES

Thanks to a dense network of seismographs covering the broader area of Christchurch a large number of ground motions were recorded during the Christchurch February 2011 earthquake. During our reconnaissance trip in April 2011, we inspected the 8 seismic station sites, depicted in the map of Figure 2.3.

Figure 2.3. Inspected seismic station sites.

2.2.1. Riccarton High School Christchurch (RHSC)

RHSC seismic station is situated at the Riccarton High School, in Upper Riccarton suburb, west of CBD. The seismograph is placed on the floor of a basement 1 m below the ground surface. The maximum PGA value recorded by the instrument is 0.3g in the EW direction (Figure 2.5). The frequency content of the recorded ground motions is rather high, affecting periods below 1 sec, as indicated by the spectra, depicted in Figure 2.6.

The school building, a steel made light structure, performed well during Christchurch earthquake, sustaining only minor damage, like superficial cracking in the walls. This may partially attributed to the fact that the building had been strengthened with steel braces 4 years four years ago. Close to the school there is large open space used for sport activities, while the buildings in the vicinity are also low light structures. These facts can lead to a safe conclusion that RHSC records are free-field motions, not essentially affected by the building response.

No evidence of liquefaction was found in the site, as confirmed by the employees of the school, which is also interpreted in the characteristics of the recorded acceleration time histories - no long period cycles and cut-off of acceleration values after a peak acceleration value is reached. Furthermore, people working in the school stated that they lots of rocking during the earthquake.

According to the employees of the school, the soil consists of old river banks, mostly gravel and some silts. In addition to that, borelog conducted 1.5 km east of the RHSC station (Figure ??) indicates that the superficial deposits belong to the Springston formation comprising well sorted gravel, sand and silt (Brown and Weeber, 1992).

Figure 2.4. Close plan view of RHSC seismic station site.

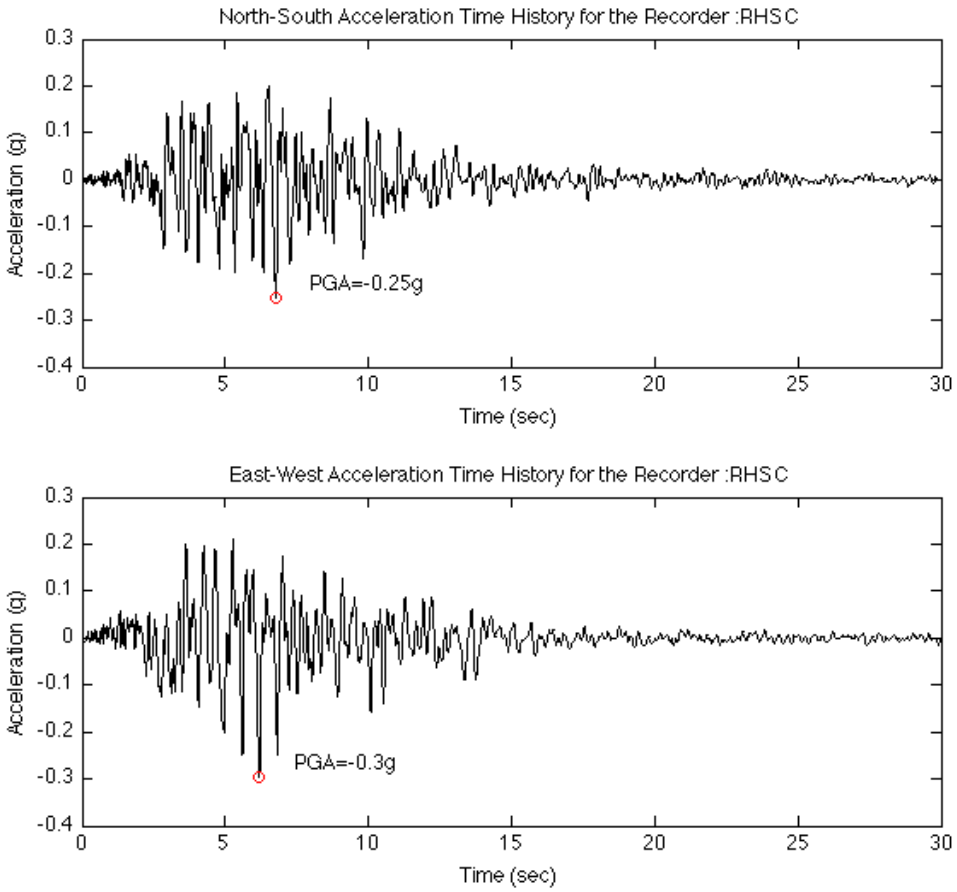

Figure 2.5. Acceleration time histories in NS-EW directions recorded at RHSC station.

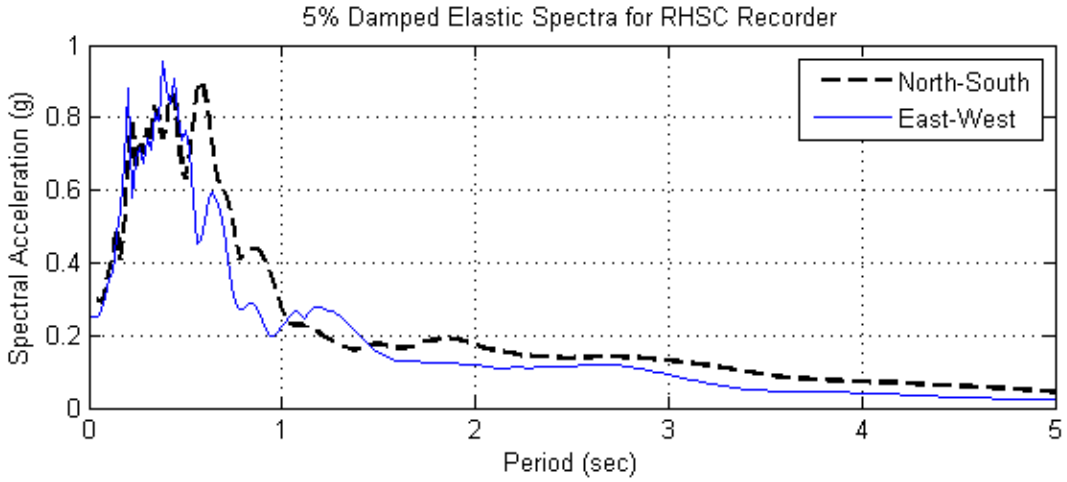

Figure 2.6. Acceleration spectra in NS-EW directions of ground motions recorded at RHSC station.

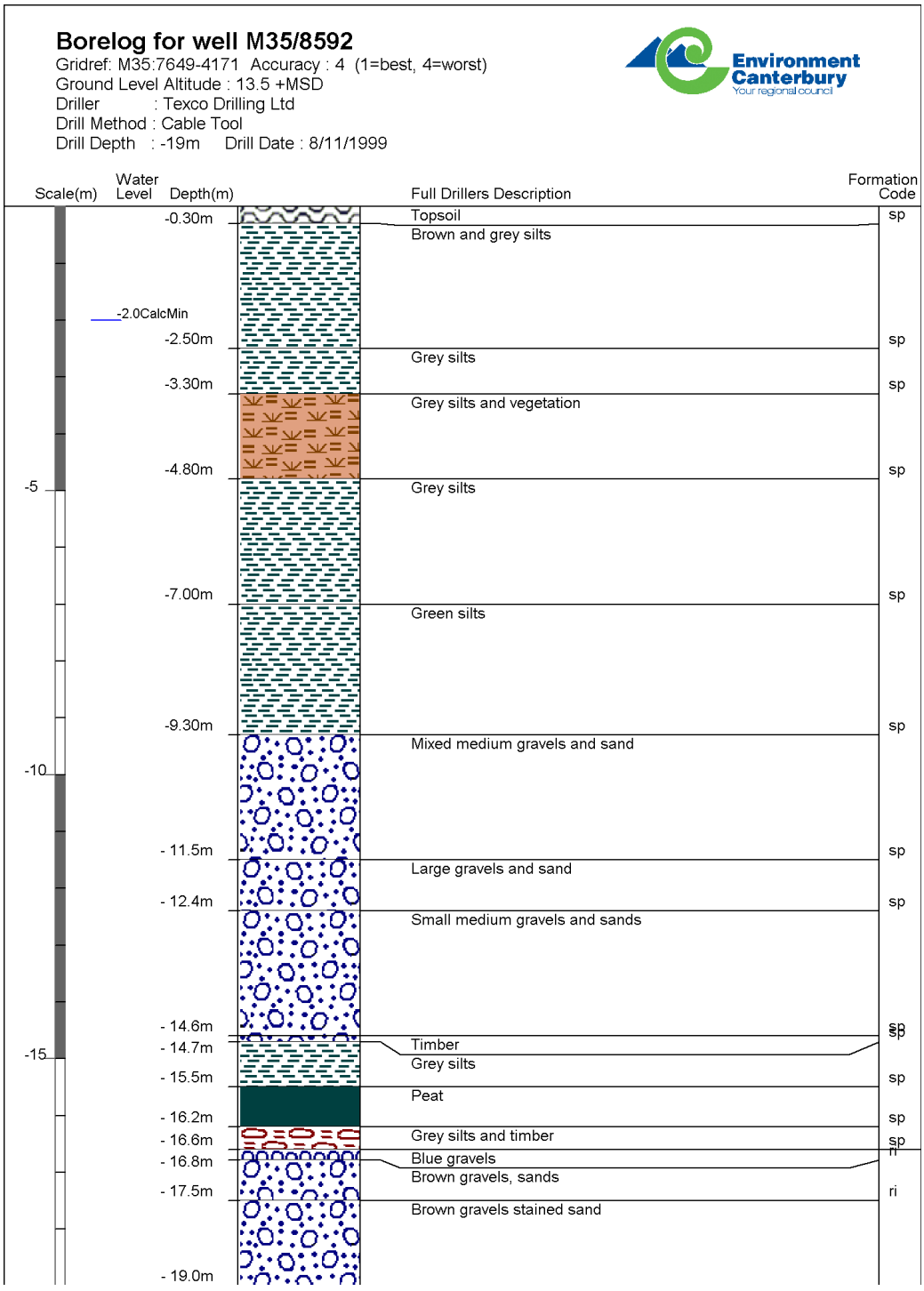

Figure 2.7. Borelog conducted 1.5 km east of RHSC seismic station (http://ecan.govt.nz/).

Figure 2.8. Riccarton High School (left) and its yard (right).

Figure 2.9. The basement accommodating the seismic station (left) and the seismograph placed in a box fixed on the solid base on the ground floor (right).

2.2.2. Christchurch Hospital (CHHC)

CHHC seismic station is situated in a 2-storey concrete building (235 Antigua St) in the neighborhood of Christchurch Hospital. The seismograph is placed on the ground floor. The maximum PGA value recorded by the instrument is 0.36g in the EW direction (Figure 2.11). A profound characteristic of the recorded ground motion - especially the EW one - is the acceleration cut-off and period elongation after a peak value has been reached. Thus, the frequency content of the recorded ground motions is rich, affecting a large range of periods up to 1.5 sec or more, as indicated by the spectra, depicted in Figure 2.12. The spectra also

comprise amplification bulges at even higher periods i.e. 2.5 sec. All the aforementioned characteristics are indicative of liquefaction.

The concrete building accommodating the station did not sustain major damage apart from gap opening between the front and the rear section in the order of 4 cm at the top and a 1 cm out of plane displacement (Figure 2.15). A crack between the building and the asphalt has been developed in the perimeter of the building allowing the liquefied sand emerge on the ground surface. The soil underneath the station mainly consists of sand (borelog of Figure 2.13), justifying the large amount of ejected sand.

Sandboils were evident all over the neighborhood, which consists of heavy steel and concrete structures. The car park building across the seismic station was seriously damaged, as well as the Nurses' Training Building adjacent to the hospital. Overall, the CHHC recorded shaking is a strong one, despite the relative low value of accelerations, due to its rich period content. Last, it should be mentioned that the recorded ground motions must have been affected by the structure response and cannot be characterized as free-field records.

Figure 2.10. Close plan view of RHSC seismic station site. The star indicates the location of the borelog.

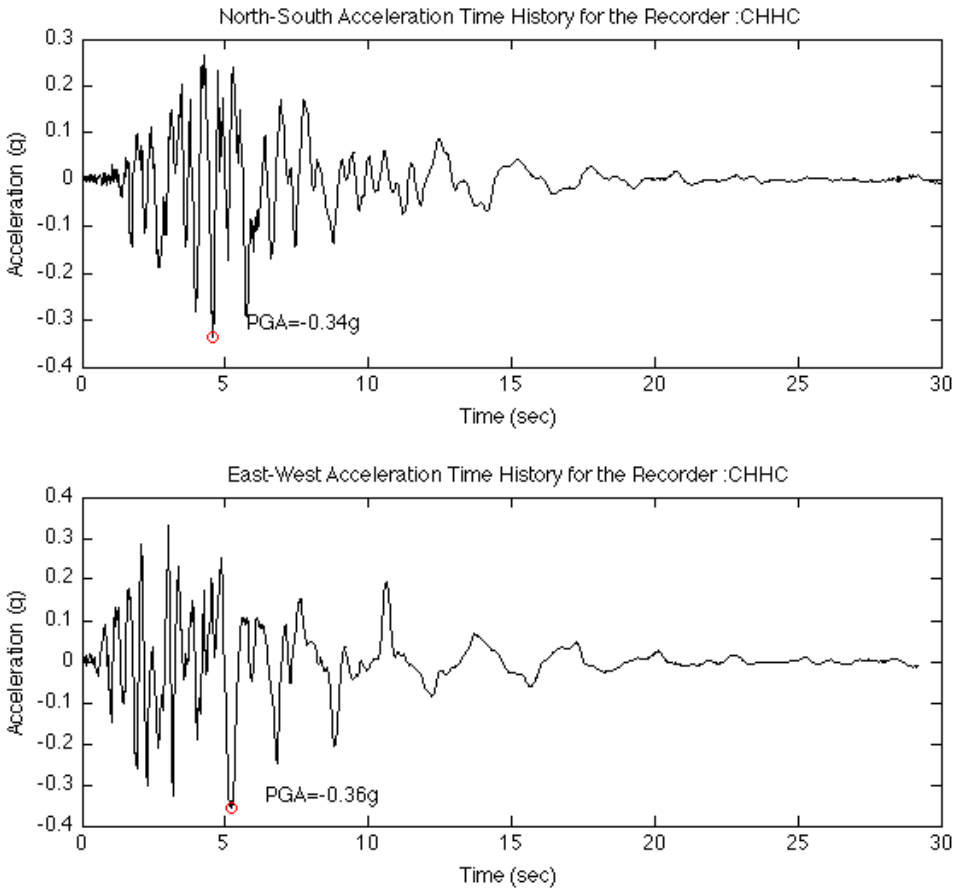

Figure 2.11. Acceleration time histories in NS-EW directions recorded at CHHC station.

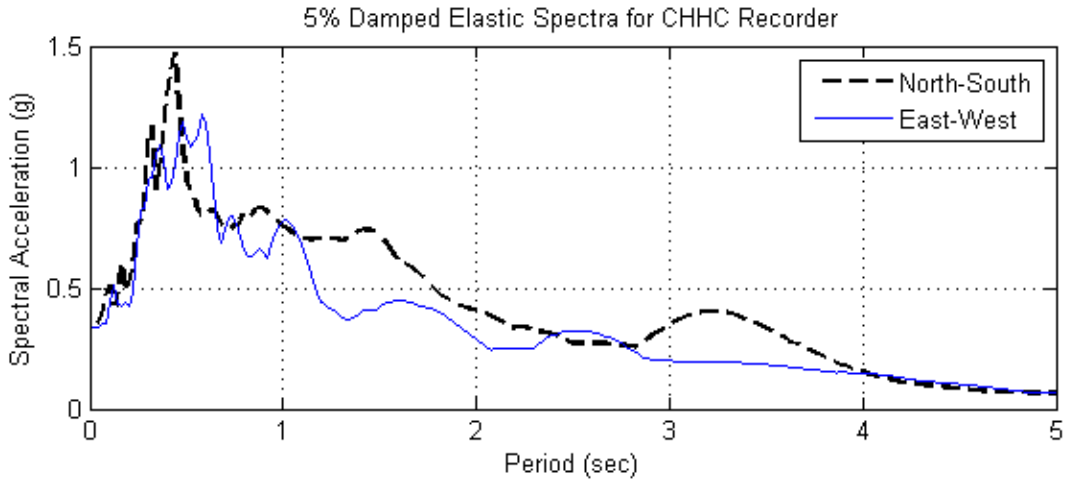

Figure 2.12. Acceleration spectra in NS-EW directions of ground motions recorded at CHHC station.

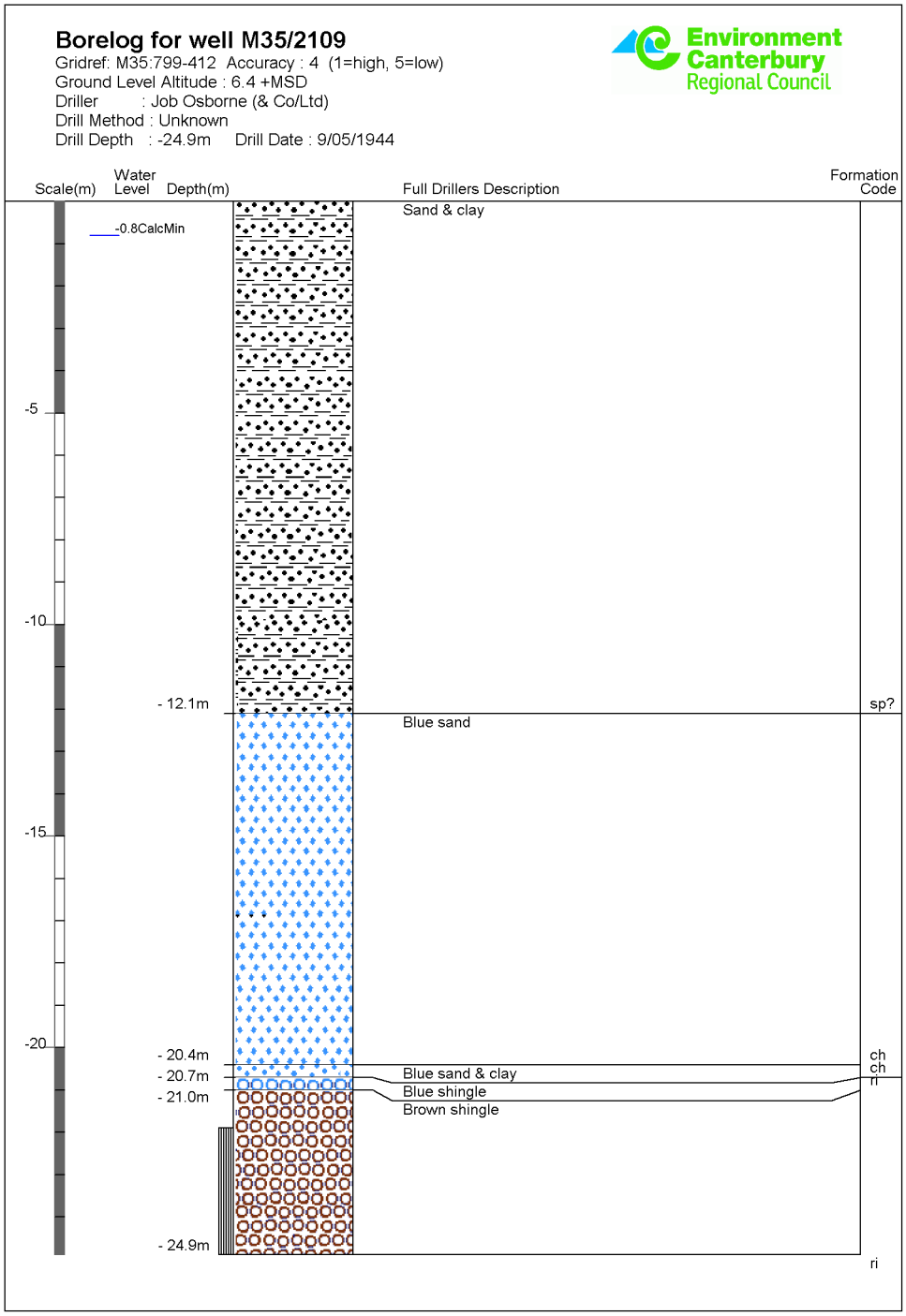

Figure 2.13. Borelog underneath the CHHC seismic station (http://ecan.govt.nz/).

Figure 2.14. 2-storey building at 235 Antigua Street, accommodating CHHC seismic station.

Figure 2.15. Gap opening between the front and rear section of CHHC seismic station building (left). Crack between the building and the asphalt due to ejected sand (right).

Figure 2.16. Seismograph placed on the ground floor (left). Shear crack in a wall adjacent to CHHC seismic station building due to liquefaction-induced differential settlement and possible heaving (right).

Figure 2.17. Christchurch Hospital Car Park (239 Antigua St) adjacent to CHHC seismic station building (left). Sand eject in front of Christchurch Hospital Car Park (right).

2.2.3. Christchurch Cathedral College (CCCC)

CCCC seismic station is situated at the Christchurch Cathedral College close to the southeast edge of CBD. We were not able to enter the building in order to exactly located the seismograph. The College is a new designed building which sustained no visible damage during the earthquake. However, the Cathredal of the Blessed Sacrament was partially collapsed. Sandboils appeared all over the site especially on the open space next to the college building. The superficial soil deposits, 20 m thick, consist of sand and clay, as indicated by the borelog conducted in the site (Figure 2.21).

The maximum PGA value recorded by the seismograph is 0.41g in the EW direction (Figure 2.19). Acceleration cut-off and period elongation after a peak value has been reached are also the main characteristics of the records, as in case of CCCC. Interestingly the acceleration spectra indicate a large amplification for a period of about 1.5 sec, rendering the ground motion particularly strong for long period structures. All this characteristics can be justified by the soft soil deposits and the occurrence of liquefaction.

Figure 2.18. Close plan view of CCCC seismic station site. The star indicates the location of the borelog.

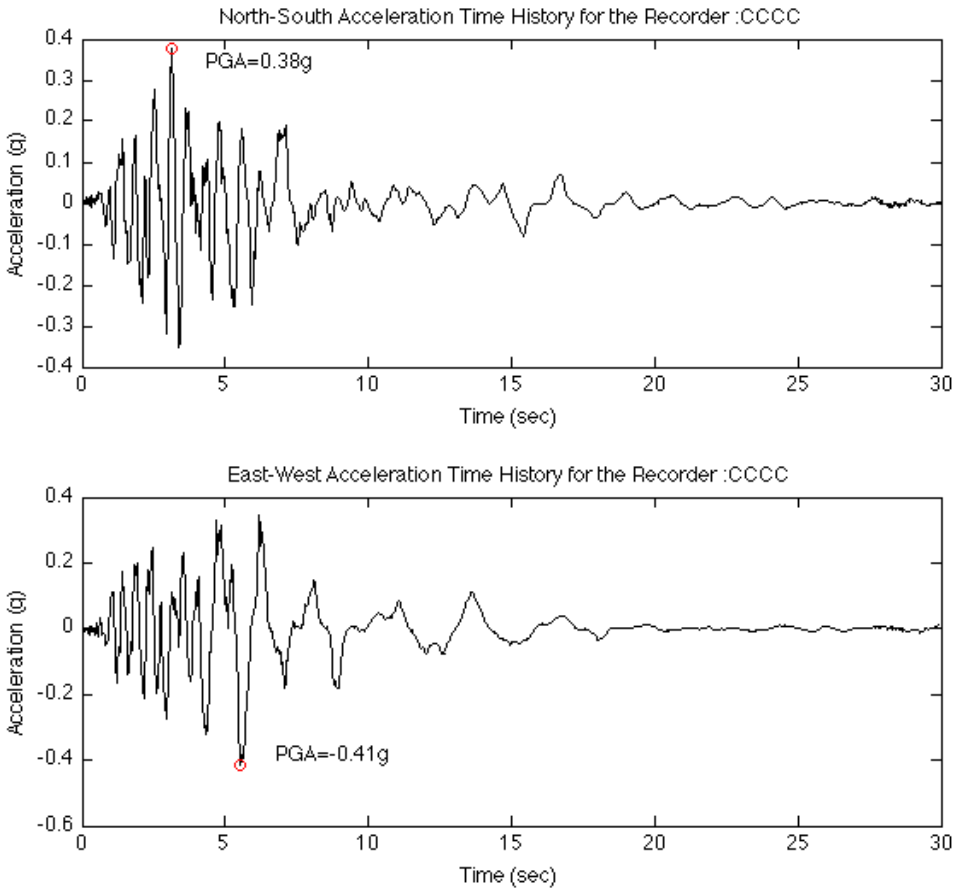

Figure 2.19. Acceleration time histories in NS-EW directions recorded at CCCC station.

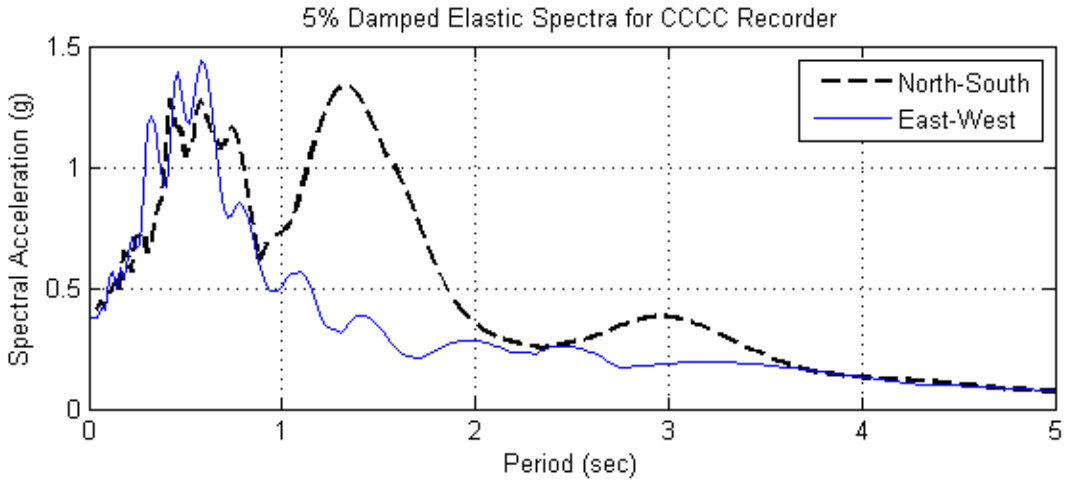

Figure 2.20. Acceleration spectra in NS-EW directions of ground motions recorded at CCCC station.

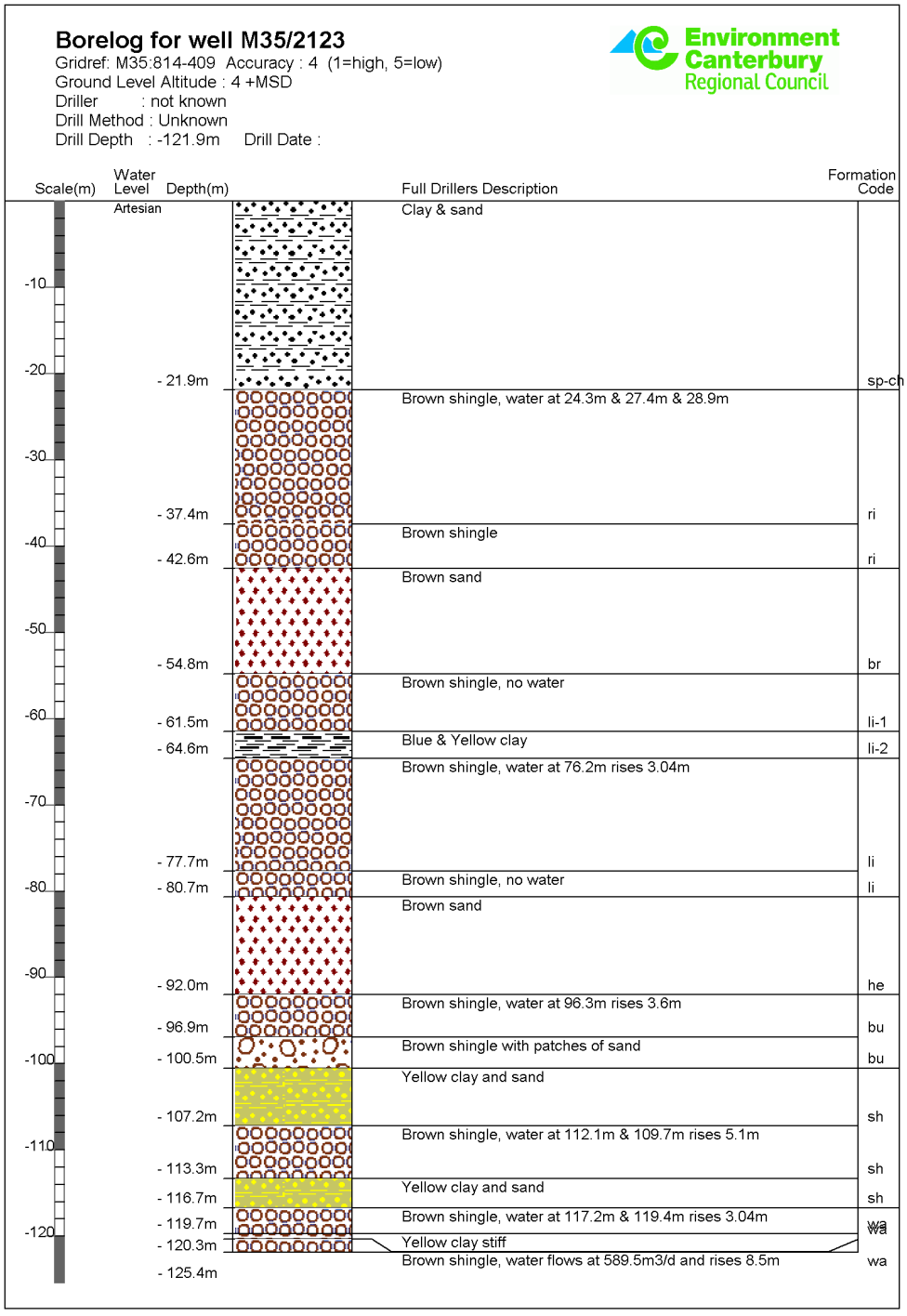

Figure 2.21. Borelog close to the CCCC seismic station (http://ecan.govt.nz/).

Figure 2.22. Christchurch Cathedral College building accommodating CCCC seismic station.

Figure 2.23. Partial collapse of the Cathredal of the Blessed Sacrament, close to CCCC station.

Figure 2.24. Liquefaction in front of Christhcurch Cathedral College (right). Ejected sand from the open space next to CCCC station cumulated in a pile (right).

2.2.4. Christchurch Resthaven (REHS)

REHS seismic station is situated at Christchurch Resthaven Care Center for old people in 901 Colomb Street, at the northern border of CBD. The seismograph is located in a separate storage within the Resthaven facilities. The recorded motion is considered a free-field response taking into account the open space around the station.

The maximum PGA value recorded by the seismograph is 0.72g in the EW direction (Figure 2.26), a rather high value corresponding to a single spike. Acceleration cut-off and period elongation after a peak value has been reached is observed in the records, which indicate that at least moderate liquefaction must have occurred, even though sand did not manage to emerge on the ground surface. The main peak of the acceleration spectra takes place for a period of about 1.5 sec, which is also indicative of severe soil softening. There are is also a bulge at 3 sec in the EW spectrum which can only be attributed by liquefaction-related effects (if directivity effects are excluded).

Figure 2.25. Close plan view of REHS seismic station site. The star indicates the location of the borelog.

The Resthaven building did not sustain any damage, though numerous timber and masonry houses in the surroundings were damages. There was no evidence of liquefaction on the site in terms of sand ejecta. The soil consists of clay, silt, sand and peat in thin alternating layers, according to a borelog conducted close to the station (Figure 2.28).

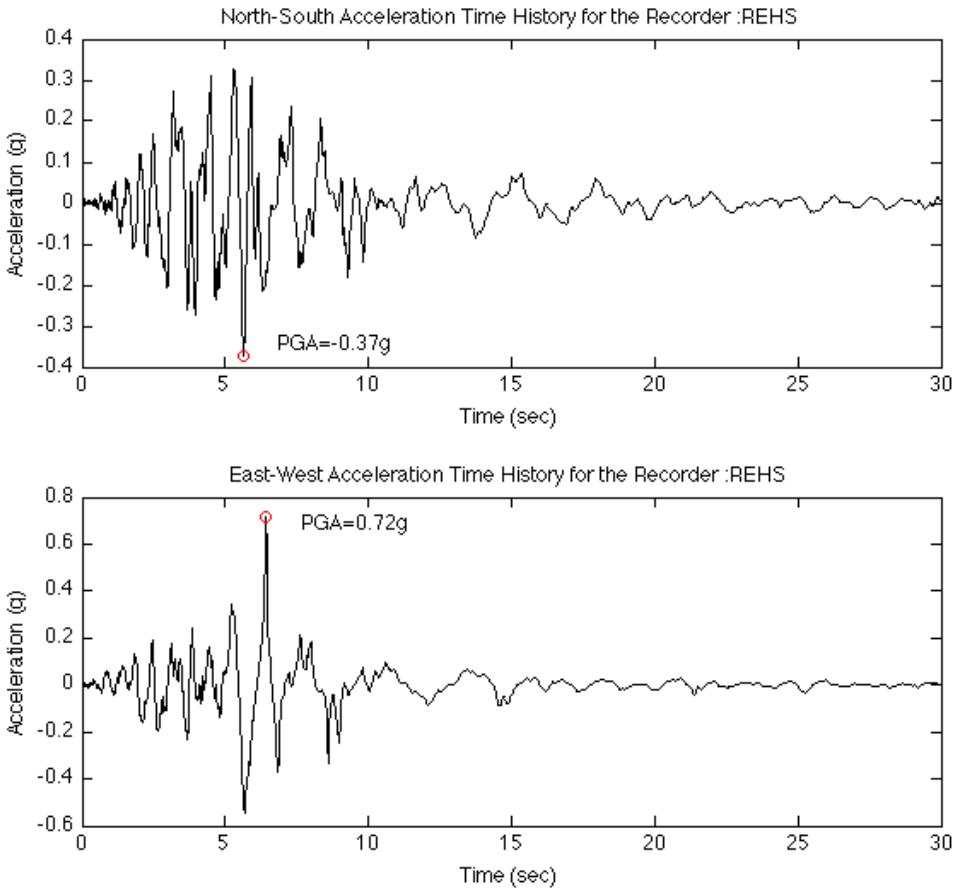

Figure 2.26. Acceleration time histories in NS-EW directions recorded at REHS station.

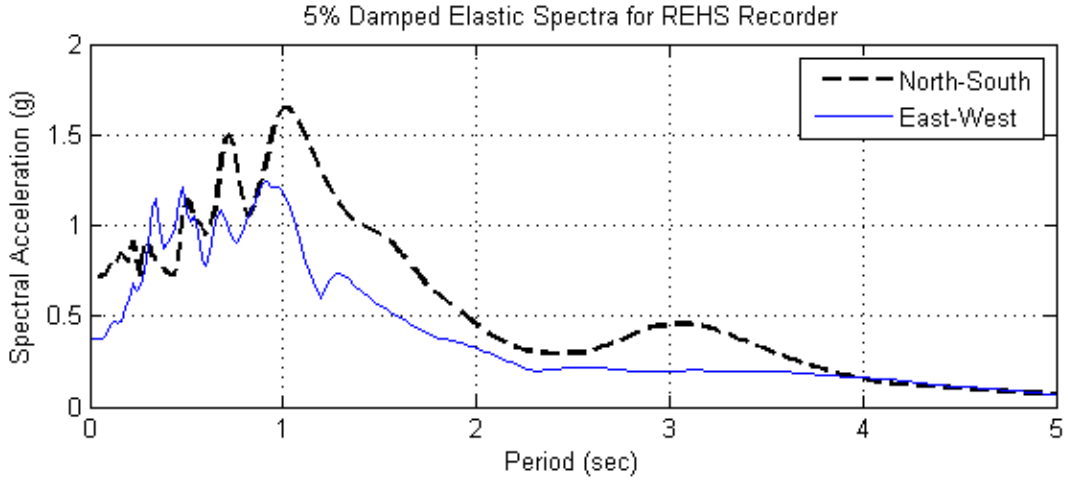

Figure 2.27. Acceleration spectra in NS-EW directions of ground motions recorded at REHS station.

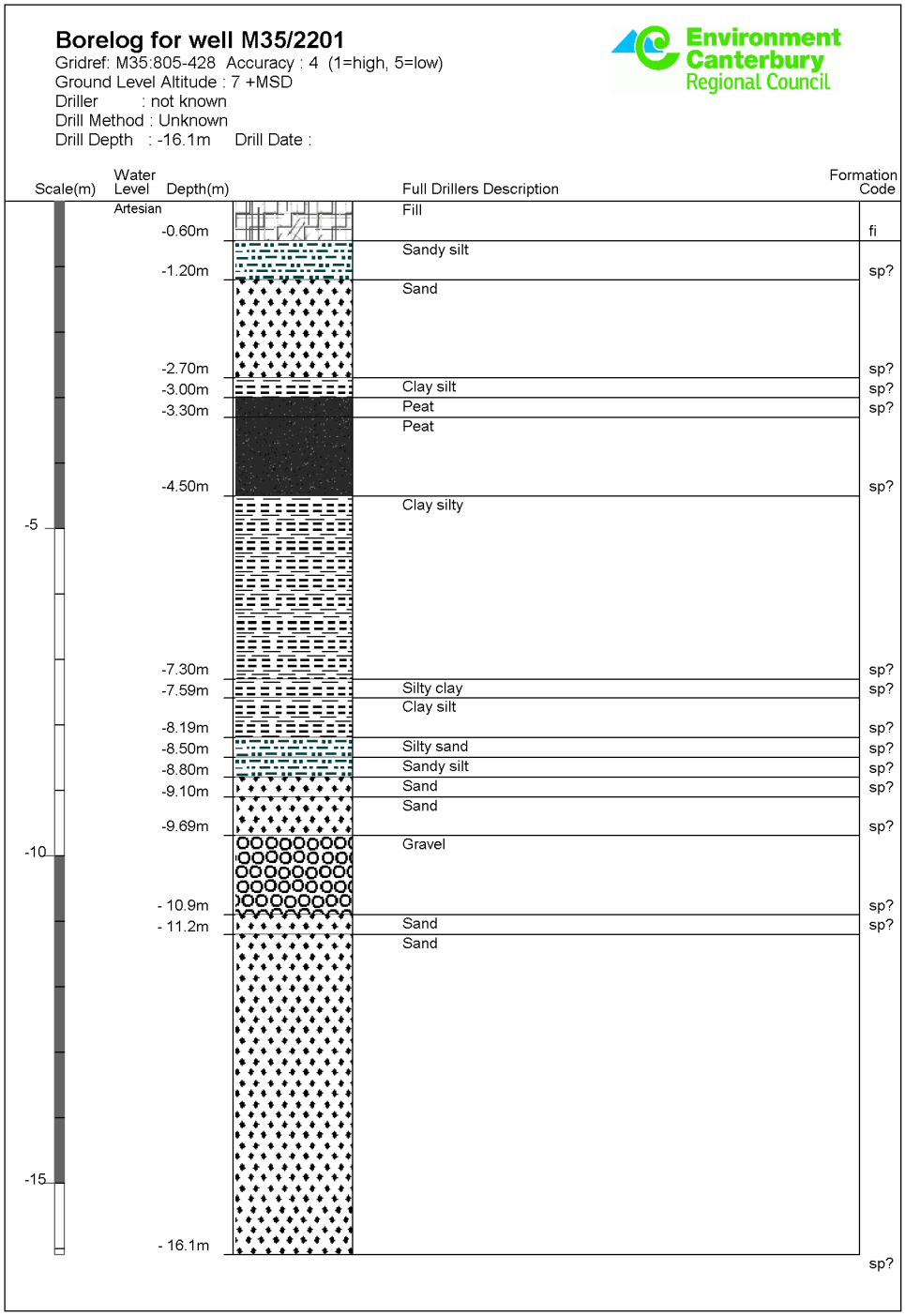

Figure 2.28. Borelog close to the REHS seismic station (http://ecan.govt.nz/).

Figure 2.29. The Resthaven Center Care accommodating REHS seismic station.

Figure 2.30. The storage (left) where the seismograph (left) is placed in.

2.2.5. Christchurch Botanic Gardens (CBGS)

CBGS seismic station is situated in Christchurch Botanic Gardens. The seismograph is placed in a light steel kiosk in a middle of a park. The ground motions recorded are totally free-field responses. The maximum PGA value recorded by the seismograph is 0.54g in the EW direction (Figure 2.32). The main characteristics of the motion records are high frequency spikes succeeding long period cycles with acceleration cut-off and reversely. This is typical for liquefied sites, as the CBGS one. Evidence of liquefaction was everywhere. The soil profile is given in the Figure 2.2 (site C2).

Figure 2.31. Close plan view of CBGS seismic station site.

The monument in the "Azalea garden" section of the Botanic Gardens, named as "An Inside Outlook" by the sculptor Stuart Griffiths, consists of a concrete base, a green granite piece on the base, 2 concrete columns (fairly regularly shaped) and a green granite top (see Figures 2.37 to 2.39). The 2 concrete columns are connected to the base by using steel tubes with 9cm diameter and 2mm wall thickness.

The monument fell down towards the South-East direction causing failure of the steel tubes. The tubes were buckled and exceeded their bearing capacity.

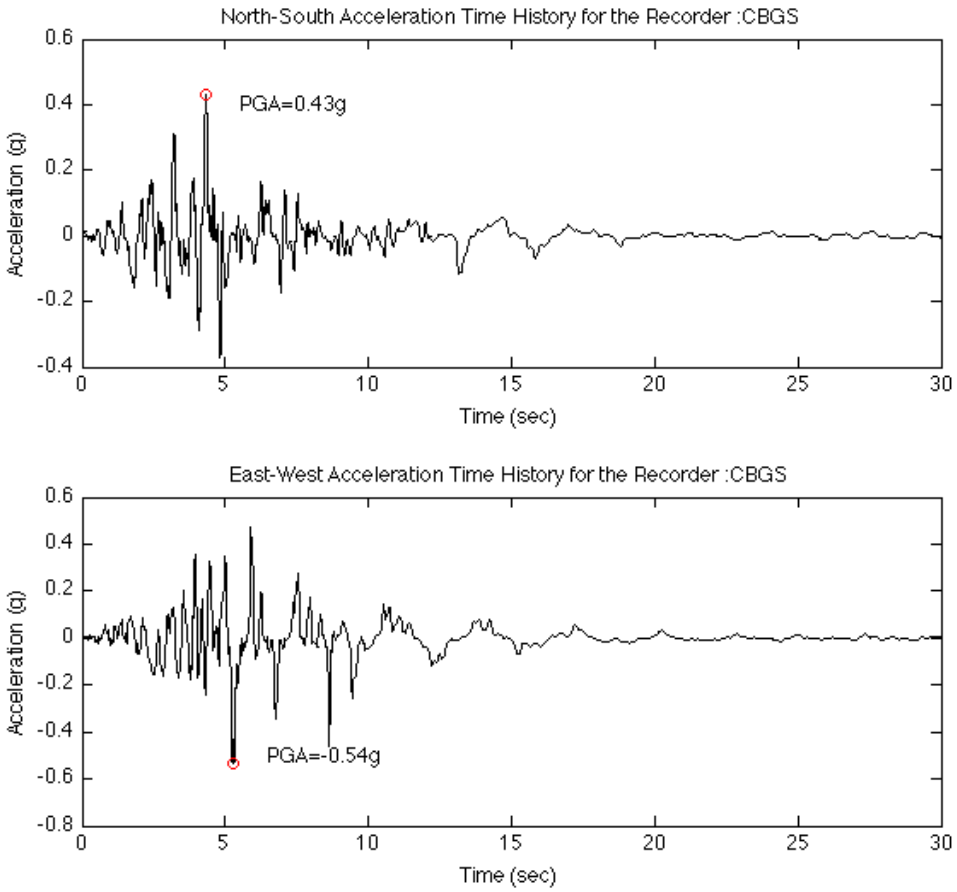

Figure 2.32. Acceleration time histories in NS-EW directions recorded at CBGS station.

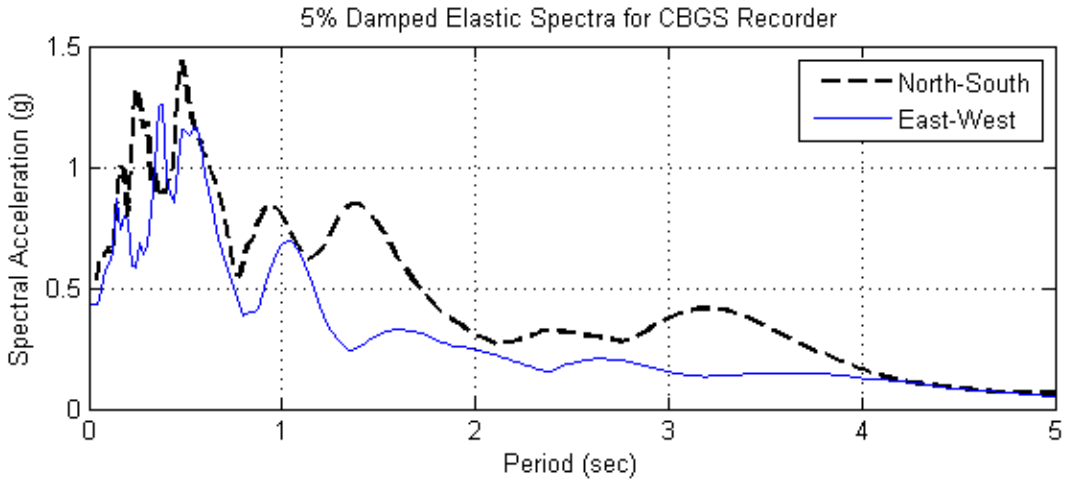

Figure 2.33. Acceleration spectra in NS-EW directions of ground motions recorded at CBGS station.

Figure 2.34. CBGS seismic station.

Figure 2.35. The seismograph in CBGS seismic station.

Figure 2.36. Excavation near the CBGS seismic station showing part of the superficial soil deposit consisting of silty sand.

Figure 2.37. "An Inside Outlook" by sculptor Stuart Griffiths in Azalea Gardens before Christchurch earthquake (left). Fallen sculpt after the earthquake (right).

Figure 2.38. Sand ejecta on the site of the fallen sculpt in Azalea gardens.

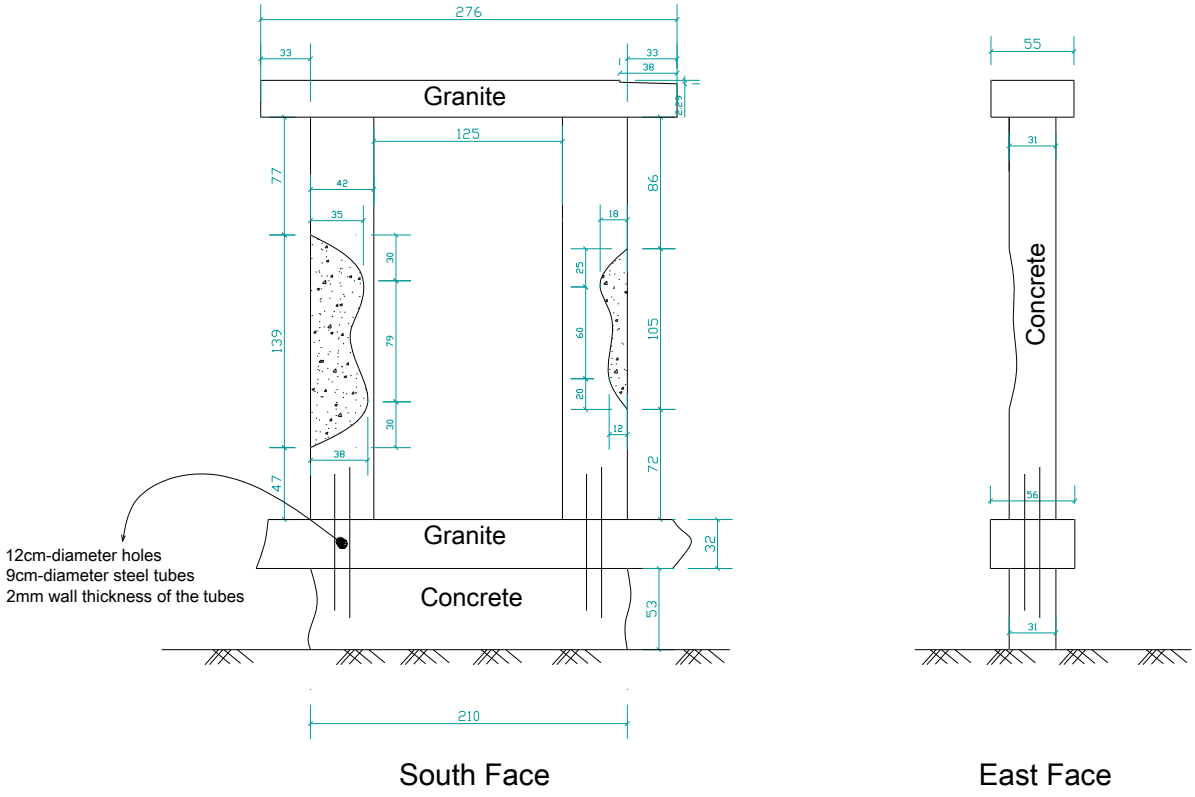

Figure 2.39. Elevation of the fallen monument "An Inside Outlook" close to the CBGS recorder

2.2.6. Pages Road Pumping Station (PRPC)

PRPC seismic station is situated in the facilities an old Pumping Station at the corner of Pages Road and Woodham Road, in Avonside suburb. In particular, the seismograph is placed in a garage/storage outside the Pumping Station (Figure 2.41). The instrument was surrounded by numerous other heavy unrelated objects, which may have affected the records (Figure 2.42).

The Pumping Station suffered significant damage during the earthquake and was unoccupied by the time of our visit. Differential displacement of one section relative to the adjacent one was the primary damage. Moreover, there was no evidence of liquefaction on the site, when we arrived, not even remnants of sand. However, a borelog contacted in the site shows that the superficial layer 27 m consists only of sand (Figure 2.44). Moreover, typical characteristics for liquefied sites, such as long period cycles and acceleration cut-off can be observed in the recorded acceleration time histories and the corresponding spectra. The maximum PGA value recorded by the seismograph is 0.72g (Figure 2.45) in the EW direction. It should be mentioned, though, that the EW record seems to have been affected by the objects surrounding the instrument.

Figure 2.40. Close plan view of PRPC seismic station site. The star indicates the location of the borelog.

Figure 2.41. PRPC seismic station site. The seismograph is placed in the garage (in the red circle).

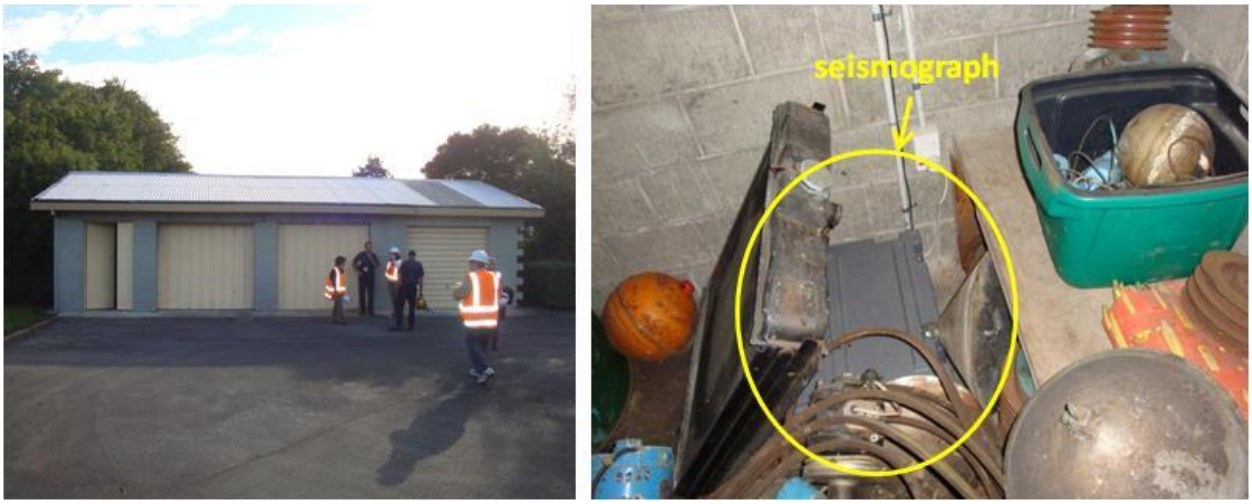

Figure 2.42. PRPC seismic station site in the garage (left). The seismograph among other unrelated stored objects.

Figure 2.43. Interior of the Pumping Station next to the garage. Differential movement at the joint of one section of the building with the other.

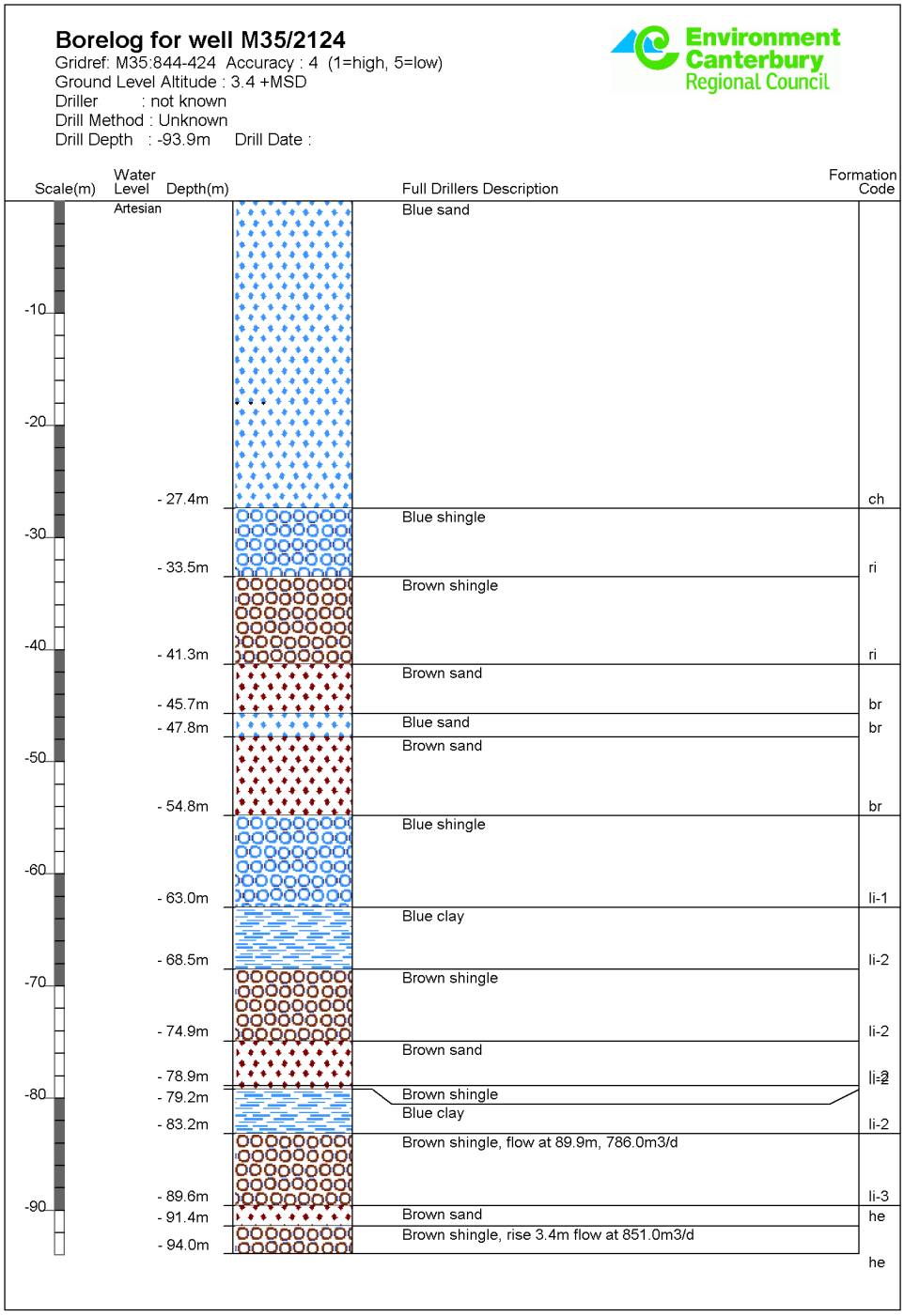

Figure 2.44. Borelog close to the PRPC seismic station (http://ecan.govt.nz/).

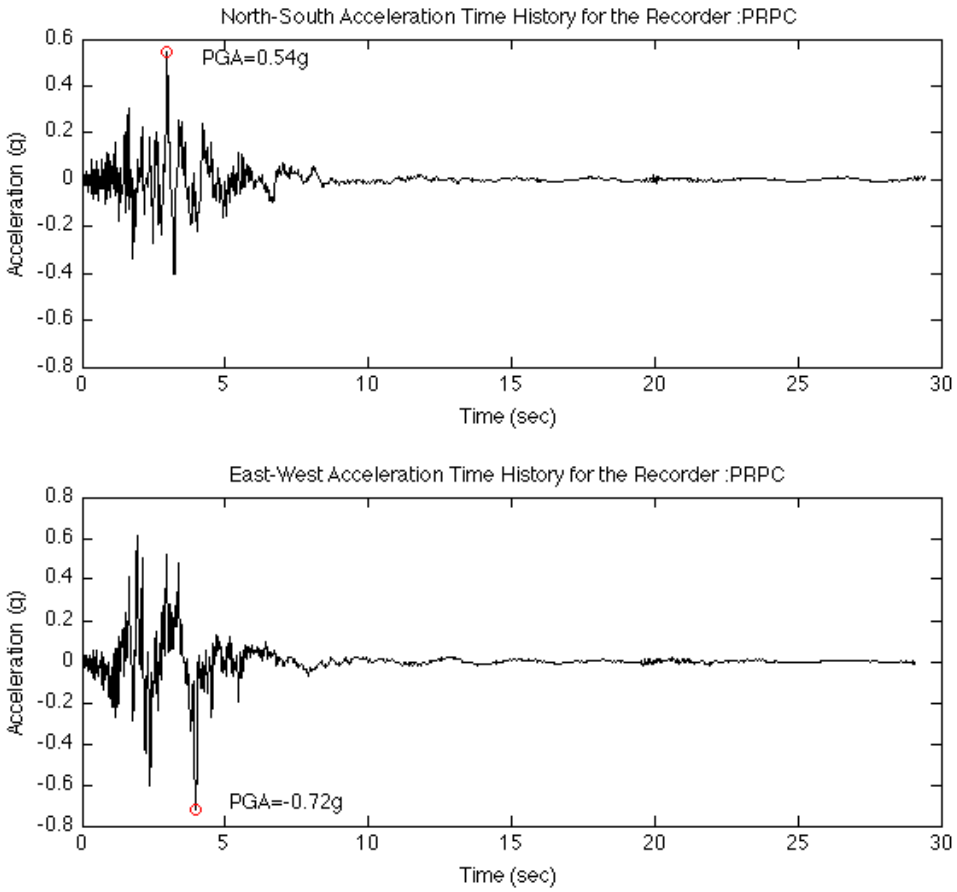

Figure 2.45. Acceleration time histories in NS-EW directions recorded at PRPC station.

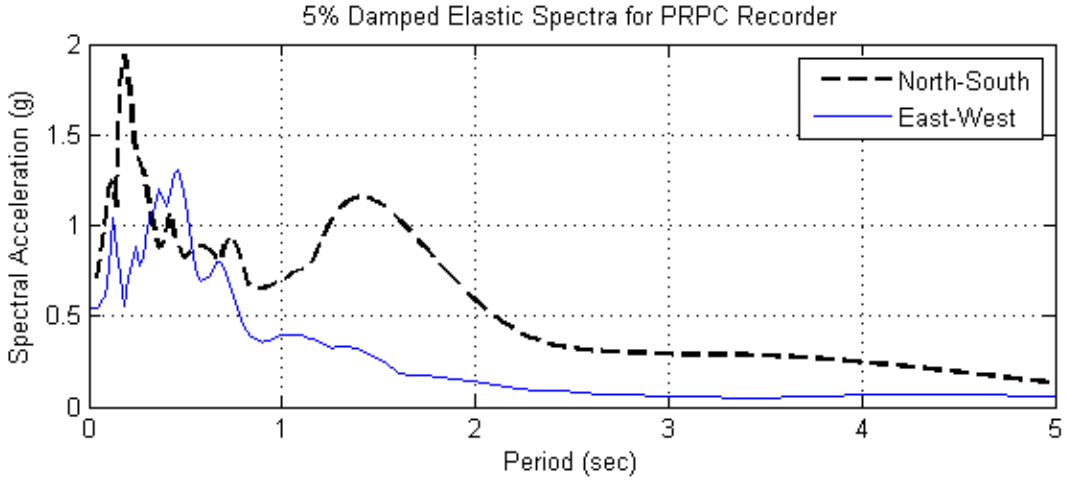

Figure 2.46. Acceleration spectra in NS-EW directions of ground motions recorded at PRPC station.

2.2.7. Heathcote Valley Primary School (HVSC)

HVSC seismic station is situated at Heathcote Valley Primary School. The school building, a very light structure, sustained moderate damage due to earthquake. The seismograph is placed in a storage kiosk located on the yard of the school close to Bridle Path Road. Adjacent to the school, there is an excavation (8 m deep approximately) leading the way to the railway tunnel passing through the Port Hills and heading to Lyttelton Port (Figure 2.47). The railway tunnel was constructed in 1864. The school was made that year for the workers' children. Ever since, this slope consisting of stiff clay stands vertical ever since (Figures 2.48 and 2.49). Both the railway damage (6 m high) and the vertical slope survived the double earthquake, sustaining no damage. The road tunnel parallel to the railway tunnel was built almost 100 years later, in 1960. The road tunnel also suffered no damage but it remained close at the time of our visit, in order to be inspected.

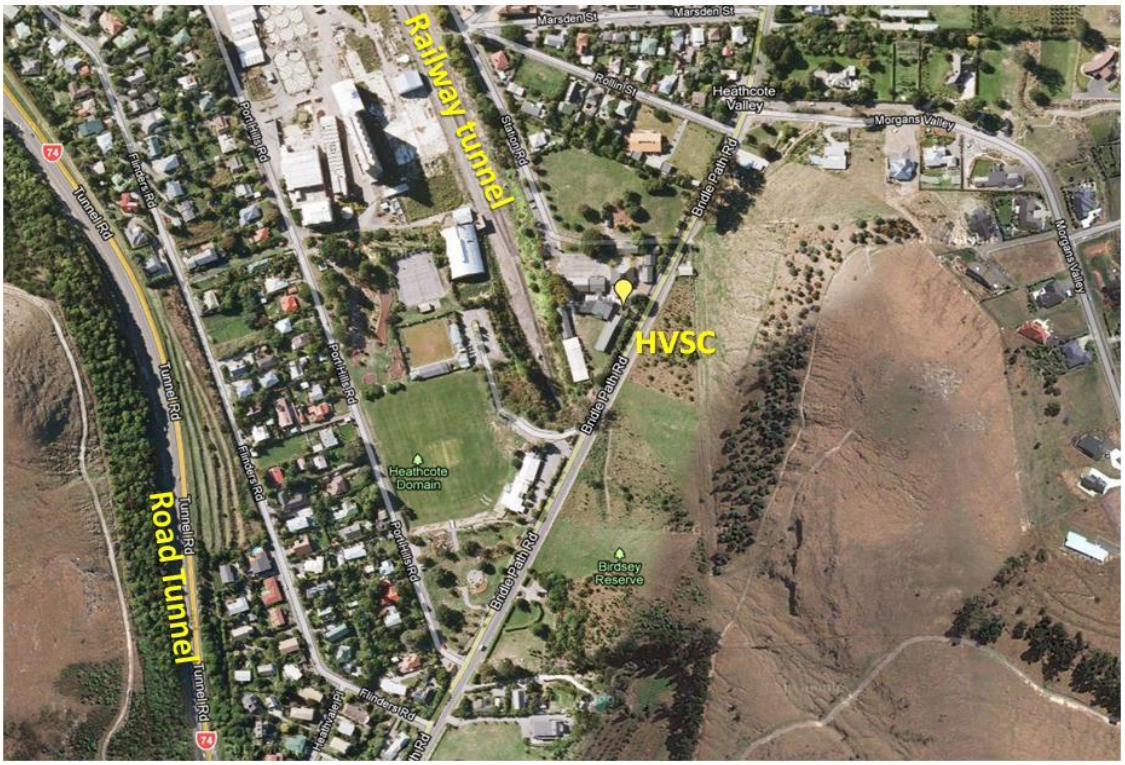

Figure 2.47. Close plan view of HVSC seismic station site.

There are not specific information about the soil conditions and mostly about the depth to the bedrock. Brown and Weeber (1993) state that the depth to bedrock in Heathcote Valley ranges from 96 to 128 m. A sketch depicted in Figure 2.49 illustrates the possible soil geometry at the location of the station. Moreover, the ground water level is not shallow indicated by the 8 m

vertical slope. Thus, there was no liquefaction occurrence in the site. The first evidence of liquefaction appears 1 km away towards the north, in Ferrymead (Figure 2.50).

Figure 2.48. The excavation adjacent to HVSC station, leading to railway tunnel. The remnants of rain water show that it cannot be easily absorbed by the soil which is indicative of clayey soil with low permeability(left). The entrance to the railway tunnel showing, no damage (right).

Figure 2.49. The vertical slope of stiff clay (8 m high) adjacent to HVSC station.

HSVC ground motion is the strongest one recorded during Christchurch Earthquake in terms of PGA values reaching 1.3g (Figure 2.52 and 2.53). It is evident that significant topographic and basin effects contributed to the amplification indicated by the high acceleration values. In addition, the frequency content is relatively high indicating strong soil conditions, such as stiff clay.

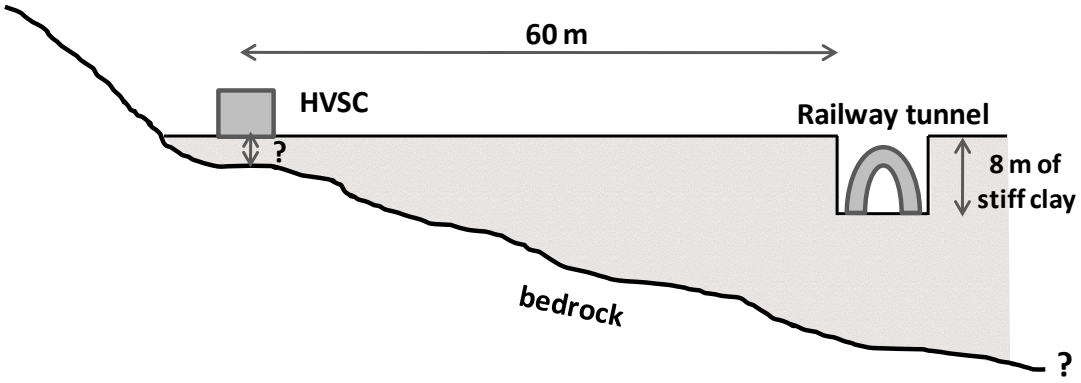

Figure 2.50. Sketch of the topography and soil geometry of the HVSC seismic station site.

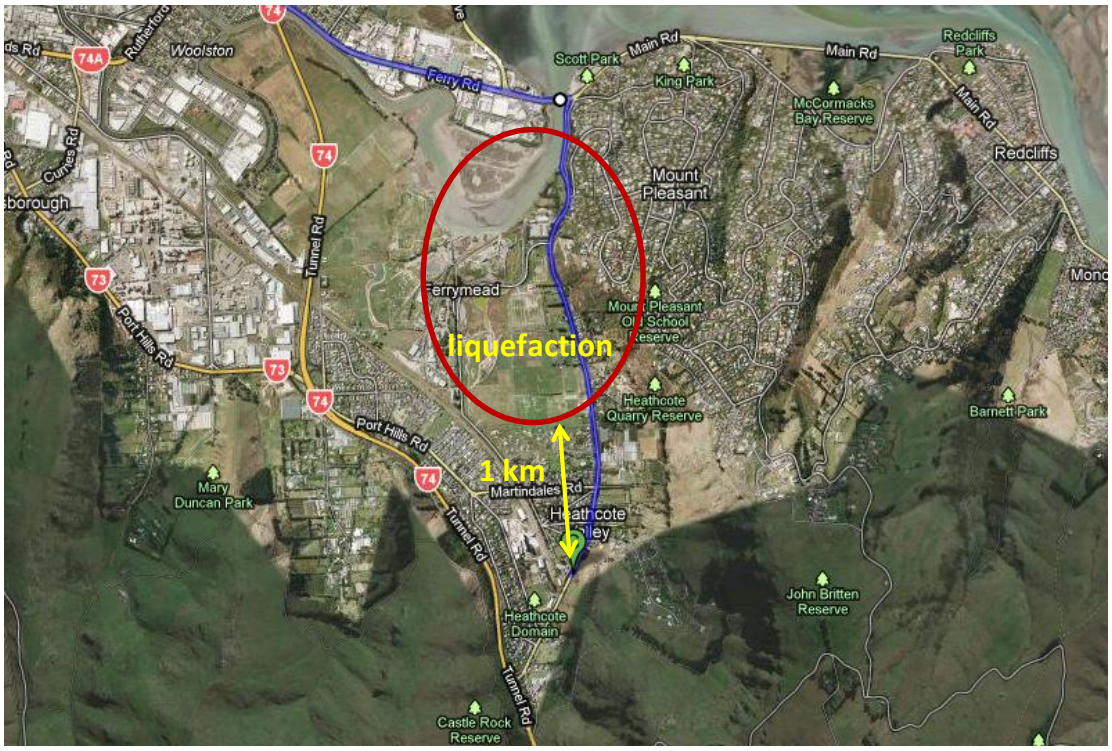

Figure 2.51. Evidence of liquefaction appears in Ferrymead, 1.5 km north of HVSC station.

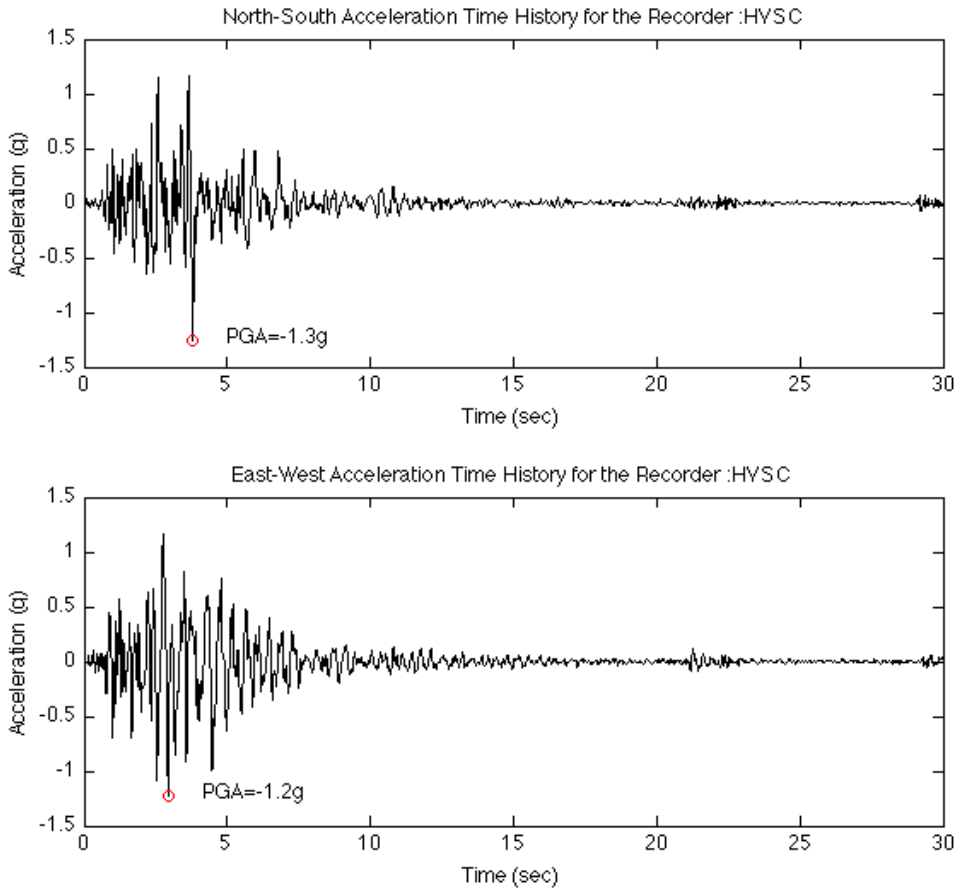

Figure 2.52. Acceleration time histories in NS-EW directions recorded at HVSC station.

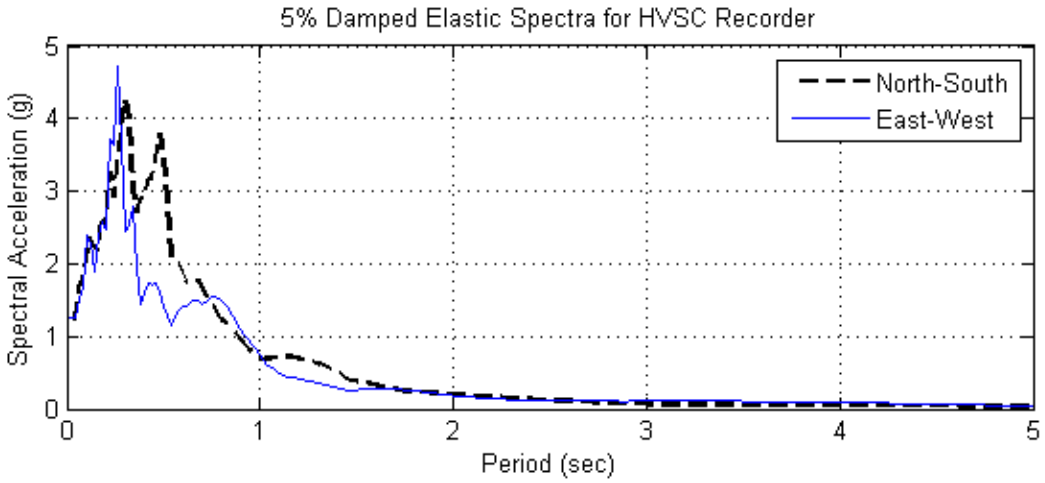

Figure 2.53. Acceleration spectra in NS-EW directions of ground motions recorded at HVSC station.

The memorial obelisk in Heathcote Valley (Figure 2.54 to 2.56) has fallen down in an angle 45 degrees towards East from Noth (see Figure 2.55). The base of the obelisk where the names are written has also tilted about 12 degrees towards in anti-clockwise direction. No shear connection is observed on the site between the tilted piece and the pieces above or below.

Figure 2.54. Obelisk at the corner of Bridle Path Road and Martinales Road close to HVSC station before Christchurch earthquake (left). Fallen obelisk after the earthquake (right).

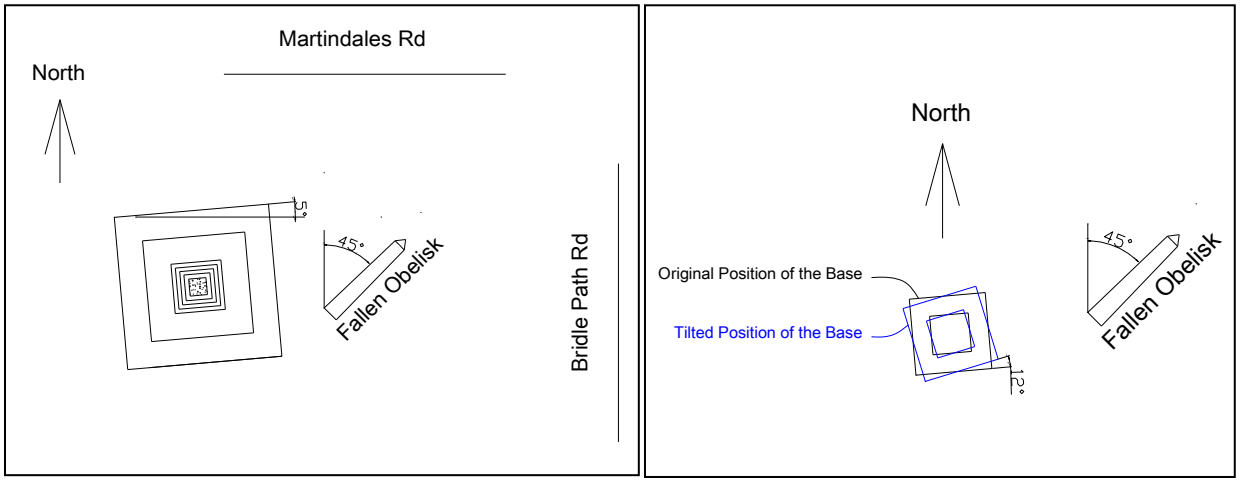

Figure 2.55. Original and tilted-fallen positions of the base of the monument and the obelisk.

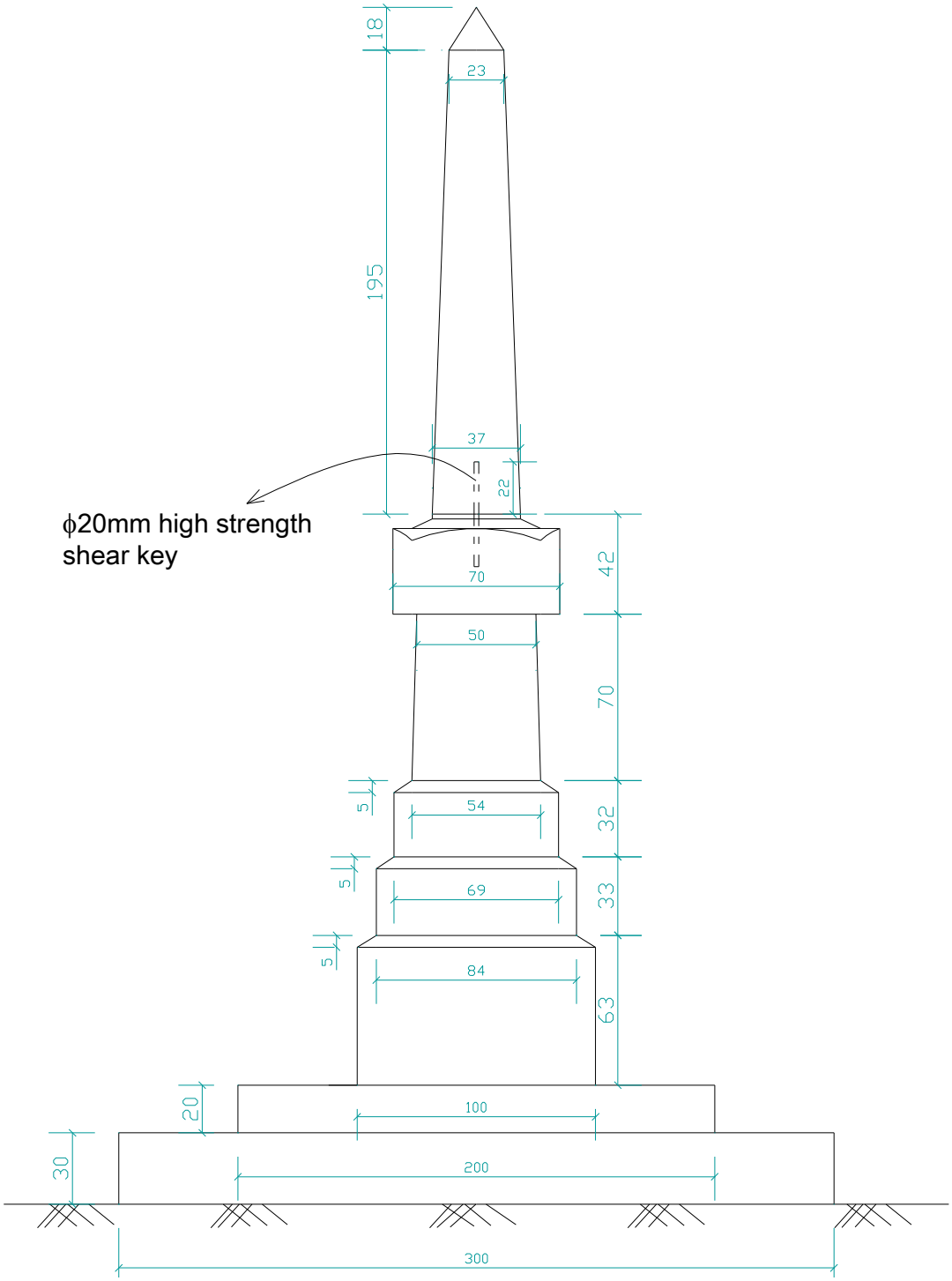

Figure 2.56. Elevation of the marble monument in the Heathcote Valley close to the HVSC recorder.

There is another fallen monument along Avon River, at the corner of New Brighton Road and Lake Terrace Road (Figure 2.57) that has almost the same dimensions with the monument in Heathcote Valley. The memorial obelisk by Avon River, at the corner of New Brighton Road and Lake Terrace Road, fell down during the Christchurch Earthquake of February 22nd. The falling direction of the obelisk is almost perfectly aligned with East. The axes of the base of the obelisk are aligned, with 3 degrees difference, with NS and EW. The base piece, just below the obelisk, is also simply placed on the rest of the bottom part of the monument but no tilting or translational displacement was observed. The monument is 2.8km far from the PRPC recording station. That monument was 1.5km away from the HPSC (Hulverstone Drive Pumping Station).

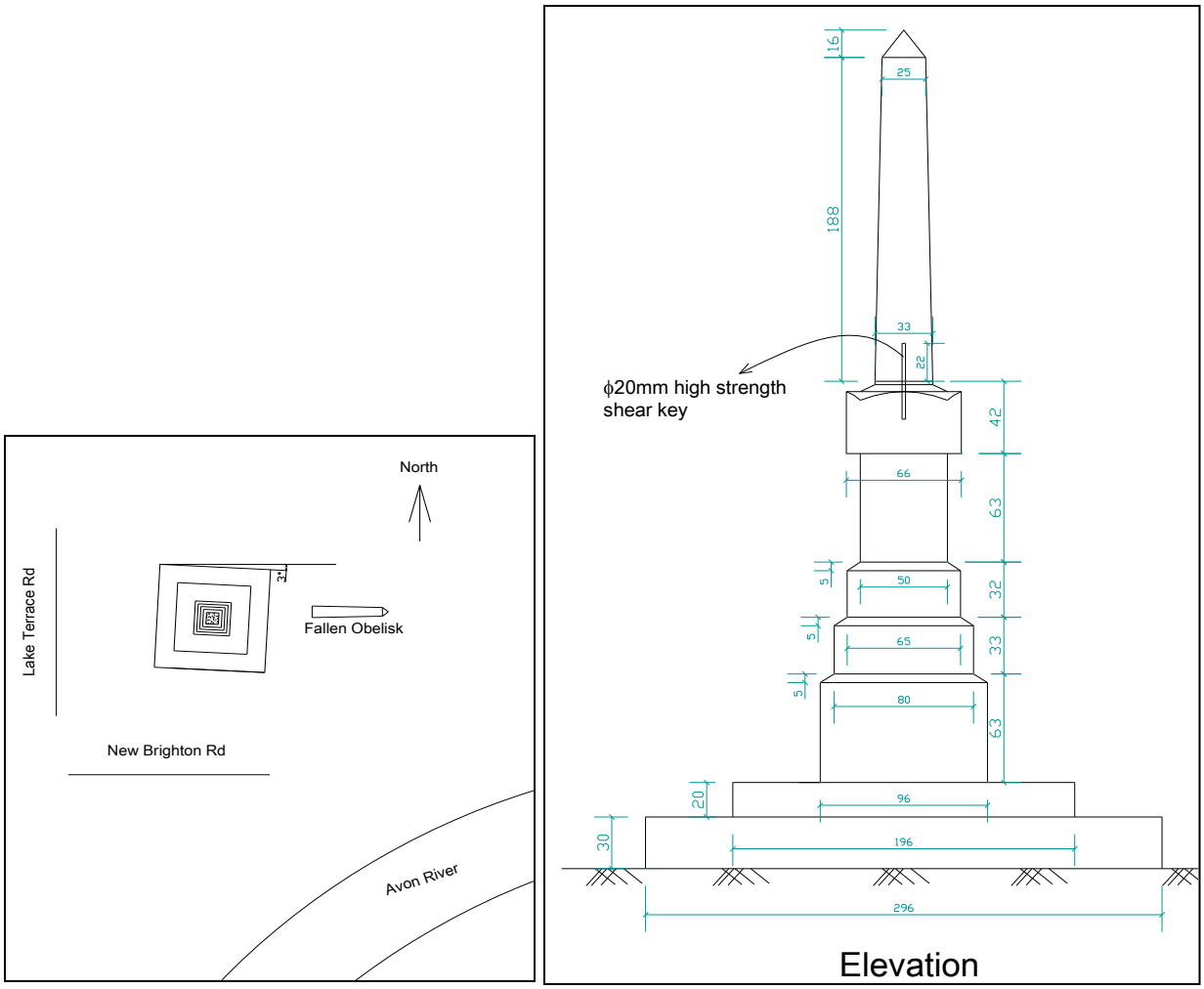

Figure 2.57. Elevation of the marble monument along Avon River, relatively close to the HPSC recorder.

2.2.8. Lyttelton Port Company (LPCC)

LPCC seismic station is situated in Lyttelton Port at the edge of the Port Hills., above 2-3 m of soil. It is considered an outcrop record, which is justified by its high frequency content. Details about the site reconnaissance are given in Chapter 5.

Figure 2.58. Close plan view of LPCC seismic station site. Lyttelton Port at the southern part of Port Hills.

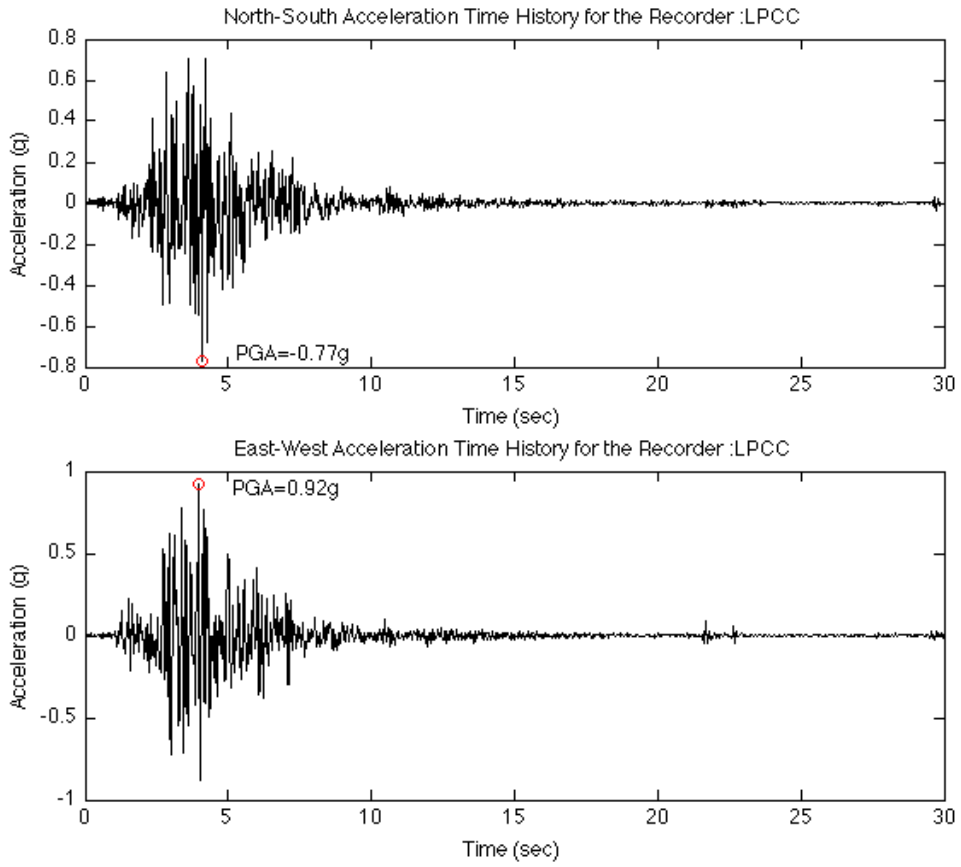

Figure 2.59. Acceleration time histories in NS-EW directions recorded at LPCC station.

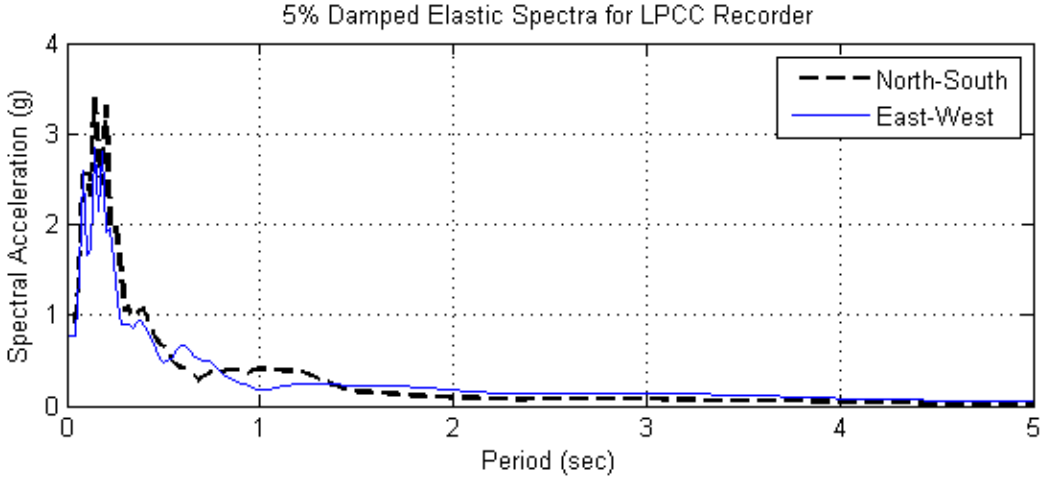

Figure 2.60. Acceleration spectra in NS-EW directions of ground motions recorded at LPCC station.

2.3. STRONG MOTION RECORDS VERSUS LIQUEFACTION

The predominant geotechnical characteristic of both earthquakes events was liquefaction and lateral spreading. The Darfield earthquake caused significant liquefaction with evident signs of surface manifestation mostly in the eastern suburbs of Christchurch along the Avon river such as Avonside, Dallington, New Brighton and Bexley (Cubrinovsky et al., 2010). The CBD was much less affected by liquefaction. The subsequent Christchurch earthquake did not only re-liquefy the previously mentioned areas, but caused a more widespread liquefaction which also affected the southern suburbs and the CBD (Figure 2.61 and 2.62). In particular, liquefaction in CBD was demonstrated by numerous sandboils formed in the perimeter of buildings and the large amount of sand emerging on to the surface.

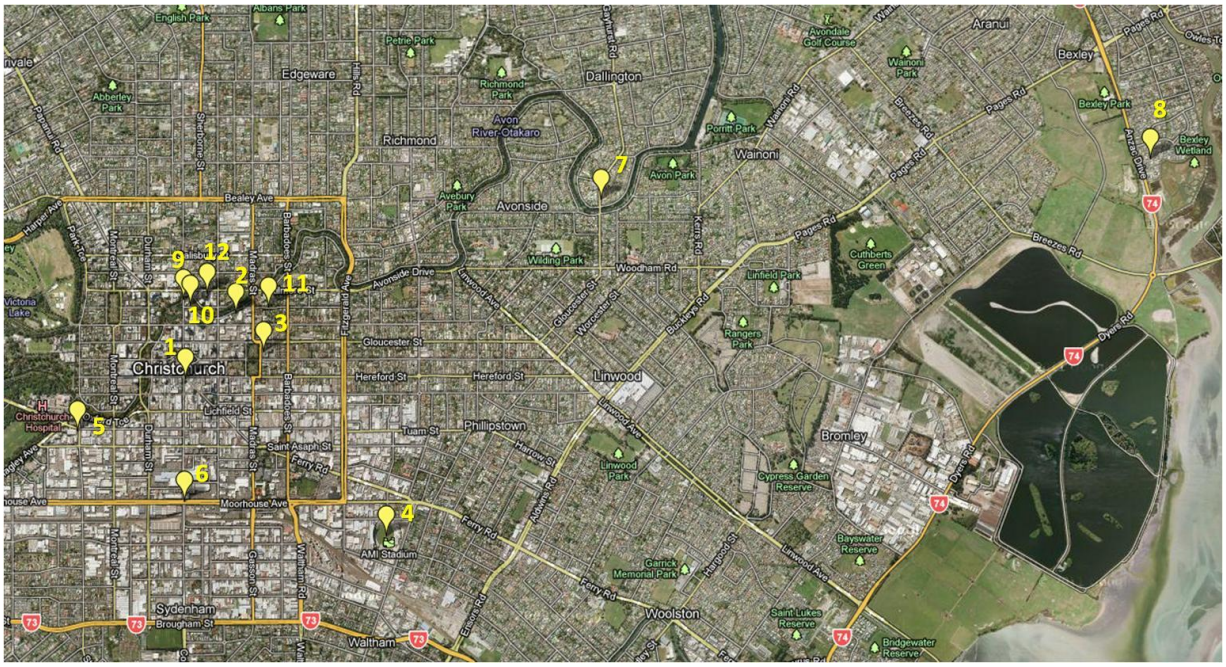

Figure 2.61. Map pointing indicative liquefied sites corresponding to the photos in Figure 2.62.

Figure 2.62. Photos of liquefied sites after Christchurch earthquake.

After Darfield earthquake several borehole tests were conducted covering a broad area of the eastern suburbs of Christchurch in order to investigate in detail the properties and the layering of the soil (Tonkin & Taylor LTD, 2011). The soil practically consists of layers of silty sand and clean fine to medium sand, with the ground water level reaching almost the ground surface (0.3 - 2.5m deep). The SPT and CPT values indicated very low cyclic shear resistance especially for the first 10m of soil. This suggests that the upper layers were those that mostly liquefied and explains why so large amount of sand reached the ground surface. Moreover, grain size distributions curves were produced for soil samples taken by Dallington and Bexley areas by sieve and hydrometer analyses after Darfield earthquake (Cubrinovski et al., 2010). Their range

is depicted in Figure 2.63 and is compared with equivalent ranges from Adapazari, Niigata and Kobe areas which area believed to have sustained liquefaction in past earthquakes. All these facts explain the extensive liquefaction occurrence during the two earthquakes and especially the second one with significantly higher PGAs.

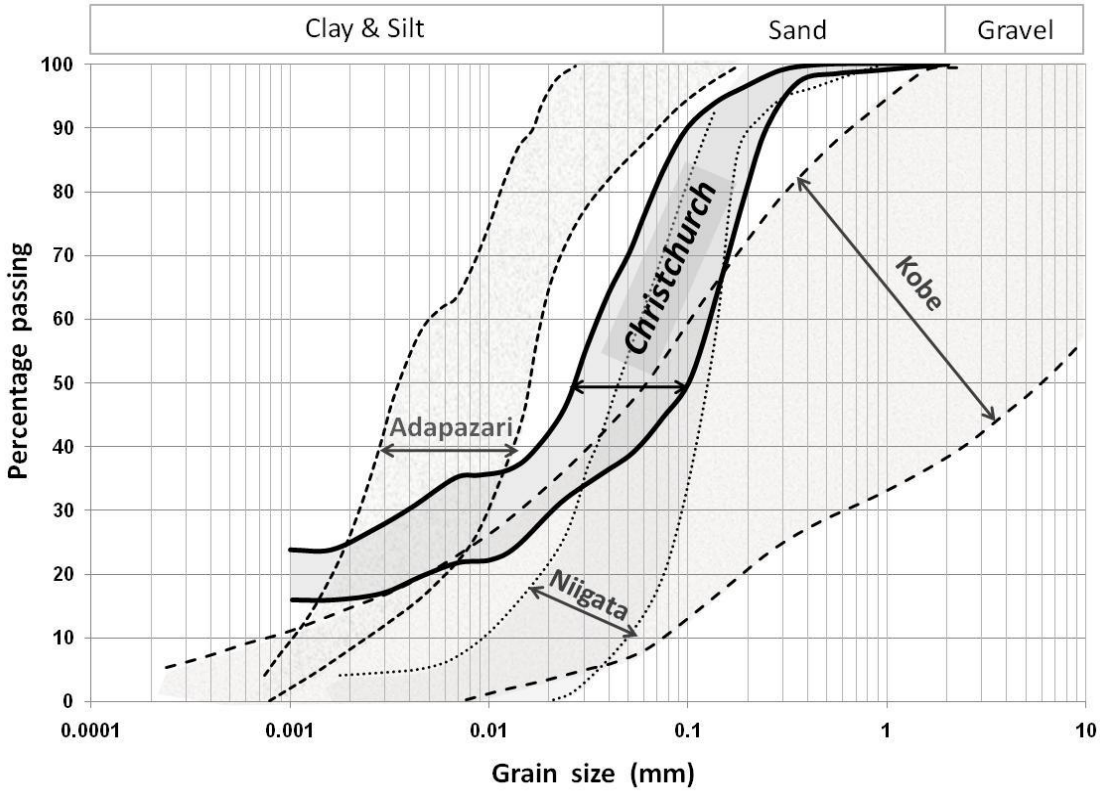

Figure 2.63. Range of grain size distribution curves of soil samples from Dallington and Bexley areas after Darfield earthquake (Cubrinovski et al., 2010), compared with curves from Adapazarı, Niigata and Kobe areas which have sustained liquefaction in past earthquakes.

Thanks to a dense network of seismographs covering the broader area of Christchurch (Figure 1) a large number of ground motions were recorded during the Christchurch February 2011 earthquake. The CBD area includes four seismic stations, i.e. CBGS, CCCC, REHS and CHHC. These ground motions may not have been the strongest ones recorded in terms of PGA values, i.e. compared to HVSC record; however, due to certain features, their effect on structures or soils was detrimental.

There is a certain variation in the recorded acceleration time histories in CBD, all depicted for comparison in Figure 2.64. For instance, the range of PGA values varies within a factor of 2, from 0.34g (CHHC-NS) to 0.72g (REHS-EW). A dominant common trend in all records affected by liquefaction is: initial lower period cycles with increasing acceleration values up to a threshold

value after which liquefaction occurs. Thus, long period cycles develop with acceleration cut-off. As explicitly explained by Smyrou et al. (2011):

"Soil softening due to excess pore water pressures in combination with sufficient acceleration values has led to amplification of large periods affecting a broad category of structures, as indicated by the acceleration spectra. Especially, the spectral amplification at periods exceeding 2 sec is attributed to the fact that once liquefaction has occurred, the overlying soil 'crust' oscillates with very low frequencies, causing the bulges observed in the acceleration spectra for periods of about 3 sec (see Youd and Carter (2005) for similar observations from the then available liquefaction-affected acceleration spectra). In addition to structural damage due to high spectral accelerations, important soil-related failures have directly affected houses and bridges."

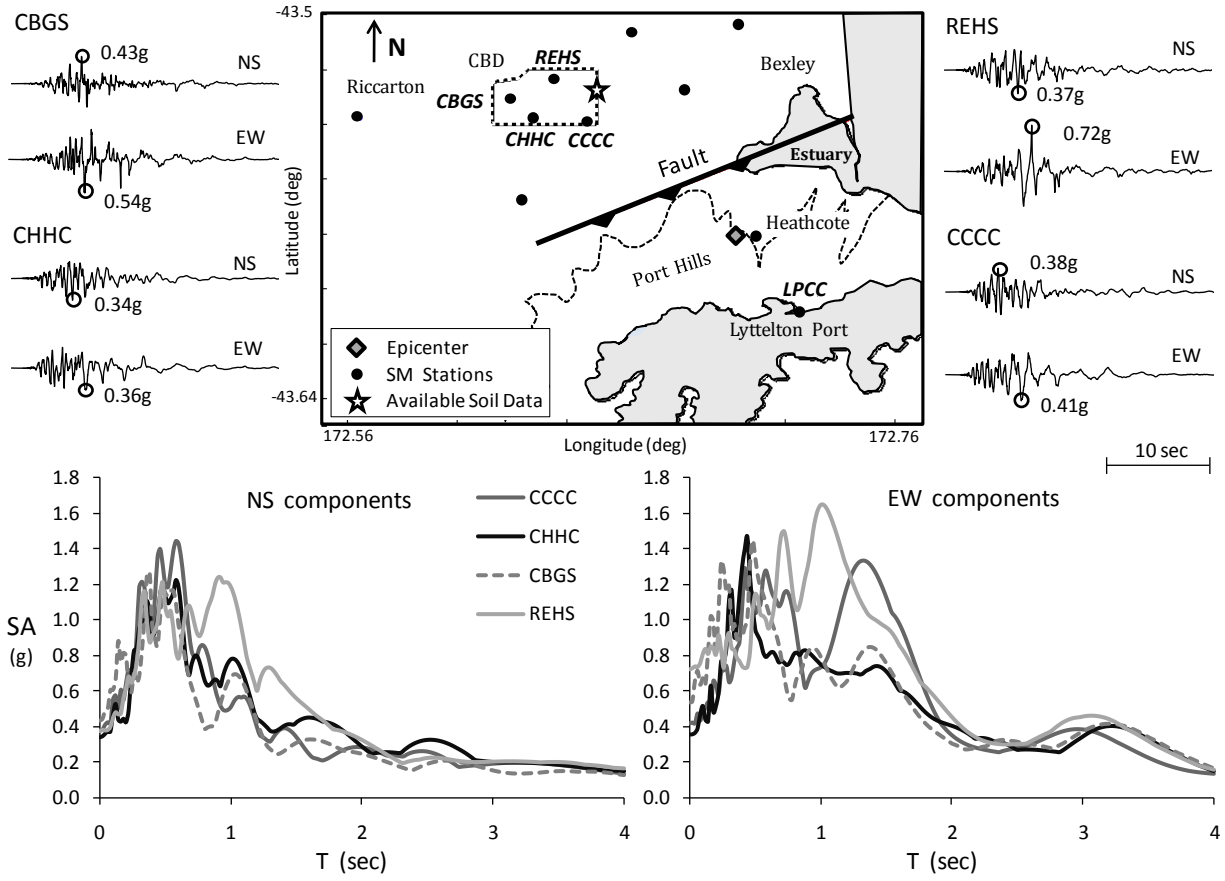

Figure 2.64 Map of the Christchurch broader area showing the intersection of the fault plane with the ground surface (from GNS Science), the location of the accelerograph stations, the epicenter, and the location with available soil data. Acceleration time histories and spectra of four CBD (Central Business District) seismic stations for NS and EW directions. Source: Smyrou et al., 2011.

Moreover, an advanced effective stress site response analysis has been performed by Smyrou et al. (2011), with LPCC as the input motion, in order to obtain a better insight on the soil response mechanism discussed above. Analysis approached effectively the reality. The comparison between the analysis and the real record, in terms of spectra, is depicted in Figure 2.65.

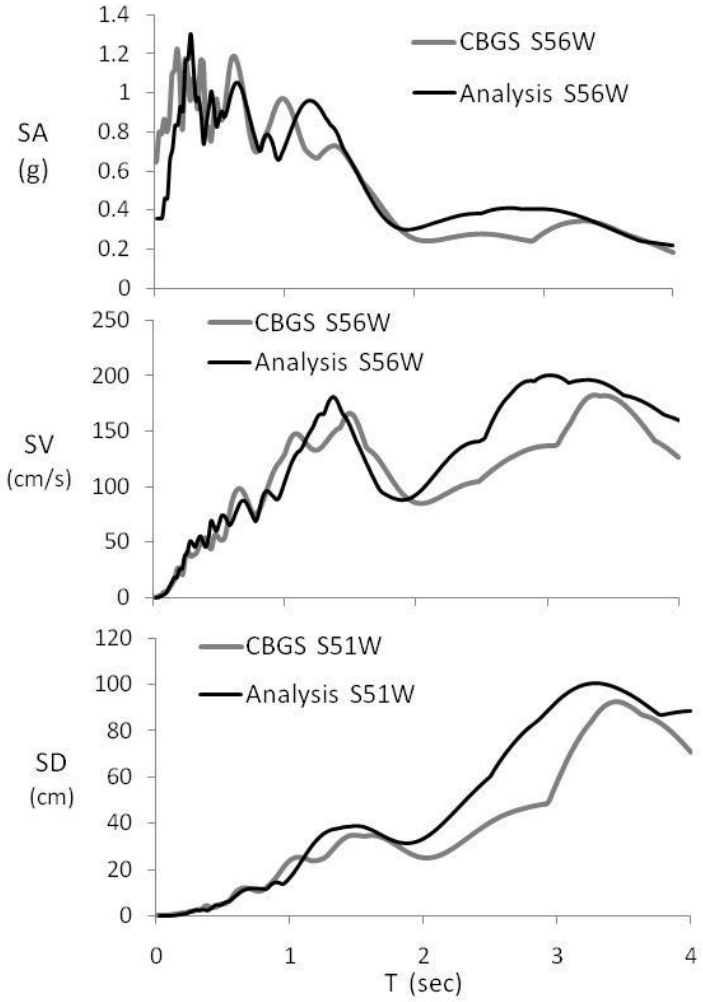

Figure 2.65 Comparison of 5%–damped spectra between CBGS record and analysis. Source: Smyrou et al. (2011).

Last, it should be mentioned that the strongest direction of all aforementioned records is the East-West, taking into account the PGA values, as well as the spectral amplification. This is key-feature towards the explanation of many structural failures discusses in the following chapter. The strong direction in Heathcote Valley seem to be different than the direction of the other records, something that may be attributed to the hanging-wall and foot-wall effects.

Chapter 3:

STRUCTURAL DAMAGE IN CBD

3.1. INTRODUCTION

This Chapter of the report is related to the observed damages in CBD (Central Business District) of Christchurch. The observations are both structural and geotechnical. A part that describes the damages in Soil-Structure Interaction (SSI) terms has also been included due to the significance of the topic for that particular event.

Fortunately, CBD consists of a grid system of streets that makes the descriptions rather easy. Several routes have been investigated in CBD during the visit of the authors to the site and these routes have been identified by using different colors, as given in Figure 3. 1.

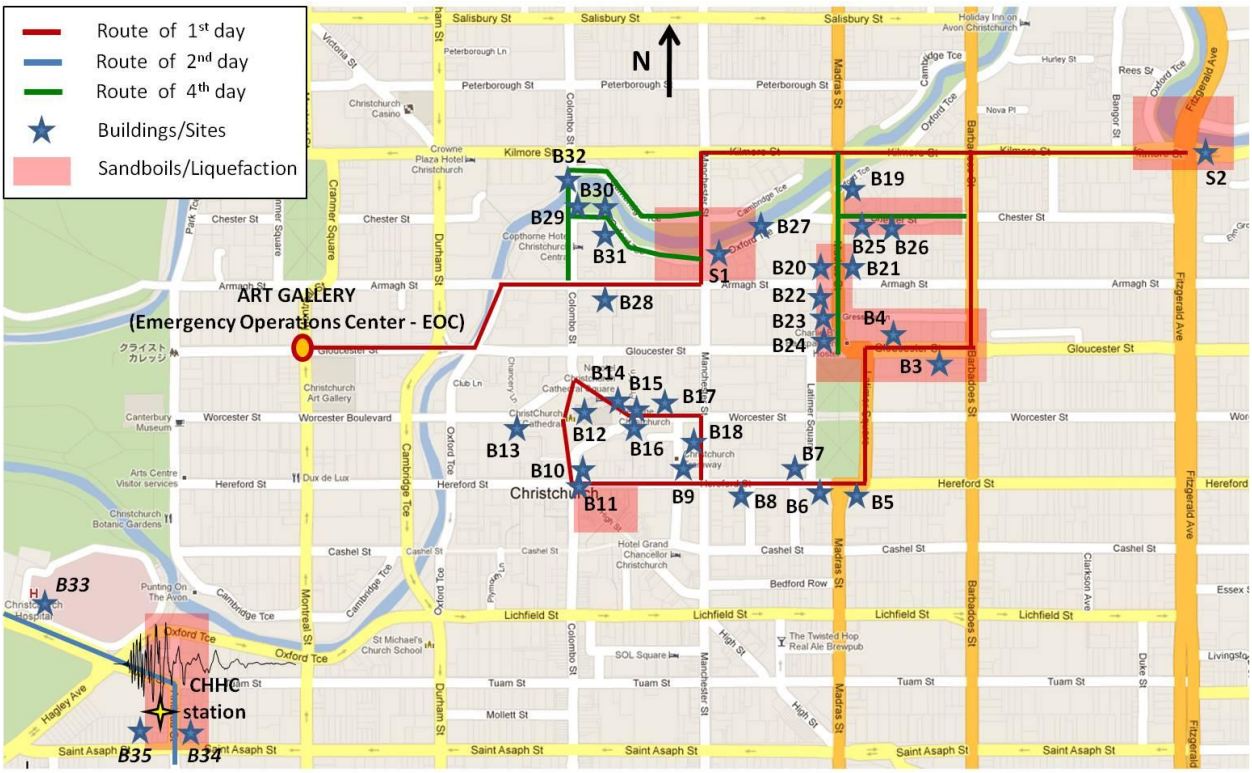

Figure 3. 1. Red, blue and green routes followed in CBD and the spatial distribution of structural damages and building sites.

3.2. THE RED ROUTE

- **Armagh St & Oxford Terrace**

The old bridge on Manchester Street, crossing Avon River and Oxford Terrace, did not have any major damage but it suffered slight rotation of abutments due to lateral spreading, road cracks at the edges of the bridge. A nearby small park with lots of sand boils and large amount of sand made liquefaction clear.

Fitzgeral Bridge has suffered some significant abutment rotation due to major lateral spreading. Piles appeared due to subsidence of lateral movement of ground soil. The most of the damage was caused by the Darfield Earthquake, 2010.

Details for the bridges will be explained in Chapter 4 of this report.

Figure 3. 2. Bridge at Oxford Terrace (left) and rotated abutment of Fitzgerald bridge (right).

- **Manchester Street**

Manchester Street consists of several unreinforced masonry buildings, most of which has suffered out-of-plane failure of the perimeter walls (see Figure 3. 3 and Figure 3. 4).

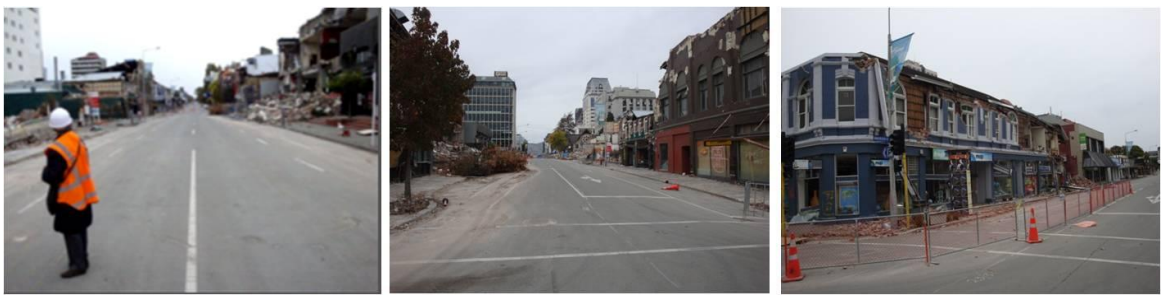

Figure 3. 3. View of Manchester Street.

There is difficulty in identifying any connection between the bearing system and the external walls, resulting in the out-of-plane collapse of the latter, probably due to incompatibility of deformation.A type of composite slab that combines wood flooring with iron or steel beams was observed in most of the unreinforced masonry buildings (Figure 3. 5).

Figure 3. 4. Damaged buildings at Manchester Street.

Figure 3. 5. A composite slab found at Manchester Street.

- **Gloucester Street towards Latimer Square**

In this part of the route, liquefaction was evident almost everywhere, tons of sand coming out of the boundaries of buildings. The area is not densely built and there are lots of free fields around. The building stock consists of low-rise structures in general. There were timber frame houses along that route which extensively damaged (see Figure 3. 6). A timber hostelbuilding with a very heavy external wall was collapsed. The hostel building also had tilting due to differential settlement of the soil (Figure 3. 7 and Figure 3. 8).

The generally satisfactory performance of most wooden structures can be attributed to their inherent flexibility. However, the lack of an appropriate lateral system of resistance led to failures such as the one shown in Figure 3. 6 in which a soft storey mechanism was formed, resulting in considerable residual displacements.Old-style timber bearing systems found in the area lack diagonal stiffening elements and moment-resisting joints at floor levels, causing formation of hinges. The modern timber structure (as shown in Figure 3. 9), some of which were found under construction; seem to be designed to resist lateral loads specifically, a fact that is confirmed with low level of damage in modern timber structures.

Figure 3. 6. Collapsed wooden residence at Gloucester St.

Figure 3. 7. Collapsed Stonehurst Hostelat Gloucester Street.

Figure 3. 8. The heavy external wall and the slab detail of the collapsed Stonehurst Hostel.

Figure 3. 9. Typical modern wooden structure under construction.

- **Hereford Street towards Cathedral Square**

No evidence of liquefaction was observed in this part of the route. Severe structural damage on masonry buildings was observed. Shear failure of masonry piers in orthogonal directions, X-shape cracks, rotation of piers and out-of-plane movement of walls were the major problems (from Figure 3. 10 to Figure 3. 16).

Buildings with similar structural pattern in EW and NS axes exhibited different level of damage in the two directions. The level of damage along the EW direction was consistently higher as observed in several buildings in CBD, which they were mostly affected in their EW side though their structural system was similar in both axes.

Figure 3. 10. Building at Hereford and Madras Streets.

For example, the building in the corner of Hereford and Madras Streets bore serious structural cracks in the EW direction (along Hereford St), while in NS direction there were damages of non-structural elements primarily (Figure 3. 10). In the damaged direction of that building, characteristic shear cracks in the joints, considerable movement resulting in the fall or detachment of non-structural elements, wide cracks in corner column, and rigid body movement of decorative one-piece column are the main observations regarding the damage.

Similarly to above, the building at Hereford St and Latimer Square exhibits major shear cracks in the EW direction, while in the NS direction has suffered limited damage compared to the opposite direction (from Figure 3. 11 to Figure 3. 13). Damages in that building are due to the existence of squat piers in the corners of rectangular openings. The situation is deteriorated by the repeated pattern of semi-circular arches resting on short columns that practically cuts the entire floor.

Figure 3. 11. Building at Hereford St and Latimer Square – EW direction

Figure 3. 12. Lateral displacement of columns in the EW direction.

Figure 3. 13. Building at Hereford St and Latimer Square – NS direction.

Massive decorative elements, badly connected to the buildings as shown in Figure 3. 14, caused loss of life during the earthquake.It should be noted that such elements' fall is due to high accelerations, that is why those in the NS side (normal to the strong component of the earthquake) are affected mostly, while the damage in EW side is primarily structural. A characteristic case of failure of non-structural elements is collapse of a massive perimeter beam element which was not structural, as shown in Figure 3. 15, constructed using bad quality concrete and reinforced with insufficient in number and area bars. That beam collapsed during the shaking and caused 1 casualty.

Figure 3. 14. Massive decorative element disconnected from the main body of the structure.

Figure 3. 15. Insufficient reinforcement, low quality concrete and bad application caused collapse of a decorative beam and 1 casualty.

The high accelerations induced by the earthquake, as recorded by the four stations in CBD, led to out-of-plane failures of the external leaf of masonry walls that were detached from the usually wooden frame of the structures (Figure 3. 16). After the earthquake the support of whole side of some masonry structures was needed in order to avoid their collapse. However, the overturning of wall segments was deterred in several cases with the application of tie rods. Again, in most of the cases, the out-of-plane movement of the facade occurred towards East.

Figure 3. 16. Out-of-plane failures around Hereford Street.

- **Stewart Square and Cathedral Square**

Liquefaction was evident around Stewart square with sand on the surface and cracks on the sidewalks. Old masonry buildings had significant damage and partial collapse (Figure 3. 17). A monumental structure with a tower and a dome has partially collapsed (Figure 3. 18).

No liquefaction was observed in Cathedral Square. Severe structural damage of the church and nearby masonry buildings was observed. The last floor of the building (left side of Figure 3. 19) has collapsed at night during an aftershock. The building seen on the right side of Figure 3. 19 did not suffer any significant damage since it was successfully retrofitted before the shakings.

Figure 3. 17. Severely damaged building at Hereford Stwith characteristic shear cracks and historical building at Stewart Square.

Figure 3. 18. Collapse of dome and view of the heavily damaged and partially collapsed Cathedral.

Figure 3. 19. Buildings in the Cathedral Square.

Figure 3. 20. Several historical masonry buildings, including the Cathedral, with significant damage.

As seen in and around Cathedral Square, many public buildings of Christchurch are masonry structures, the external leaf of which is constructed of characteristic grey stone during the first years of Christchurch (Figure 3. 20). They follow the British architectural style and construction of practice which was developed with no consideration of earthquake. Among of them the Cathedral Church, the most emblematic building in Christchurch is referred. These structures exhibited striking consistency in the type of failures observed, fact that indicates that these structures have certain weaknesses (i.e. weak buttresses, lack of tie rods etc) in their structural system which were revealed during earthquake and led to the partial collapse of most of them.

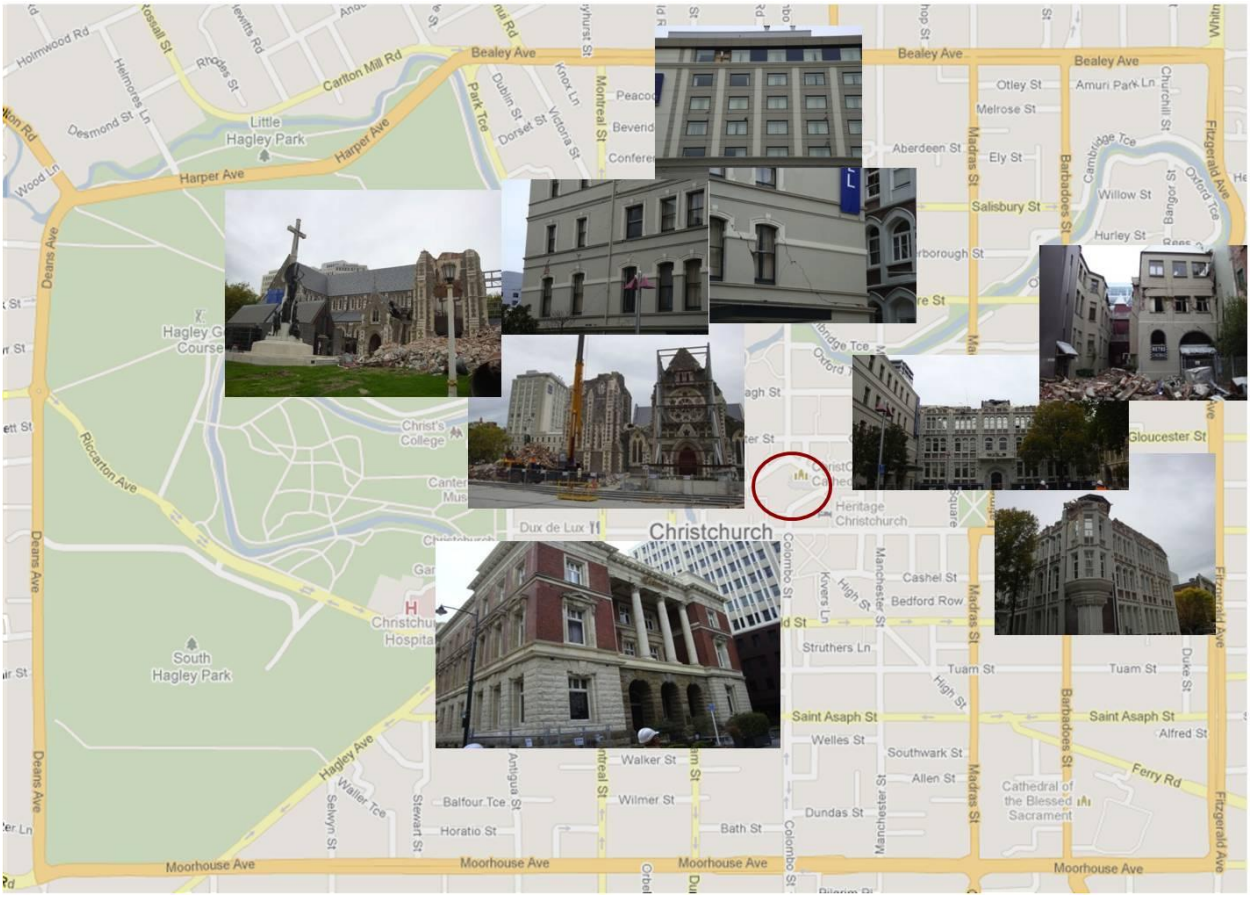

Figure 3. 21.Buildings around the Cathedral Square.

Pounding effect was also observed in CBD, among structures with varying height and stiffness. Large ground deformations might have also helped pounding of adjacent structures (Figure 3. 22).

Figure 3. 22. Observedpounding effect in CBD.

An emblematic building of the city, Grand Chancellor Hotel, had failure of one of the ground floor shear walls leading thus to progressive failure in the floors above. The building is the tallest in the city with 26 storeys and 85m height. Grand Chancellor exhibited severe damage and more than 1m residual top displacement, rendering it unusable. A safe region around the Grand Chancellor Hotel was close to any access even by the search and rescue teams, due to the high level of danger associated.

Figure 3. 23. Views of the Hotel Grand Chancellor.

3.3. THE GREEN ROUTE

- **Madras Street and Around**

Figure 3. 24. Buildings (B20 left and B22 right) damaged due to differential settlements induced by liquefaction.

Figure 3. 25.Heavily damaged buildings at Madras Street.

Traces of liquefactions were obvious along Madras Street. Severe damage was observed in EAST-WEST direction once more. A six storey building (see the left building in Figure 3. 24) was extensive liquefaction, shallow foundation comprised of isolated footings with tie beams and perimeter grade beam, differential settlements in the range of 26cm, structural deformations. The building shown on the right side of Figure 3. 24 suffered a substantial settlement of the front side resulting in tilt of ~2 degrees. Uniform lateral displacement of 15cm towards the area of significant liquefaction near the right front of the building was observed. Both these buildings were considered uneconomic to repair and were (will be) demolished in the months following the 22 February 2011 earthquake. Other multi-storey buildings also suffered this type of damage, which in many cases was exacerbated by the 13 June 2011 earthquakes (Cubrinovski and McCahon 2011).

Due to the architecture of the commercial buildings in CBD, characteristic short column shear failure as indicated in by the diagonal cracks are common (Figure 3. 25).

Figure 3. 26. Sand boils after liquefaction and collapsed masonry structure at Madras Street.

- **Chester Street**

Figure 3. 27. Historical wooden structures at Chester Street.

Chester Street East has a series of historical timber houses sustained significant structural damage, plastic hinges to the columns of the ground floor, large deformations, liquefaction, large amount of sand covered the yards.Unfortunately, among the heavily damaged wooden

structures are the three out of four identical heritage residences in 86-100 Chester Street East, which were included in the as per 13/04/2011 demolition list.

- **Oxford Terrace**

ACC Building on 262 Oxford Terrace across Avon riveris very close to the river. The elevator tower suffered significant seismic load and was sheared horizontally creating a large crack. All things inside the building have fallen indicating high levels of accelerations.

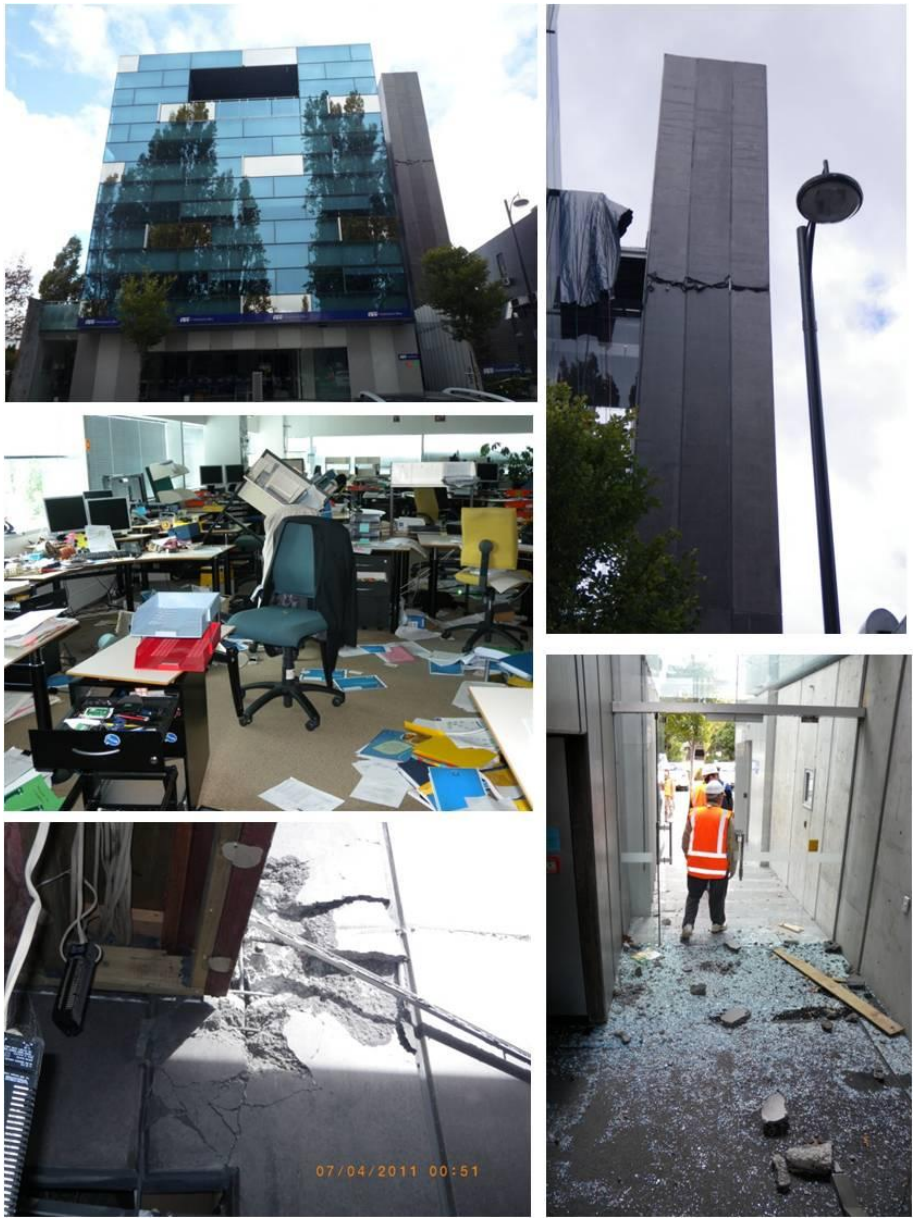

Figure 3. 28. ACC building.

One reasonable explanation of the failure of the cantilever wall at the side of ACC building may be that the displacement profiles along the height of a frame and a cantilever wall structure considerably differ, however, in a frame-wall structure the diaphragms at floor levels, rigidly linking frames and walls, ensure common displacements. Due to the presence of frame the drifts of the cantilever wall, expected to be maximum at the top height, are limited. Nevertheless, in the case of ACC building the lack of a connecting link at the top is suspected to have been the reason for this displacement incompatibility between cantilever wall and frame, with the latter restraining the displacements of the former at all levels but for the one at the top, leading to wide crack at the immediately lower level.

- **Forsyth Barr Building**

Forsyth Barr Building is one of the tall structures of the city. The stairs in the first three floors fell down during the earthquake trapping people upstairs since there was no other means of passage. The stairs were fixed on top and rebars were inserted inwards the floor slab. The other side of the stairs, the lower part, was simply sitting on the slab but obviously the sitting length was not sufficient (**Error! Unknown switch argument.** and Figure 3. 30).

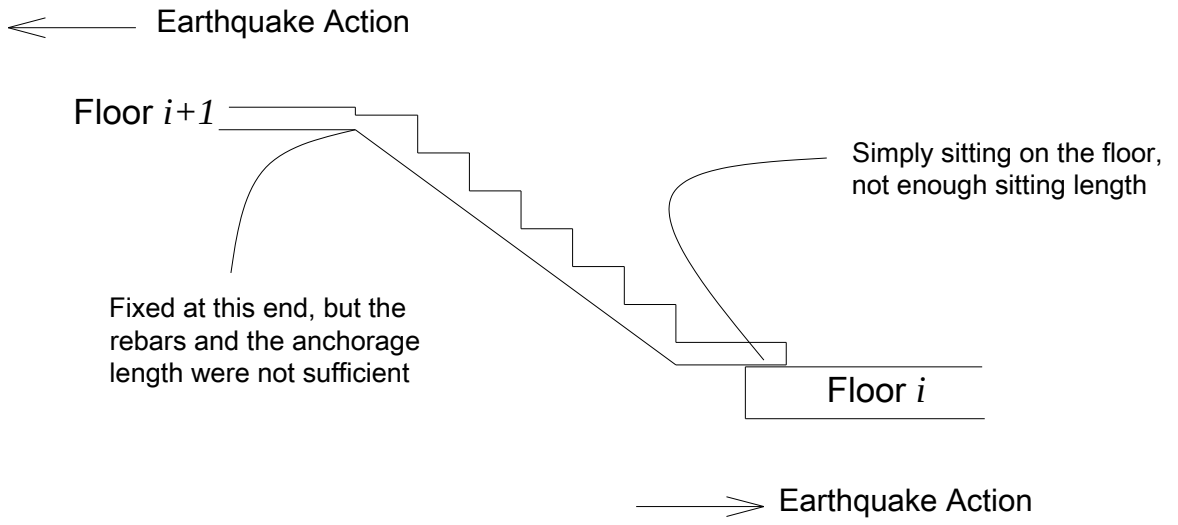

Figure 3. 29. Collapsed stairs of the Forsyth Barr Building.

Figure 3. 30. Damage in the Forsyth Barr Building and its collapsed stairs.

- **Colombo Street and Oxford Terrace**

Colombo Street and Oxford Terrace are along Avon River where liquefaction is evident everywhere and large ground deformations due to liquefied soil and lateral spreading are common. Wide and deep cracks on the ground along the river bank were observed. There is a crust of clay 0.5 m thick on the surface. Usually the bottom of the river is covered with gravels but it is now filled with sand. The river is now more shallow (15 cm), which means that large amount of sand came up to the surface.

Lateral spreading of the river banks is restrained in the locations of bridges with rigid body. Spreading is limited by the abutments. The old bridge on Colombo Street, crossing Oxford Terrace, had significant buckling due to lateral spreading but the bridge is still operational (Figure 3. 32).

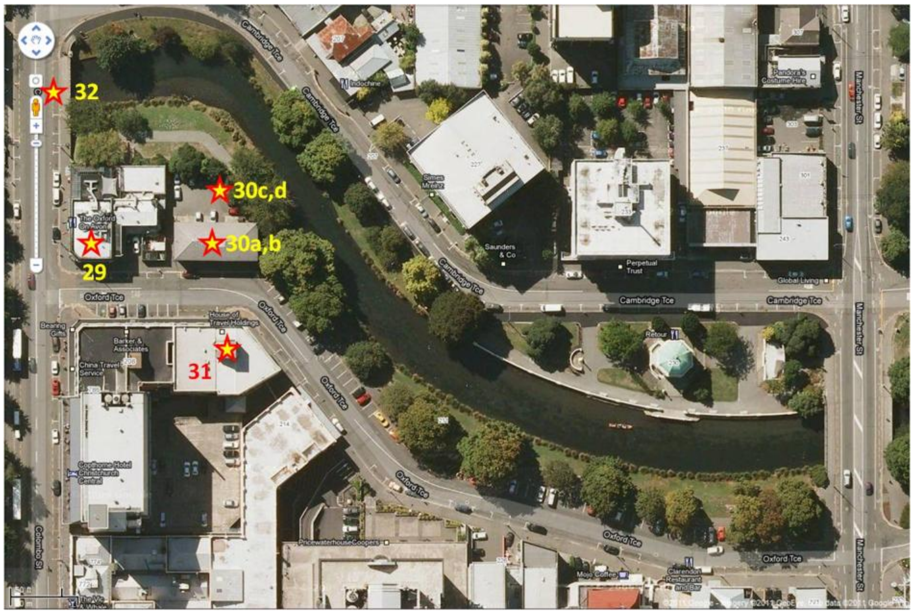

Figure 3. 31. Colombo Street and Oxford Terrace.

Figure 3. 32.The old bridge at Colombo St and Oxford Terrace.

An old masonry building (B30) and a reinforced concrete building (B31) were subjected to large ground deformations that caused tilting of the structure and differential settlements (Figure 3. 33 and Figure 3. 34). As firemen reported, there was increase of cracks days after the earthquake causing further damage (B31). Wide cracks and opening of expansion joints are attributed to phenomenon of lateral spreading.

Figure 3. 33. Building at Colombo St and Oxford Terrace (B30).

Figure 3. 34.River bank at Oxford Terrace and the nearby building (B31).

- **Kilmore Street**

The building shown in Figure 3. 35was constructed on piles. 30-35 cm settlement was observed due to liquefaction. The ground subsided where the cars were parked, the columns founded on piles did not settle, no significant structural damage was observed. Major structural damage of the superstructure was prevented thanks to deep foundation type.

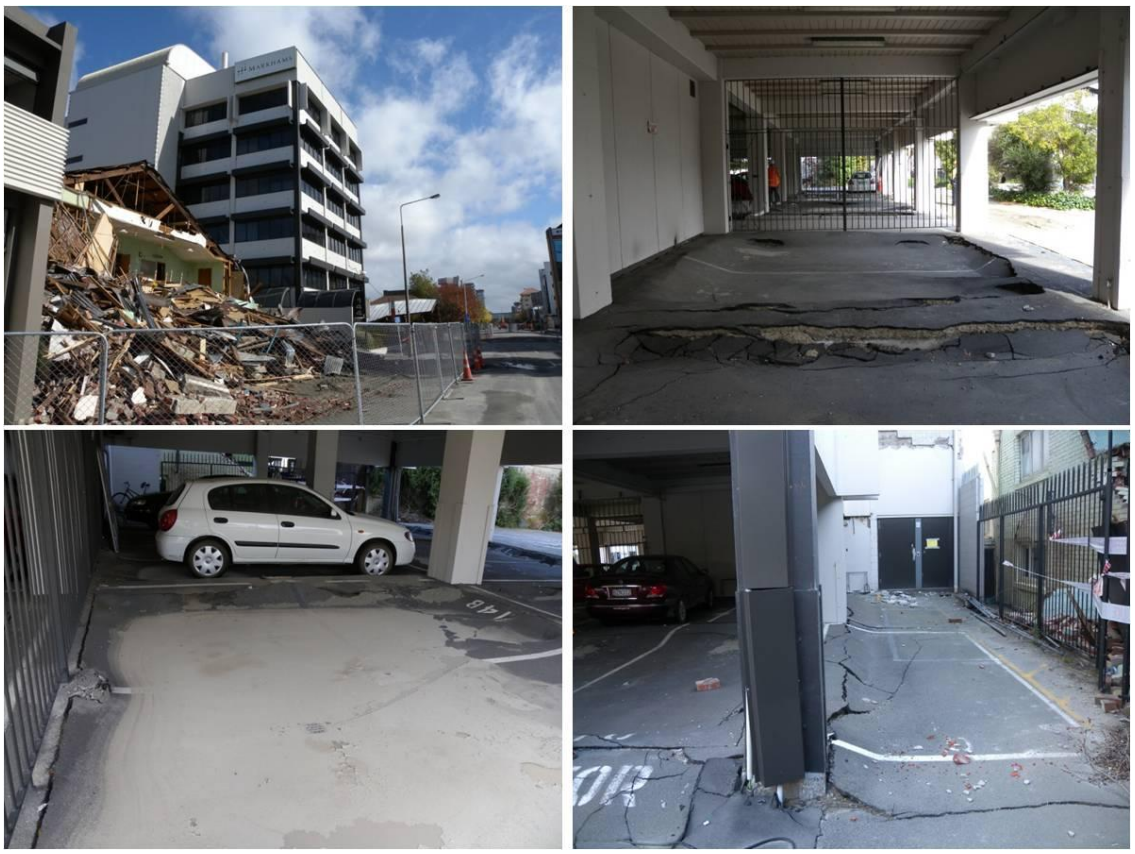

Figure 3. 35. A RC building on piles (B33) with large soil settlements and insignificant damage.

Another modern RC building at Kilmore Street, shown in Figure 3. 36, had no differential settlement though liquefaction was evident. Sand came up at the perimeter of the building but no bulging or sand-boil was observed inside the building. A large crack of ground and side walk was observed in front of the main entrance but no structural damage or shattered window glasses were witnessed.

Figure 3. 36.A modern RC building at Kilmore Street with raft foundation.

3.4. THE BLUE ROUTE

- **Hospital Staff Car Park**

Staff Car Park of Christchurch hospital is one of the structures with moderate to significant The structure consists of eccentrically braced frames (EBFs) where prefabricated beams and columns form a continuous frame. The slabs are also prefabricated, wood members with prefabricated RC joists and a topping concrete, a common construction practice in New Zealand. The damage was concentrated on 2 bracings and one column on the ramp. The bracing that had a severe failure at the zone, which connects the top beam profile to the diagonals, had a construction error (the flange of the diagonal profiles were not placed aligned with the ribs of the beam-diagonal joint).

The building is 10-20m from the CHHC recorder across the street. It is known that the CHHC records exhibited some acceleration bulges caused by liquefaction. The liquefaction was also observed on site, especially inside the car park (Figure 3. 37). There was a bulging of ground, inside the building, due to liquefaction. Signs of sand-boilsand bulges on the sidewalks are also evident. Formation of bulges in the car park was restrained by the wheels and bottoms of the cars parked during the earthquake as the traces of car wheels show.

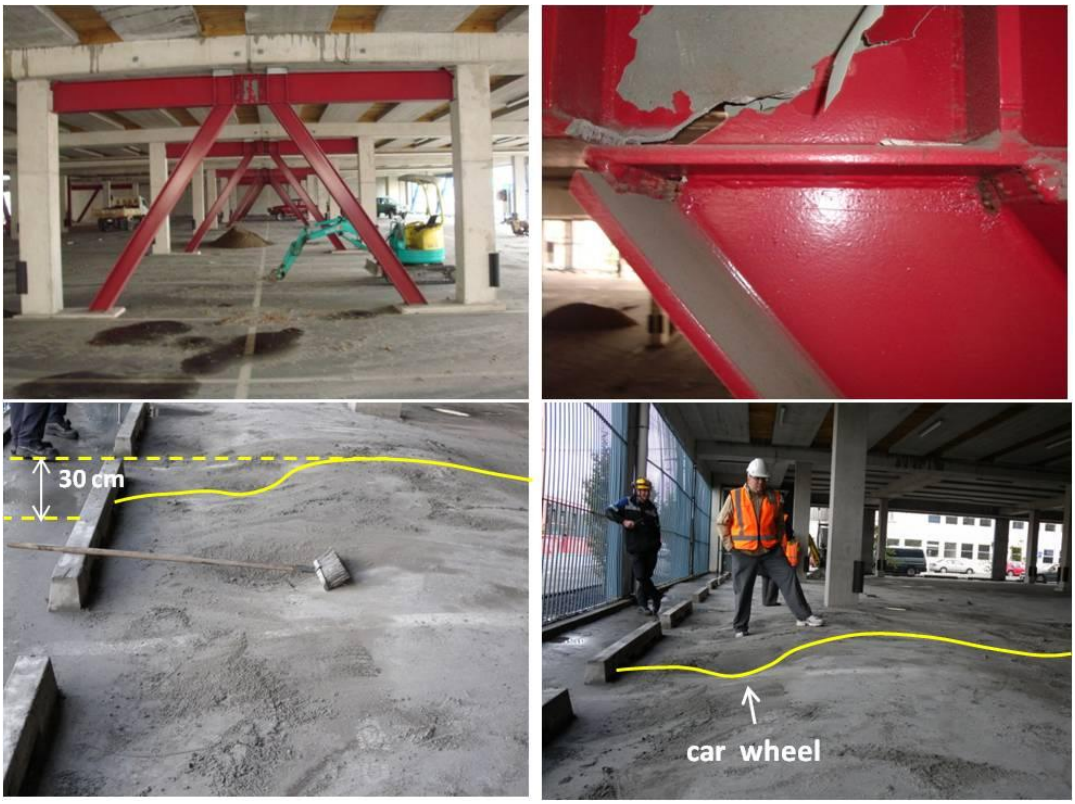

Figure 3. 37. Hospital Staff Car Park (B34).

- **Utility Buildings of the Hospital and the Chimney**

A tall RC chimney was found with no significant damage, next to the building where the acceleration recorder is installed (CHHC station). The integrity of the structure was checked after the first earthquake. The inspection showed no damage on the chimney. The utility buildings of the hospital did not suffer any significant damage as well.

Figure 3. 38. A tall RC chimney next to the CHHC recorder (B34).

- **Women's Hospital**

The newly built Women's Hospital is integrally linked to the existing central hospital facilities to provide effective interaction (Figure 3. 39). The building is planned in 2100 m^2 floor area and over ten floor levels, siting on an already busy hospital site adjacent to Hagley Park. The superstructure was also constructed with upmost concern of aseismic design. The structure has several steel bracings (Figure 3. 40), to decrease the effects of the shaking and the rest of the RC frame was built by implementing the ductile design rules. Thanks to the aseismic design, the operation of the building did not interrupt during any of the earthquakes.The unreinforced masonry building next to the Women's Hospital (Figure 3. 41), for example, suffered moderate level of damage due to the same shaking.

The hospital is a 10-level (including 2 underground levels). It has been completed and opened on May 2005 after two years of construction. It has been designed for 2000-year return period earthquake. It has over 2000 sqm of space. 10000m^3 of concrete and 1100 tons of reinforcing steel were used for the construction. The structure is designed to be able to move up to 45cm to any direction.

Women's Hospital was base-isolated by using 41 lead rubberrubber bearings (Figure 3. 45) of 800mm diameter (Oiles Corporation), 4 sliding bearings (double-curvature sliding mechanism) of 700mm diameter (Figure 3. 43), 9 smallersliding bearings, and anchorage cables (Figure 3. 45). The stressing strands are connecting the building to the 1.6m thick basement slab so it would not bounce in an earthquake.

Non-structural details such as building separation joints, outside drainage channels, life-line cable passages and staircases (from Figure 3. 44 toFigure 3. 48) were organized to prevent non-structural damage during the differential movement the isolated floor and the superstructure.

The bearing of the hospital had 25mm residual displacement after the September 2010 Darfield Earthquake of M_w= 7.1, and they were almost perfectly placed back during the Christchurch Earthquake of February 2011 (M_w=6.3). The local responsible engineer reported that the isolators experienced maximum of 10cm displacement during the Darfield Earthquake. There was no evidence of liquefaction inside and in the perimeter of the Women's Hospital.

Figure 3. 39. General view of the Women's Hospital

Figure 3. 40. Eccentrically placed steel bracing in the superstructure of the Women's Hospital.

Figure 3. 41. The old unreinforced masonry block for nurses, that has moderately damaged during the earthquake.

Figure 3. 42. Rubber bearing (left) and the restraining ground anchorage.

Figure 3. 43. 700mm diameter sliding bearings (double-curvature sliding mechanism).

Figure 3. 44. Detail of the staircase that connects the isolated floor with the rest of the building (the sitting part of the stairs is allowed to slide freely)

Figure 3. 45. Slab-beam detailing to allow the lifeline cables to slide freely.

Figure 3. 46. Non-structural detailing in Women's Hospital to allow differential displacements due to the isolators.

Figure 3. 47.Gap allowance in the perimeter of Women's hospital.

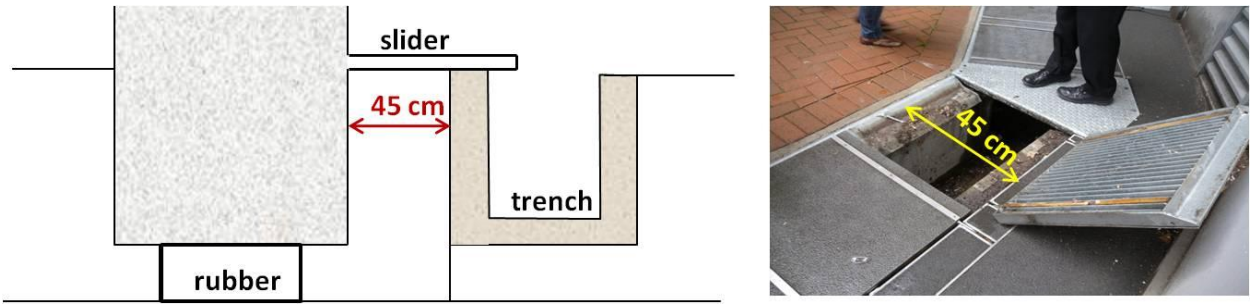

Figure 3. 48. Gap allowance in the perimeter of Women'shospital.

3.5. EFFECTS OF THE EARTHQUAKE ON PARTICULAR STRUCTURAL TYPES

As opposed to the European building stock, the structures in New Zealand exhibit a great variety. Structures built with wood and masonry constitute around 80% of the building stock (Uma at al., 2008). Christchurch in particular has many single storey or 2-storey masonry and timber residential buildings outside the Central Business District (CBD) and very few modern RC high-rise buildings (Figure 3.49). The building composition in the CBD differs from the rest of the city with medium-rise modern steel and RC structures, as well as mid-rise unreinforced masonry (URM) and timber dwellings and office buildings, some of which have historical value.

It can be said, very roughly, that the Christchurch City, outside of CBD, consists of relatively low-period structures, whilst the long-period structures are more common in CBD. This might be

one of the reasons of the high concentration of damages in the CBD area during the February 2011 earthquake. A preliminary study presented in this paper investigates the spatial distribution of the spectral amplifications of the recorded strong motions for several yield period ranges as explained below, noting that the period ranges examined have been chosen in accordance with the observed building characteristics of the region.

Figure 3.49.Characteristic timber (left), masonry (middle) and modern RC (right) structures outside of CBD.

3.5.1 Damage to Building Structures during the Darfield and Christchurch Earthquakes

Darfield earthquake inflicted severe damage to residential houses and infrastructure mainly due to soil liquefaction and lateral spreading. The damage was concentrated in areas close to major streams, rivers and wetlands throughout Christchurch and the town of Kaiapoi (Cubrinowski et al., 2010). All buildings were assigned a usability rating of green, yellow or red tag. Green indicted no limitation of access and usability, yellow signified restricted use only, while red meant that a building was unsafe and access was banned. According to the Civil Defence Council, 80% of the buildings inspected were tagged green, 14% yellow and 6% red, while no building collapse was reported. As for the unreinforced masonry structures, a preliminary assessment on approximately 600 such buildings (Ingham and Griffith, 2010) resulted in 21% of the URM structures to be assigned red, 32% yellow and 47% green tag.

As for the Christchurch earthquake, at the time of writing this paper the final statistics regarding the building safety evaluation were not yet available. However, as per 18th of March, the data by Civil Defence (Kam et al., 2011) referred to 3621 buildings checked within CBD, out of which 1933, 862 and 826 were posted red, yellow and green respectively. Being more specific, of the “red” buildings 19% were reinforced concrete structures, 14% timber structures and only 7% the steel buildings, which performed in general satisfactorily. The respective percentage for reinforced masonry structures was 16%, jumping to 62% for unreinforced masonry buildings, reconfirming the poor behaviour of such structures, most of which have been built following the dominant construction practice or earlier design codes. Insufficient detailing and bad construction techniques, mostly related to non-structural elements,

deteriorated the damage. Although the aforementioned data have come up before the completion of the 2nd level of building safety assessment and thus reflect the situation in CBD one month after the earthquake, they offer a representative picture of the extent and severity of damage in CBD

3.5.2. Correlation of Damage to Spectral Values

3.5.2.1.Estimation of Yield Period of Characteristic Structural Types

The yield period of a building refers to the stiffness at the point of yielding, which essentially signifies the limit beyond which the structure enters inelasticity and starts to experience substantial damage that may require structural repair.

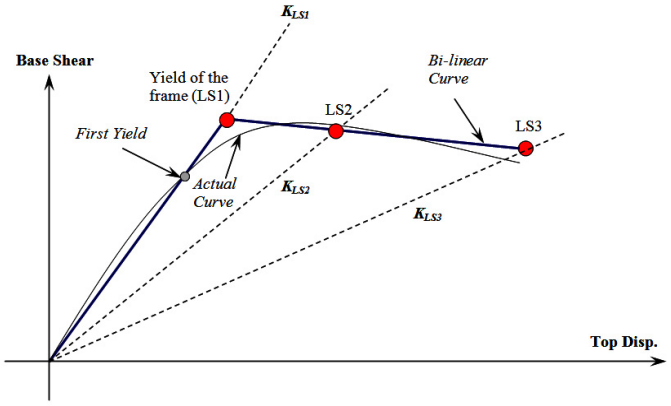

Figure 3.50. Structural response in base shear vs top displacement format, structural limit states and the bi-linearization process (by Bal et al., 2007).

A schematic representation of the characteristic limit states and the relevant bi-linearization of the system are given in Figure 3.50. A multi-degree-of-freedom (MDOF) system can be represented by an equivalent single-degree-of-freedom system (SDOF) precisely enough, as first suggested by Gülkan and Sözen (1974) and Shibata and Sözen (1976), as long as the equivalent SDOF substitute structure's characteristics are determined. An effort to define the yield period that corresponds to the K_{LS1} is made in this study aiming to have an overall idea about the spatial distribution of the damage.

Only two structural types have been considered in the preliminary analyses presented. The first group is the typical mid-rise RC structures in the city, most of which have been built with RC walls around stairs and elevator shafts (Uma et al., 2008), a situation also observed in European building stock (Bal et al., 2007). Studies by Vuran et al. (2008) and Enrique (2010) on such structures, where RC walls have not been built with the primary concern of earthquake resistance, but in reality, nevertheless, they contribute to the seismic response, show that a period value as given in Equation (1) would be a fairly good approximation to the yield period of similar structures.

$$T_y \approx 0.075H \qquad (1)$$

where H is the total height in m. The yield period of a 6-storey representative structure with RC walls around the elevator shaft then becomes 1.36sec.

As described above, the majority of residential buildings in Christchurch consist of 1 to 2-storey unreinforced masonry buildings with timber floors and ceiling, thus, this group was also examined. A study by Bothara et al. (2007) on a representative laboratory structure suggests that the threshold drift limits describing slight, moderate, extensive and complete damage states are 0.1, 0.4, 0.9 and 1.3% respectively. The elastic period found in their study is 0.09sec in average for the two transversal directions. This elastic period, refers to the stiffness that corresponds to the drift limit of 0.1%, which defines the limit for the slight damage. If real-size structures with two floors and 2.8m storey height are considered, in conjunction with an assumed value of 0.6 (ATC, 1996) for the ratio of the force where the first crack occurs over the yield force, then the yield period can be calculated as 0.26sec.

3.5.2.2.Distribution of Spectral Values

The spectral values of acceleration and displacement for the two consecutive earthquakes have been computed and plotted in the contour maps shown below. Only the maximum of the EW and NS components are presented here due to space restrictions. A range of spectral values within a band of ±10% has been averaged in order to produce the following plots, noting that the values have been calculated per station and linearly interpolated among the stations, thus, the plots should be considered more indicative rather than definitive.

Spectral acceleration and spectral displacement plots given in Figure 3.51indicate that for the short period range where the low-rise timber and URM buildings fall into, the concentration of spectral amplifications occurs near the western end of the fault. This is somehow interesting sinceFigure 3.51 reveals a concentration of PGAs along the fault rupture line, implying that the motion right along the fault may contain mostly long period components. Another observation derived from Figure 3.51 is the displacement demand for the SDOF systems. Uma et al. (2008) claims that the drift limit state for URM buildings for the moderate damage is 0.4%, which is translated to a 0.012m displacement demand for an equivalent SDOF system, explaining thus the damage concentration of such structures in the Darfield area after the September'10 earthquake.

An interesting feature in Figure 3.52, in relation to the comments given above on Figure 3.51, is that the long period spectral amplifications appear more pronounced on the western end fault, a probable outcome of forward rupture directivity effects that affect the frequency content of the strong motion records with respect to the position and the site distance from the fault (Somerville, 2003). The spectral acceleration values in Figure 3.52 highlight the very high acceleration demands imposed (in the range of one g), but, as the building exposure in that region is mostly low-rise residential, extensive damage of mid-rise RC structures was not observed after the September'10 earthquake.

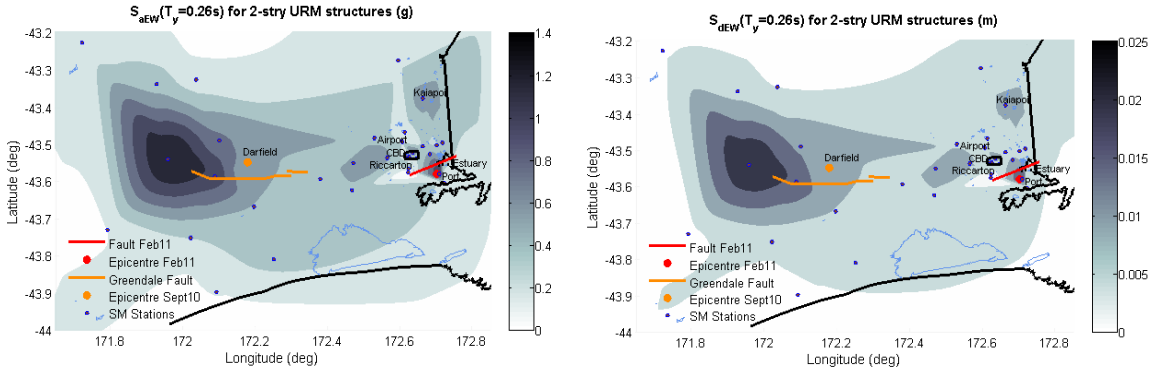

Figure 3.51. Spatial distribution of spectral accelerations (left) and displacements (right) for Darfield earthquake for yield period of 0.26sec (2-storey typical URM houses-EW direction).

The spatial distribution of PGAs and long-period spectral values exhibit a gradual reduction of values with increasing distance from the source, as readily shown by the contour lines, referring to a point-source for the February'11 earthquake rather than a line source as happened in the September'10 earthquake. The seismological definitions concerning the Christchurch earthquake are yet not settled, due to the fact that there was no surface rupture, and even the debate on whether the February'11 earthquake belonged to the aftershock sequence of the Darfield earthquake or not is still open. Nevertheless, from an engineering point of view it is rather interesting noticing in Figure 3.53 that the short-period components are concentrated in Heathcote Valley, where the epicentre of the earthquake was, while Figure 3.54 suggests that the long period components are stronger close to CBD, 7km away from the epicentre. This finding can correlate the damage expected to certain structural types in specific areas to the damage really observed.

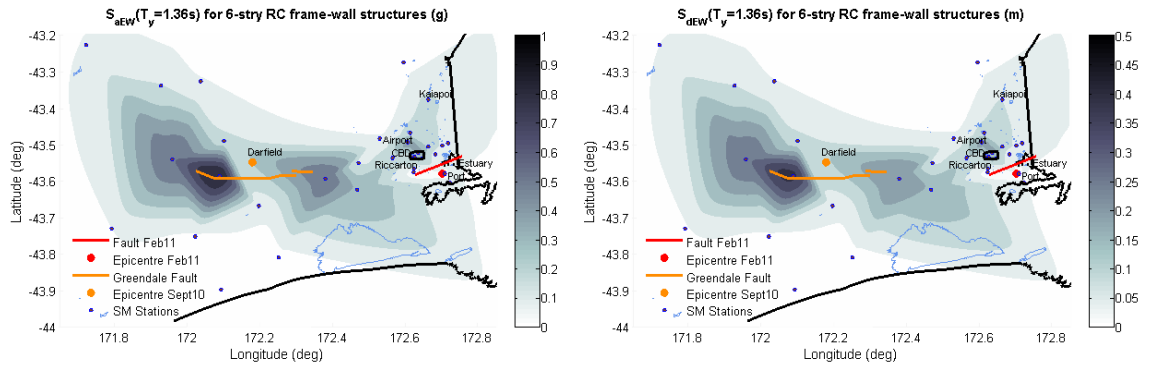

Figure 3.52. Spatial distribution of spectral accelerations (left) and displacements (right) for Darfield earthquake for yield period of 1.36sec (6-storey typical RC frame-wall structures - EW direction).

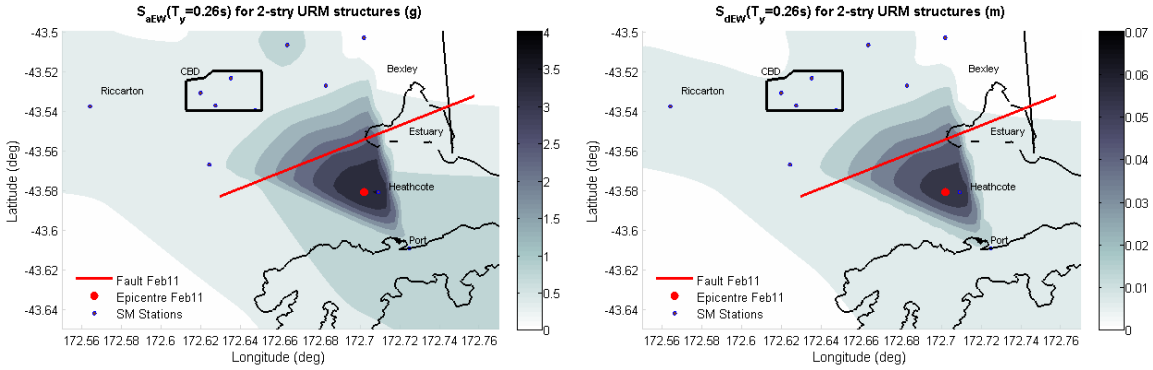

Figure 3.53. Spatial distribution of spectral accelerations (left) and displacements (right) from Christchurch earthquake for the yield period of 0.26sec (2-storey typical URM houses - EW direction).

As mentioned, the life losses from the second earthquake were primarily due to the heavy damage or collapse (mostly partial) of mid-rise and relatively tall RC structures in the CBD. Indicatively, the case of Grand Chancellor Hotel, which is a 26-storey structure with severe damages and more than one meter residual top displacement, is mentioned as an example of a tall RC building with substantial structural damage that rendered it unusable. Figure 3.54 presents this issue quite clearly showing that the spectral amplification around CBD is much higher than the one close to the fault epicentre. Nevertheless, the effects of the Christchurch earthquake on tall structures in CBD needs to be investigated in detail with respect to the soil-structure interaction and the soil plastification recorded in several parts of the centre.

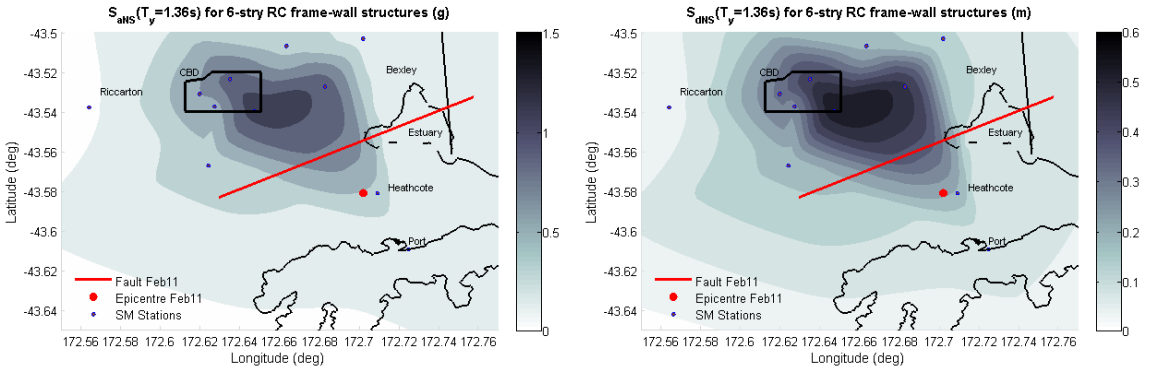

Figure 3.54. Spatial distribution of spectral accelerations (left) and displacements (right) for Christchurch earthquake for the yield period of 1.36sec (6-storey typical RC frame-wall structures - NS direction).

Finally, it is worth noticing the different composition of the spectral values for short and long periods in different regions in respect to the fault (Figure 3.51 to Figure 3.53), which could be partly attributed to potential source effects. However, another plausible explanation is the soil softening due in particular to soil liquefaction that occurred in large scale in both earthquakes. Response spectra obtained in liquefied areas are often characterised by bulges in the long-period range, signifying substantial amplification of the spectral values, much further than the constant acceleration plateau (Figure 3.54). Such a change in the frequency content, evident also in the spatial plots, has a significant impact on the seismic demand imposed and thus on the response of mid-rise and tall structures.

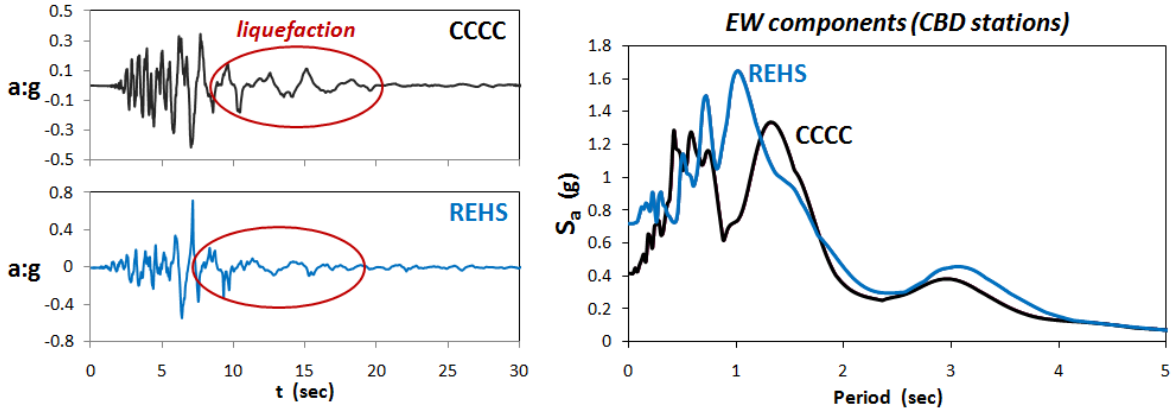

Figure 3.55. Recorded acceleration time-histories (left) and response spectra from REHS and CCCC stations (right) indicative of liquefaction.

3.6. SUMMARY OF OBSERVATIONS

Most of the damage during the Darfield and Christchurch earthquakes of 2010 and 2011, respectively, were in CBD area. The buildings in the perimeter of CBD, some of which also multi-storey modern RC structures, did not suffer significant damage. Most of the multi-storey buildings outside CBD were intact, without any damage (Figure 3. 56).

Figure 3. 56. Modern RC buildings performing satisfactorily.

Other observations related to the structural performance of the building stock in Christchurch and particularly in CBD are listed below:

- Where liquefaction was not evident on the surface, structural damage was more severe.
- The structural damage was more severe in the EAST - WEST direction which is parallel to the fault. Ground motion must be stronger in that direction. Directivity effects may have occurred as well.
- Non-structural damage was extensive and caused losses of lives.
- Satisfactory behavior of modern RC buildings was observed.
- Structures with mid to long period range were affected. Structures sitting directly on the surficial layers, without any deep foundation, are expected to be affected badly from the shaking.
- Composite elements (i.e. masonry with steel, steel with timber, masonry with concrete, etc...) were extensively used in construction but this proved to be not a good choice in a strong shaking.
- Several buildings on shallow foundations within the CBD are supported on loose to medium-dense sands and silty sands that liquefied during the 22 February earthquake. The liquefied foundation soils lost the capacity to support the buildings leading to non uniform (differential) settlements of the foundations and tilt of the buildings. Uneven settlements across the footprint of the building inevitably induce structural deformations which are often damaging to the structure (Cubrinovski and McCahon 2011.

Chapter 4:

DAMAGE ASSESSMENT OF BRIDGES

4.1. BRIDGES OVER AVON AND HEATHCOTE RIVER

Liquefaction along Avon River caused lateral spreading of the ground. Evidently, bridges were the structures mostly affected by lateral spreading. As Avon river forms several meanders within the city, there is a large number of bridges crossing the river. During our visit in April 2011, we inspected 9 bridges (8 crossing Avon river and 1 crossing Heathcote river shown on the map of Figure 5.1). Typically, most of them are concrete bridges with small to moderate spans none to two piers, continuous deck and seat type abutments on piles, with the exception of the two pedestrian bridges, i.e. the steel truss Medway bridge and the arch Snell Footbridge. The Table 5.1 includes all nine bridges and illustrates their response during Darfield and Christchurch earthquakes according to certain performance states described in the legend below the table. It can be clearly concluded that: i) most of the bridges performed very well during Darfield earthquake, apart from Gayhurst and South Bridge Bridge with moderate visible damage and the two pedestrian bridges with significant damage and ii) the performance of the bridges was worse, but still satisfactory in general, during Christchurch earthquake. This is partially attributed to the smaller ground accelerations of Darfield earthquake and thus, to the smaller inertial forces developed to the bridge decks. However, the deflection of the bridges points out lateral spreading as the prevailing source of load.

The deformation pattern of the concrete road bridges consists of lateral displacement of the abutments towards the river and their rotation around their contact point with the deck, accompanied by subsequent settlement of the fill behind the abutment and distress of the piles. This typical pattern of deformation is attributed to lateral spreading of the ground.

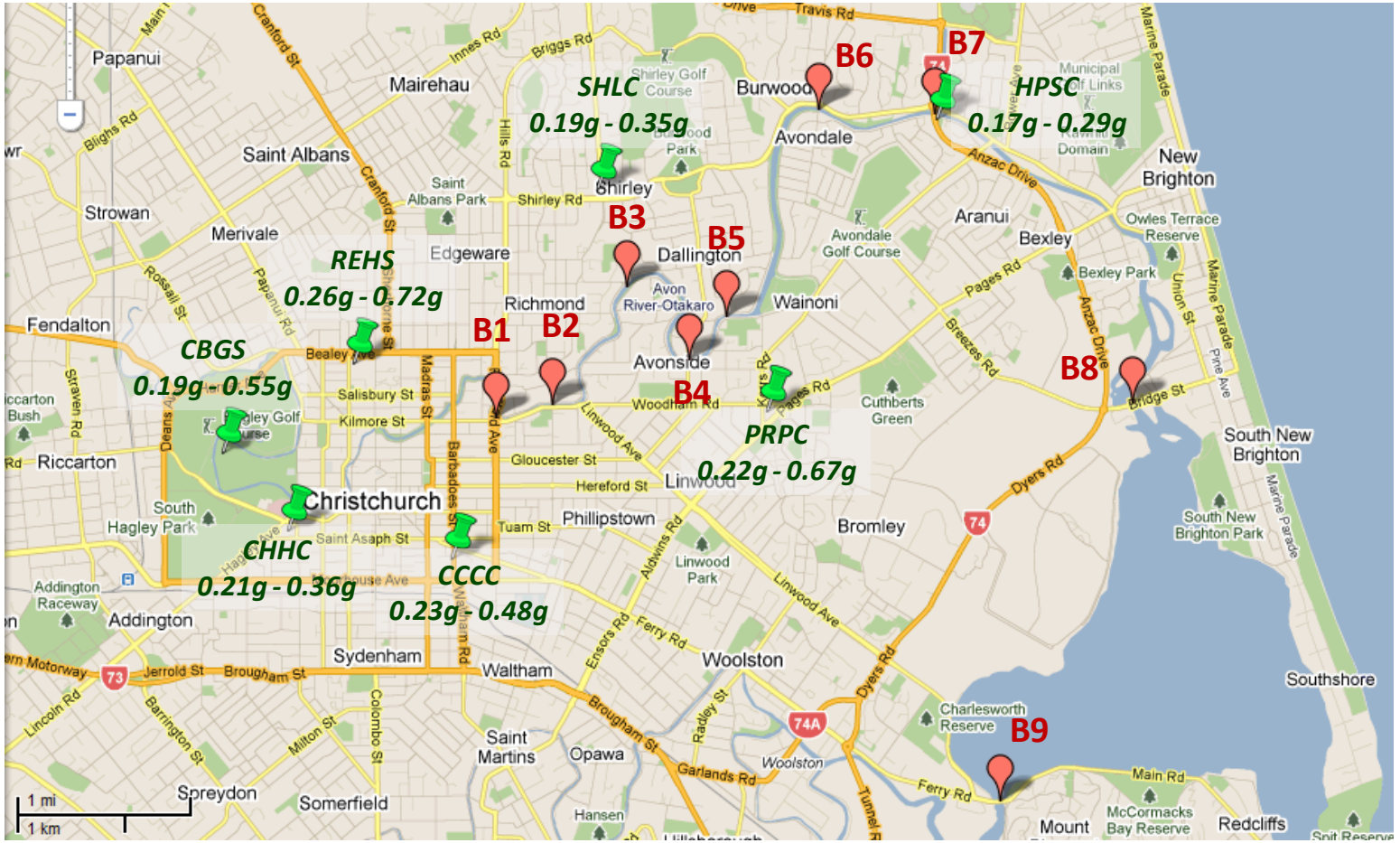

B1: Fitzgerald Bridge B2: Stanmore Bridge B3: Medway Pedestrian Bridge B4: Gayhurst Bridge
B5: Snell Footbridge B6: Avondale Bridge B7: Anzac Bridge B8: South Bridge Bridge B9: Ferrymead Bridge

Figure 5.1. Map illustrating the location of the bridges (red signs under the names B1, B2 etc) and the seismic stations (green signs) with the corresponding recorded PGAs (1st and 2nd value correspond to Darfield and Christchurch earthquakes respectively) in the broader area occupied by the bridges.

BRIDGES	***DARFIELD 2010****	***CHRISTCHURCH 2011*** **
Fitzgerald Bridge	A	B
Stanmore Bridge	A	B
Medway Pedestrian Bridge	C	D
Gayhurst Bridge	B	C
Snell Footbridge	C	C
Avondale Bridge	A	B
Anzac Bridge	A	B
South Bridge Bridge	B	B
Ferrymead Bridge	A	B

A	*without visible damage or completely undamaged*
B	*safe bridge for use **but** with visible damage*
C	*bridge closed due to large but repairable structural and foundation damage*
D	*bridge failed completely*

** from Bridge Research Group (Natural Hazard Platform) inspection (SEPTEMBER 2010)*
*** from our inspection (APRIL 2011)*

Table 5.1. Damage assessment of bridges along Avon and Heathcote rivers due to lateral spreading during Darfield and Christchurch earthquakes.

Aiming to investigate the reason why the bridges that were damaged during the Christchurch earthquake performed really well in Darfield earthquake, despite the fact that liquefaction occurred in both earthquakes, especially in the eastern suburbs, an evaluation of the liquefaction potential with depth was conducted for Anzac Bridge and Fitzgerald Bridge, for both earthquakes (Smyrou et al., 2011, conference paper). Following the classical Seed and Idriss (1971) procedure for assessing the liquefaction potential (as updated by Idriss and Boulanger (2006)), the Cyclic Resistance Ratio (CRR) of soil and the applied Cyclic Shear Ratio (CSR) were computed. The former was obtained from the CPT (in case of Anzac Bridge) or SPT

data (in the case of Fitzgerald Bridge) and the latter from the PGAs of the corresponding site. The results will be demonstrated in the following.

4.1.1. Fitzgerald Bridge

Fitzgerald twin bridges are situated at the eastern border of CBD (B1 on map of Figure 5.1). They are two-span bridges supported on seat type abutments and one central pier. The abutments are founded on a group of 8 piles of 30 cm diameter and 8 m depth (Bradley et al., 2010). Lateral spreading caused rotation of abutments, subsidence of the backfill and exposure of pile foundation, especially in the northern side. However, the central pier and bridge superstructure did not sustain any damage, so that the bridge was safe to be used after the earthquake.

Figure 5.2. Fitzerald Bridge (B1 on map of Figure 5.1). Performance of southern abutment after ChCh earthquake. No signs of lateral ground deformation occurred at the southern abutments of the twin bridges. The soil is still attached to the abutment.

Figure 5.3. Fitzerald Bridge (B1 on map of Figure 5.1). Performance of southern abutment after ChCh earthquake. No lateral ground deformation occurred at the southern abutments of the twin bridges. Thus, there was no rotation of the abutment. However, the southern abutment suffered moderate cracks due to seismic and inertial load.

Figure 5.4. Fitzerald Bridge (B1 on map of Figure 5.1). Performance of northern abutment after ChCh earthquake. Lateral spreading of the ground has exposed the pile heads.

Figure 5.5. Fitzerald Bridge (B1 on map of Figure 5.1). Performance of northern abutment after ChCh earthquake. Rotation of abutment is evident due to lateral spreading. The backfill has differentially subsided relative to the abutment.

Figure 5.6. Fitzerald Bridge (B1 on map of Figure 5.1). Rotation of northern abutment has caused tension cracks at the pile-tops.

Figure 5.7. Fitzerald Bridge (B1 on map of Figure 5.1). Performance of northern abutment of the twin bridge after ChCh earthquake. Rotation of abutment and slump of the backfill took place. Concrete spalling of the deck developed close to the abutment-seat.

In the case of Fitzgerald Bridge the complete soil profile geometry profile (Figure 5.8) is available (Bradley et al., 2010). There is an inclination of the third soil layer towards the southern abutment, which tends to cause an additional lateral soil movement at the side of the northern abutment towards East, even below the pile foundation (8m deep), as indicated by the red arrows. This is also supported by the liquefaction potential analysis of the soil profile below the northern and southern abutment (Figure 5.9) which indicates that in the soil between 11 and 14m depth the liquefaction susceptibility is greater in the case of the northern abutment (Smyrou et al., 2011, conference paper). It should be noted that CSR was estimated using an average PGA value of the REHS and CCCC records which are the closest to the bridge site. The southern abutment, shown in Figure 5.3, after the Christchurch earthquake, suffered only some moderate cracks, with no significant horizontal displacement or rotation. Moreover, there were no signs of lateral spreading (cracks, gap between abutment and soil) in front of the toe of the abutment. On the other hand, the northern abutment (Figure 5.5 and 5.7) sustained substantial rotation, the backfill has settled and the ground in front of the toe has spread towards the river, exposing the top of the piles.

The fact that there was no visible damage of the bridge during Darfield earthquake can be explained by the lower liquefaction potential of the soil profiles (shadowed areas) and its smallest range in depth compared to that obtained for Christchurch earthquake. In addition, there was no ground manifestation of liquefaction close to the bridge site in the case of Darfield earthquake, in contrast to the case of Christchurch earthquake. This observation is also supported by the analysis showing deeper liquefaction (practically below the depth of 8m) during the first earthquake. Thus, it is more difficult for the sand to be ejected on the ground surface.

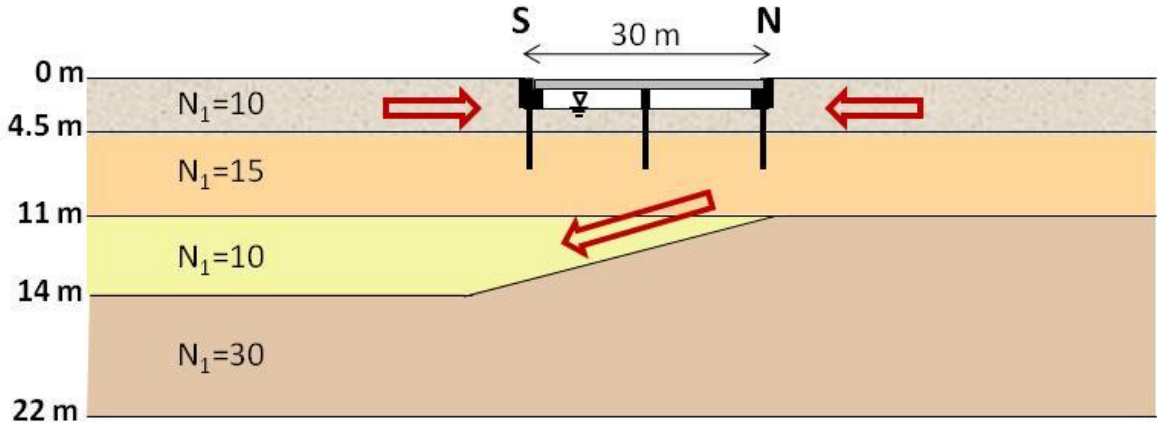

Figure 5.8. Soil profile geometry along Fitzerald Bridge (B1 on map of Figure 5.1). The soil mainly consits of sandy gravel and sandy silt prone to liquefaction. The red arrows indicate the soil displacement due to lateral spreading.

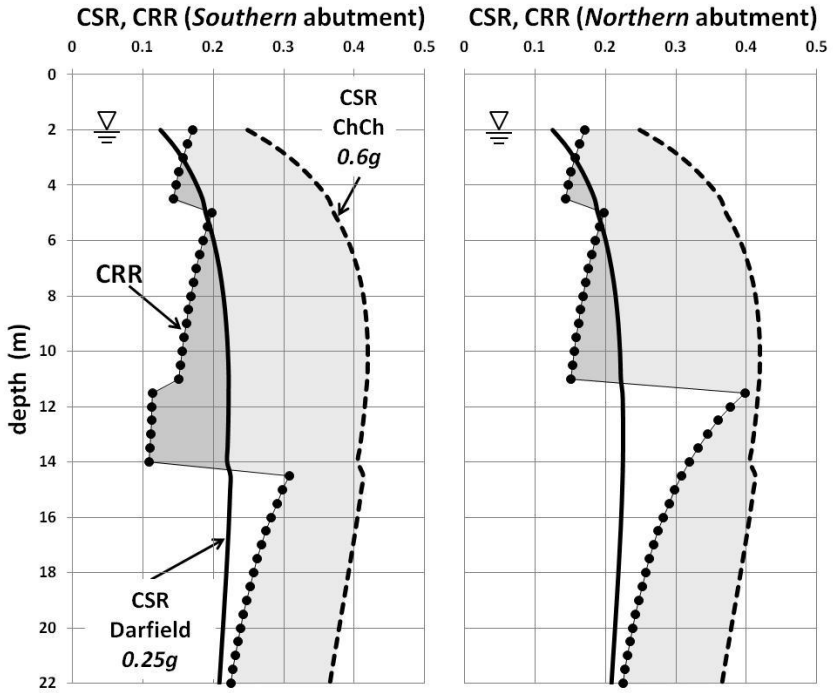

Figure 5.9. Fitzerald Bridge (B1 on map of Figure 5.1). Distribution of CRR with depth based on SPT values compared with the CSR for the northern and southern abutments.

4.1.2. Stanmore Bridge

Stanmore Road Bridge (Stanmore Rd & River Rd) is a concrete two span bridge which was completed in 1995 (B2 on map of Figure 5.1). The bridge sustained rotation of abutments and slump of the backfill due to lateral spreading, but overall its performance was satisfactory. Thus, it remained open to traffic after the Christchurch February earthquake.

Figure 5.10. Stanmore Bridge (B2 on map of Figure 5.1).

Figure 5.11. Stanmore Bridge (B2 on map of Figure 5.1). Rotation of the abutment around the deck. The street lighting column next to the abutment has rotated riverwards, following the lateral deformation of the ground, while the light column seated on the abutment indicates that the abutment has back rotated due to the deck constraint. Slump of the approach fill is not visible because at the time of our visit, the cracked ashalt between the two abutments had been replaced by new. However the large cracks in the road parallel to Avon river (in the order of 40 cm) due to lateral spreading were still there.

Figure 5.12. Stanmore Bridge (B2 on map of Figure 5.1). Large cracks in the asphalt due to significant lateral spreading in the free field (away from the bridge). The cracks tend to decrease towards the bridge, as the axial stiffness of the deck combined with the bending stiffness of piles limits the lateral ground deformation.

Figure 5.13. Stanmore Bridge (B2 on map of Figure 5.1). Cracks in the abutment and concrete spalling close to the joint with the deck. Gap opening between the abutment and the soil, tending to expose the foundation.

4.1.3. Medway Pedestrian Bridge

Medway Bridge (B2 on map of Figure 5.1) is a pedestrian steel truss bridge. The light superstructure buckled axially under the horizontal displacement of the abutments due to lateral spreading. The bridge had already developed large deformations after Darfield earthquake and remained closed. Buckling was even more severe after Christchurch earthquake.

Figure 5.14. Medway Pedestrian Bridge (B3 on map of Figure 5.1). Comparison of bridge damage between Darfield and Christchurch earthquakes. Source: NHP- Bridge Research Group.

4.1.4. Gayhurst Bridge

Gayhurst Bridge is located on Avonside (B4 on map of Figure 5.1) running in the NS direction and consists of precast reinforced concrete deck supported by wall piers, forming three spans. The abutments are seat-type with wingwalls. A borehole conducted close to the northern abutment indicates that the soil profile consists of a superficial layer (5 m deep) of silty sand/sandy gravel, with SPT values lower that 8 indicating high liquefaction susceptibility, overlying denser sand/gravel layers with SPT grater that 30 (Tonkin and Taylor, 2011).

The bridge was damaged during Darfield earthquake due to liquefaction-induced lateral spreading (Cubrinovsky et al. 2010). Even more extensive liquefaction and subsequent lateral ground deformation occurred during Christchurch earthquake, deteriorating the already initiated damage from Darfield earthquake. The damage was almost completely localized on the northern abutment and pier wall. Cracks in the northern wingwalls due to lateral spreading first caused by Darfield seismic event, widened inducing concrete spalling. The pier wall also sustained tension horizontal cracks. However, the cracks were not considered major ones. Thus, the bridge closed only temporarily until the settled approach fills were re-graded.

Figure 5.15. Gayhurst Bridge (B4 on map of Figure 5.1) after Christchurch earthquake. The southern abutment appears practically undamaged on the right side of the photo.

Figure 5.16. Gayhurst Bridge (B4 on map of Figure 5.1) The pier wall close to the northern abutment developed horizontal tension cracks, about 1 m below the deck due to intense shaking and lateral spreading.

Figure 5.17. Northern abutment of Gayhurst Bridge (B4 on map of Figure 5.1). Rotation and differential riverward displacement (in the order of 70 cm and more) of the eastern wingwall relative to the abutment caused concrete spalling and cracking at the joint of the abutment with the wingwall.

Figure 5.18. Northern abutment of Gayhurst Bridge (B4 on map of Figure 5.1). Rotation and displacement of the western wingwall not only riverwards but also away from the abutment (15 cm approximately at the top) perpendicular to the deck.

Figure 5.19. Western side of the northern abutment of Gayhurst Bridge (B4 on map of Figure 5.1). Comparison of damage between Darfield and Christchurch shaking events. The cracks have widened and extended, while the differential lateral riverward displacement of the abutment and wingwalls relative to the deck has increased after Christchurch earthquake Source: NHP-Bridge Research Group.

Figure 5.20. Closer look on the cracks of the western wingwall at the north of Gayhurst Bridge (B4 on map of Figure 5.1). The cracks have widened and deepened, while concrete spalling has occurred during Christchurch earthquake.

Figure 5.21 Eastern side of the northern abutment of Gayhurst Bridge (B4 on map of Figure 5.1). Comparison of damage between Darfield and Christchurch shaking events. The cracks have widened and the differential lateral riverward displacement of the abutment and wingwalls relative to the deck has increased after Christchurch earthquake. SOURCE.

4.1.5. Snell Footbridge

Snell Footbridge is an arch-shaped overpass crossing Avon River in Dallington (B5 on map of Figure 5.1). The bridge damage was initiated in Darfield eathquke by cracking at the midpoint due to lateral spreading. In Christchurch earthquake, the cracks at the mid-point widened forming a plastic hinge. The abutments also sustained cracks, indicating that a 3-hing mechanism formed. The arch is still standing due to its ached geometry.

Figure 5.22. Snell Footbridge (B5 on map of Figure 5.1) after Christchurch earthquake.

Figure 5.22. Snell Footbridge (B5 on map of Figure 5.1) after Christchurch earthquake. Cracks in the abutments.

Figure 5.23. Snell Footbridge (B5 on map of Figure 5.1) after Christchurch earthquake. Comparison of damage between Darfield and Christchurch shaking events. The cracks have widened and extended at the mid-point. Source: NHP- Bridge Research Group.

4.1.6. Avondale Bridge

Avondale Bridge (B6 on map of Figure 5.1) runs almost in the NS direction and consists of three span of precast reinforced concrete deck supported by two bents of three columns and two seat type abutments. Steel brackets have been placed to tie the girders with the piers and abutments.

A borehole conducted close to the southern abutment indicates that the soil profile consists of a superficial layer (11 m deep) of sand and silt of low plasticity, with SPT values lower that 12 indicating high liquefaction susceptibility, overlying a denser fine sand layer with SPT grater that 30 (Tonkin and Taylor, 2011).

The bridge sustained no damage in Darfield earthquake. In contrast, the bridge suffered rotation of abutments and moderate slump of the approach fills due to liquefaction-induced lateral spreading during Christchurch earthquake. Lateral spreading was more severe at the southern river coast. Thus, the rotation of the southern abutment (8 degrees) was larger than that of the northern abutment (4 degrees). The damage was not severe though, and the bridge was kept open to traffic.

Figure 5.24. Avondale Bridge (B6 on map of Figure 5.1) after Christchurch earthquake.

Figure 5.25. Southern abutment of Avondale Bridge (B6 on map of Figure 5.1) after Christchurch earthquake. Back rotation (8 degrees) and subsidence of the backfill.

Figure 5.26. Southern abutment of Avondale Bridge (B6 on map of Figure 5.1) after Christchurch earthquake. Concrete spalling and gap opening at the joint of the deck with the abutment.

Figure 5.27. a) Back rotation of southern abutment of Avondale Bridge (B6 on map of Figure 5.1), cracks in the backfill, b) Large lateral spreading cracks in the south coast parallel to the river extending in a great distance at both sides of the southern abutment.

Figure 5.28. Northern abutment of Avondale Bridge (B6 on map of Figure 5.1) after Christchurch earthquake. Moderate back rotation (4 degrees) with only slight settlement of the backfill.

4.1.7. Anzac Bridge

Anzac Bridge is a one of the most recent bridges in Christchurch, built in 2000 *(B7 on map of Figure 5.1)*. It is a totally precast structure, with a three-span deck supported on two bents of three columns and concrete abutments with wingwalls on piles. The bridge was almost undamaged in Darfield earthquake. However, severe liquefaction and subsequent lateral spreading occurred during earthquake causing significant back rotation and horizontal displacements of abutments.

Figure 5.29. Avondale Bridge (B7 on map of Figure 5.1) after Christchurch earthquake. a) Back rotation of teh abutments and slump of the approah fill, b) Large lateral spreading cracks in the ground parallel to Avon river coast extending in a great distance from the abutments indicating horizontal ground displacement more than 1, c) Riverward ground displacement in front of the abutments forms a gap of 50 cm exposing the top of the piles, d) Concrete spalling and cracks at the top of the pier-column due to intense shaking and lateral spreading, e) Significant quantity of sand ejecta close to the bridge, f) Nearby shallow excavation shows a top crust of clay containing thin beds of sand.

The liquefaction potential analysis of the soil profile (Smyrou et al., 2011, conference paper), obtained from a borehole between the southern abutment of the Anzac Bridge and the HPSC seismic station (located at a distance of 100m approximately) using the PGA records of the aforementioned station (Figure 5), indicates that during the Darfield earthquake (0.17g) the liquefaction took place practically from the ground water level to a depth of 8m (shadowed area). The applied CSR values are larger but close enough to the CRR values, so that liquefaction may not be severe. In the case of Christchurch earthquake (0.29g), the applied CSR is significantly larger than the CRR to a larger depth (10m). These facts imply that liquefaction is certain during Christchurch earthquake and definitely more extensive than the one during Darfield earthquake, causing larger soil lateral movement and at a greater depth – perhaps even below the pile foundation. This justifies partly why the Anzac bridge sustained no damage during Darfield, but 50cm horizontal displacement, plus rotation of abutments during Christchurch earthquake.

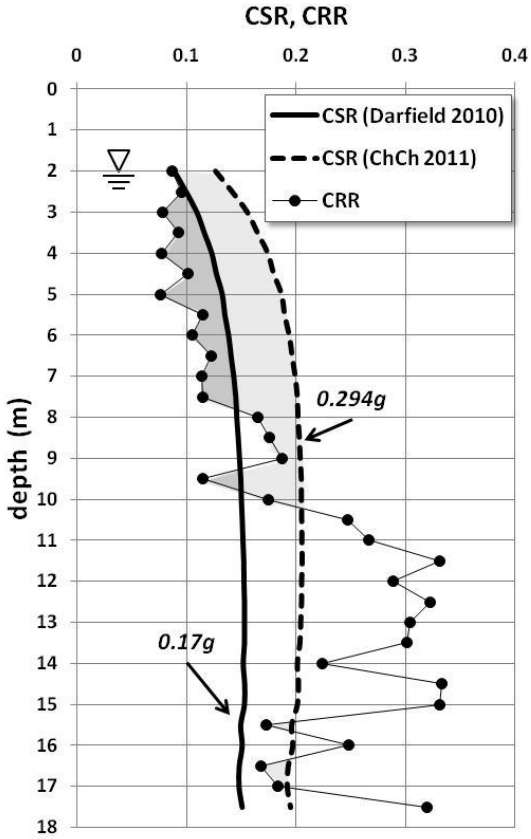

Figure 5.30. Avondale Bridge (B7 on map of Figure 5.1) The graph depicts the distribution of CRR with depth of a site between the HPSC station and Anzac Bridge compared with the CSR one during Darfield and Christchurch earthquakes. The shadowed areas indicate liquefaction susceptibility.

4.1.8. South Bridge Road Bridge

South Bridge Road Bridge (B8 on map of Figure 5.1), built in 1980, runs in the EW direction, crossing Avon river at the Avon-Heathcote Estuary. The skewed bridge consists of a three-span reinforced concrete deck supported on two piers and seat-type abutments founded on two rows of 5 octagonal precast prestressed concrete piles of 40 cm diameter with 3.4 m spacing.

The bridge suffered significant damage during Darfield earthquake due to lateral spreading. The soil in the wetland is very prone to liquefaction. Thus, the ground deformation induced by liquefaction caused back rotation of the abutments (around 6^o vertically and 8^o horizontally as measured on site), slumping of the approach fills and exposure of the pile foundation due to large soil "flow" and settlement underneath the abutments. During Christchurch earthquake, lateral spreading was even more severe, forming cracks in the ground which expanded several meters inland. The initiated damage from Darfield earthquake was extended with evidence of plastic hinging at the top of piles, cracks and concrete spalling in the abutments, as well as even greater subsidence of the backfill. Overall, the rotation and horizontal displacement of the abutments only slightly increased compared to how much large was the soil movement in Christchurch earthquake. This is due to deck restraining and pile bending resistance. Thus, the main damage of the bridge is attributed to the first earthquake.

Figure 5.31. South Bridge Road Bridge (B8 on map of Figure 5.1) after Christchurch earthquake.

Figure 5.32. South Bridge Road Bridge (B8 on map of Figure 5.1) after Christchurch earthquake. Large lateral spreading cracks in the ground parallel to the coast and adjacent to the abutments extending at a great distance inland.

Figure 5.33. Western abutment of South Bridge Road Bridge (B8 on map of Figure 5.1) after Christchurch earthquake. Back rotation of the abutment around the deck and slump of the approach fill.

Figure 5.34. Western abutment of South Bridge Road Bridge (B8 on map of Figure 5.1) after Christchurch earthquake. a) Large tension horizontal crack at the base of the abutment, b) The gabion map used for erosion protection in front of the abutment has laterally and vertically moved so that a great part of the pile heads has been exposed.

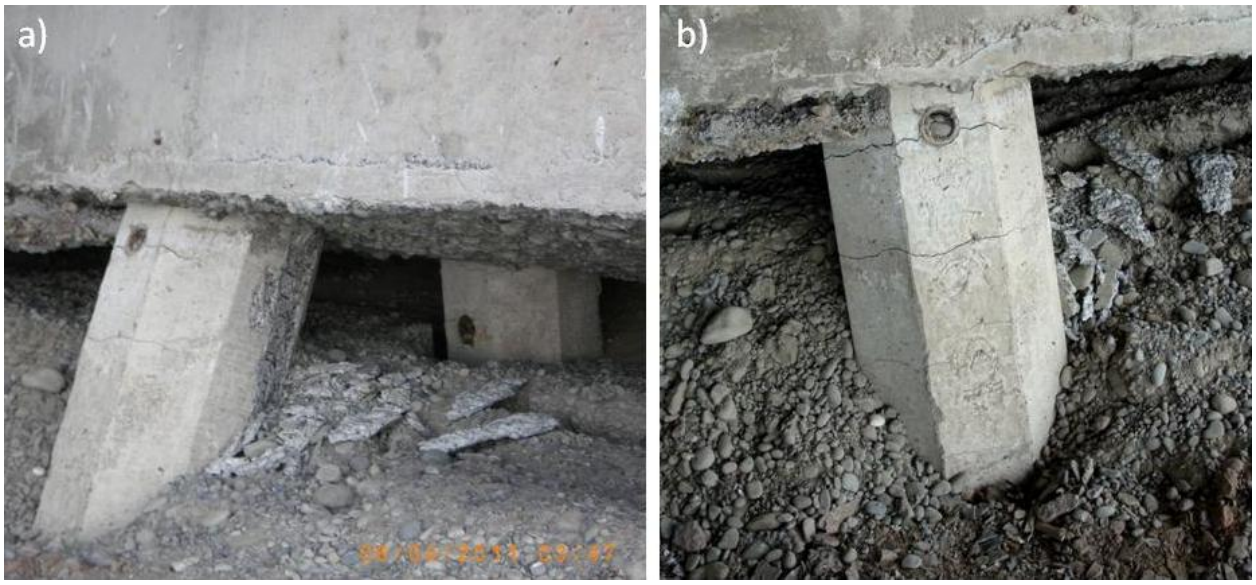

Figure 5.35. Western abutment of South Bridge Road Bridge (B8 on map of Figure 5.1) after Christchurch earthquake. a) Concrete spalling exposing the pile reinforcement, b) Flexural cracks developed at the top of the piles indicating plastic hinging.

Figure 5.36. Eastern abutment of South Bridge Road Bridge (B8 on map of Figure 5.1) after Christchurch earthquake. a)Back rotation of the abutment around the deck and slump of the approach fill, b) the soil underneath the abutments has moved riverwards exposing both rows of piles.

Figure 5.37. Eastern abutment of South Bridge Road Bridge (B8 on map of Figure 5.1) after Christchurch earthquake. a) Differential movement of abutments relative to the deck in the skew line direction is up to 20 cm accumulatively, b) the soil underneath the abutments has moved riverwards opening large cracks in the superficial crust and crating gaps in the front side of the piles.

Figure 5.38. Western abutment of South Bridge Road Bridge (B8 on map of Figure 5.1). Differences between Darfield and Christchurch shaking events. The rubber bearing pad had sheared and slided laterally in Darfield earthquake. After Christchurch earthquake the rubber pad has deformed and displaced even more. The timber pad, used as a stop probably has been placed after Darfield earthquake, because it seems to have sustained certain deformation. Source: NHP- Bridge Research Group..

Figure 5.39. Western abutment of South Bridge Road Bridge (B8 on map of Figure 5.1). Differences between Darfield and Christchurch shaking events. After Christchurch earthquake the piles have been more exposed due to greater lateral spreading of the soil and some cracks have been developed in the abutment. Source: NHP- Bridge Research Group.

Figure 5.40. Western abutment of South Bridge Road Bridge (B8 on map of Figure 5.1). Slight differences between Darfield and Christchurch shaking events in terms of differential displacement of the abutment relative to the deck in the skew line direction. Source: NHP-Bridge Research Group.

Figure 5.41 Western abutment of South Bridge Road Bridge (B8 on map of Figure 5.1). Differences between Darfield and Christchurch shaking events. After Christchurch earthquake,

the lateral soil movement has at least twice as much as in Darfield earthquake. Thus the piles are more exposed. Source: NHP- Bridge Research Group.

4.1.9. Ferrymead Bridge

Ferrymead Bridre (B9 on map of Figure 5.1), built in 1967, runs in EW direction crossing Heathcote River close to Avon-Heathcote Estuary. It consists of a prestressed reinforced concrete deck, one solid rigid unit, supported by seat-type wall abutments with two sections (front attached to the deck and rear block) and two bents of four piers. The abutments and the piers are founded on piles. The east abutment and pier are on piles fixed on engineering bedrock while the west abutment and pier are on floating piles. The bridge longitudinal section along with the soil geometry are sketched in Figure 5.42. The soil overlying the bedrock consists of clayey and silty sand, characterized as recent Christchurch formation by Brown and Weeber (1992). This soil was liquefied during Christchurch earthquake inducing lateral spreading. The considered engineering bedrock comprises older gravel formations overlying the volcanic rock of Port Hills.

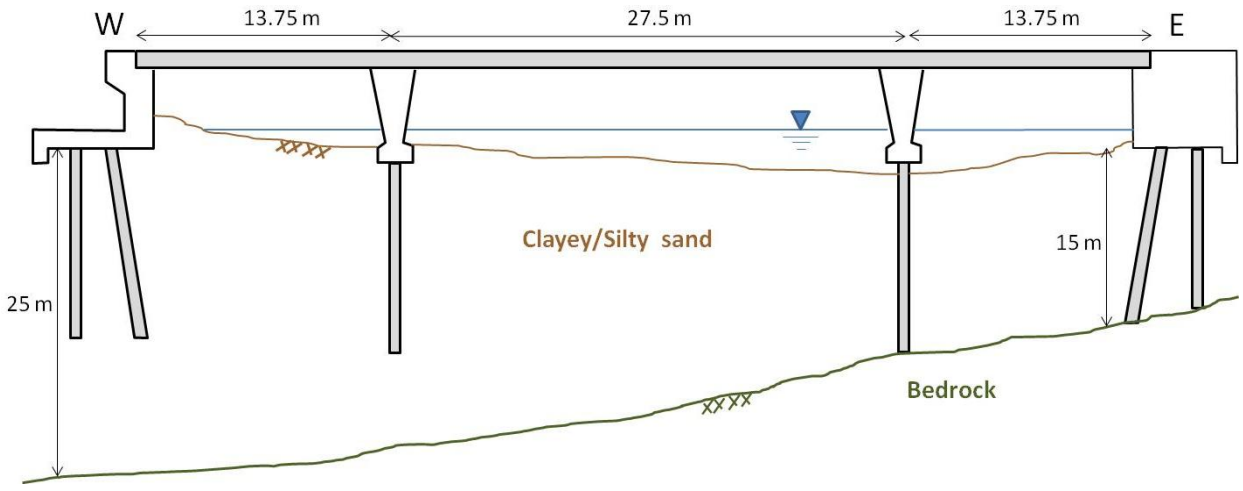

Figure 5.42 Sketch of Ferrymead Bridge and soil geometry (B8 on map of Figure 5.1). The rear sections of the abutments do not appear in the sketch.

Ferrymead Bridge was being widened and strengthened in order to accommodate the increase in users and meet the current earthquake resistance standards, when Christchurch earthquake occurred. In particular, at the time of the earthquake, a new abutment had only been

constructed in the east coast adjacent to the old one. The new abutment was founded on piles driven half a meter in the bedrock and was not yet attached to deck (yellow circle in Figure 5.43).

Figure 5.43. Ferrymead Bridge (B8 on map of Figure 5.1). Construction site in the process of strengthening and widening of the bridge. Photo taken after Christchurch earthquake. The new east abutment, in the yellow circle, was built one month before the shaking event.

On the day of our visit to the construction site, Mr. Guy Quaife, engineer in HEB Construction Ltd, working on the widening and strengthening project, described to us in detail the damage sustained by the bridge during Christchurch earthquake, illustrated in Figure 5.44. The Bridge was undamaged in Darfield earthquake.

Lateral spreading of the ground towards the center of the bridge was the main kinematic load applied to the bridge causing horizontal and vertical displacement of abutments and piers. After damage assessment of bridge was completed, deck was the only structural element of the bridge in good condition.

- ***Abutments:***

The abutment tended to move laterally following the soil deformation but the deck restrained the horizontal displacement at top, acting as a truss. Thus the abutments, being kind of pinned to the deck, back rotated. In contrast, the new east abutment, not being attached to the deck, rotated inwards moving by 50 cm at the top which is significantly smaller displacement that that of the existing abutments, indicating the beneficial role of a rigid solid deck.

The west abutment displaced horizontally at its base in the order of 20 cm, while it settled by 20cm (founded on floating piles). The east abutment, founded on pile fixed on the bedrock, was uplifted by 10 cm, following the vertical movement of Port Hills (40 cm) due to tectonics.

- ***Piers:***

The west pier moved 20 cm inwards at its base, under the soil pressure acting on the pile cap, causing rotation of the pier. The deck is connected with the piers through bearing pads. Thus, the deck rotated around a fixed point at the top-edge close to the center of the bridge, opening a large gap at the other side. The pier also settled by 20 cm (on floating piles).

The east pier moved 5 cm inwards, less that the west one, because the pile cap was not surrounded by soil, and consequently the soil pressure due to lateral spreading was smaller. The rotation of the east pier caused also a smaller opening at its connection with the deck. Moreover, the vertical displacement was zero.

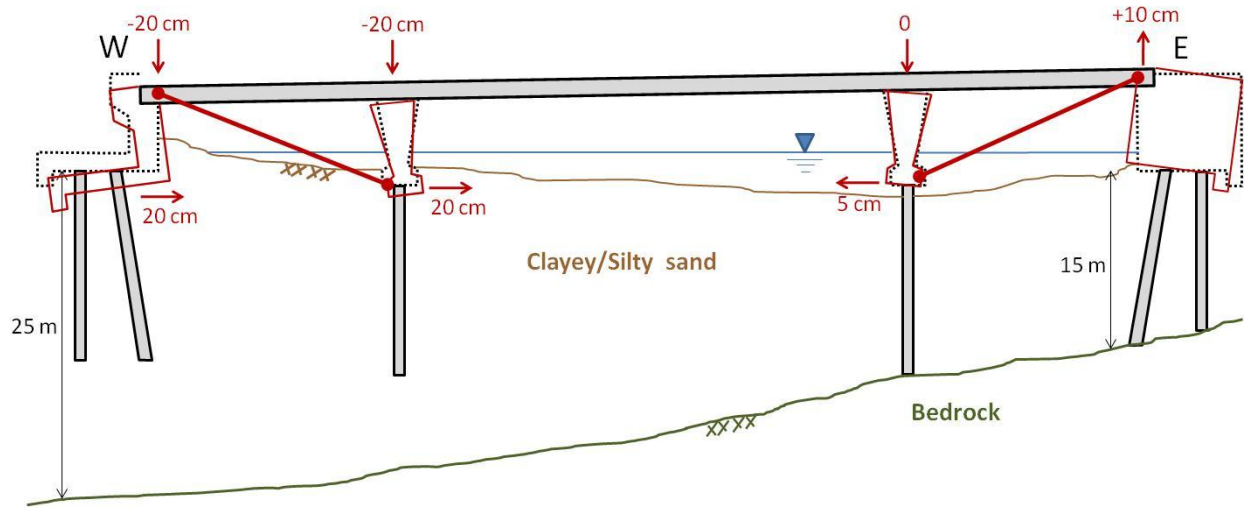

Figure 5.44. Sketch of Ferrymead Bridge deformation after Christchurch earthquake (B8 on map of Figure 5.1). The base of the piers has been tied to the deck edges after Christchurch earthquake in order to keep them in place and restrain any further inward movement until the strengthening project of the bridge is completed.

Figure 5.45. East abutment of Ferrymead Bridge after Christchurch earthquake (B8 on map of Figure 5.1). The front section of the abutment has back rotated and moved upwards by 10 cm. The rear section of the abutment has been displaced in a similar trend.

Figure 5.46. East abutment of Ferrymead Bridge after Christchurch earthquake (B8 on map of Figure 5.1). Horizontal cracks in the abutment wall have developed. The major crack is located at the height of the lower part of the deck.

Figure 5.47. East abutment and pier of Ferrymead Bridge after Christchurch earthquake (B8 on map of Figure 5.1). The base of the piers has been tied with tensors to the edges of the deck in order to keep and restrain any inward movement (left). Timber pads have been placed between the new abutment and the deck after the earthquake (right).

Figure 5.48. New east abutment of Ferrymead Bridge after Christchurch earthquake (B8 on map of Figure 5.1). The abutment have moved towards the center of the bridge. The gap opening at the back side of the pile is a result of this movement.

Figure 5.49. West pier of Ferrymead Bridge after Christchurch earthquake (B8 on map of Figure 5.1). The gap opening between the top of the pier and the deck was caused by the inward movement of the pier.

4.2. COLOMBO STREET OVERPASS IN CBD

The bridge on Moorhouse Avenue, officially named as "Colombo Street Overpass" is a reinforced concrete bridge with 11 axes consisting of twin columns. The top and bottom sections of some of the columns are hinged to the deck by using a special reinforcement detail (Figure 5.51). The deck is pre-stressed in transverse direction. The damage observed in the bridge concentrates in one of the middle columns (Figure 5.52) where the column section is halved and two columns are used side by side, exactly at the separation joint. Despite the intensive liquefaction in the area (Figure 5.53), the main reason of the damage is not liquefaction-related. The reason of the damage is restraint of the deck on one side and free

movement on the other side, leading thus increased forces on the columns at the separation joint.

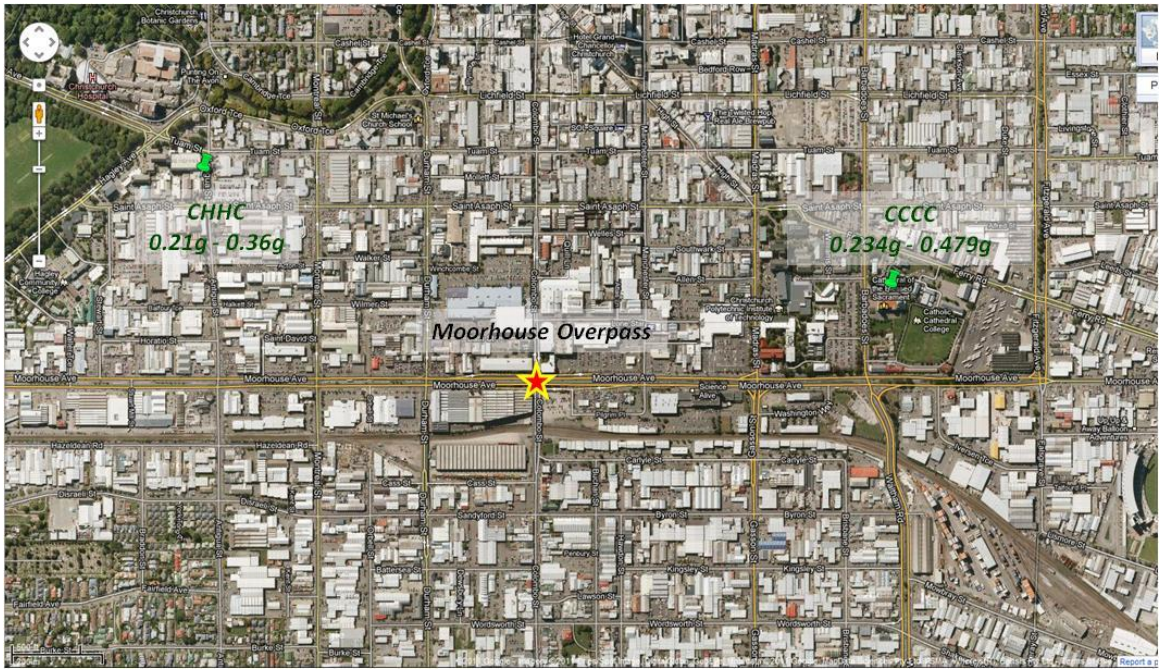

Figure 5.50. Location of Moorhouse Overpass.

Figure 5.51. Special reinforcement detail used at the bottom and top sections of the main piers to create hinges.

Figure 5.52. Failure of the pier due to shear and then buckling of the rebars under axial loads.

Figure 5.53. Sand-boils indicating liquefaction.

Chapter 5:

PORT HILLS - LYTTELTON PORT

5.1. PORT HILLS

Port Hills of Banks Peninsula are located on the southern border of Canterbury Plains (Figure 5.1), in a distance of about 6 km from Christchurch city. The volcanic bedrock, situated at an approximate depth of 400 m below CBD, emerges on the surface at the south, forming the 400-500 m high ridge of Port Hills (Brown and Weeber, 1992). The synthesis of the volcanic rocks, comprising mainly basalt and lava flows, results in a blocky rock mass, strong enough to stand in steep angles. In the urban areas of Redcliffs and Sumner, the sea-cliffs stand nearly vertically in a typical height of 15 - 30 m. However, erosion of the superficial loess and volcanic rock lead to widespread slope instability mainly in terms of rock falling along steep slopes, often causing damage to buildings and roads.

Thus, the aforementioned urban coastal areas, already vulnerable to slope instability, were most affected during the Christchurch February 2011 earthquake by landslides, rock falls and debris flows. In most cases, the earthquake triggered a relative large amount of rock blocks to roll down the steep slope faces, causing severe damage to buildings situated in the proximity of the cliffs (Hancox and Perrin, 2011).

Lyttelton urban area, including the major port of Canterbury region, Lyttelton Port, is situated on the mild slopes of the southern part of Port Hills (S5 on the map of Figure 5.1). Two seismic stations, LPCC and LPOC have record the ground motions of Christchurch February 2011 Earthquake. LPCC seismic station is situated on the lower part of a slope and considered to be practically founded on volcanic rock. Thus, LPCC record is considered a strong outcrop ground motion with peak ground acceleration of 0.92g, which may explain the large number of landslides triggered by the earthquake.

On our way to Lyttelton Port (S5) the sites S1, S2, S3 and S4 have been inspected. Our observations are reported in the following.

Figure 5.1. Map of Port Hills and Lyttelton Port located 6 km south of Christchurch - CBD (obtained from Google Earth). Reconnaissance sites are shown in the map with the yellow-reddish symbols under the names S1, S2, S3, S4 and S5. Seismic stations LPCC and LPOC situated at Lyttelton Port are also illustrated on the map.

Figure 5.2. Boulder struck through a house at 241 Governors Bay Road in Rapaki (site S1 in the map of Figure 5.1).

During Christchurch earthquake, a huge boulder was detached from the upper part of a steep slope close to the peak (400 m approximately) and rolled down the slope face, travelling about 600 m horizontally until it stopped at the Governors Bay Road. Along its travel path, the boulder struck through a house, causing severe damage. Fortunately, the house was vacant at the moment, so that there were no victims.

Figure 5.3. House collapsed by rock fall at Reakura Pl. in Redcliffs (site S2 in the map of Figure 5.1).

Rock fall destroyed a house built very close to the steep cliff at Raecura Pl. in Redcliffs, as illustrated in Figure 5.3 before the shaking event. Smaller and larger blocks of rock were detached from the cliff due to slope instability, occurring during the February earthquake, rolled down the slope and crushed the residential house built adjacent to the cliff. The volcanic rock blocks were very brittle and relatively hard, as one could smash them in smaller pieces with his hands.

Figure 5.4. The "Shag Rock" has reduced to half its height (site S3 in the map of Figure 5.1).

Christchurch New Zealand's local landmark, known as "The Shag Rock" or "Rapanui", is a prominent sea stack stands close to the southern shore on Main Road leading to Sumner. The rock had a height of 11m depending on the tide level, until it crumbled during the February 2011 Christchurch earthquake. Now, the Shag Rock is reduced to half its height and the remains are are still easily seen from the road.

Figure 5.5. Extensive rock fall behind the RSA building at 34 Wakefield Ave, in Sumner *(site S4 in the map of Figure 5.1).*

Rock boulders tumbled from the cliff at 34 Wakefield Ave, in Sumner during February earthquake. The rock fall caused damage to the adjacent RSA building (Returned Services Associaltion), but collapse was avoided in this case.

5.2. LYTTELTON PORT

5.2.1. General

Lyttelton Port is the major port of Canterbury region accommodating numerous facilities related to coal, automobile and fuel products. It is situated on the southern part of Port Hills, 12 km approximately south of CBD. The port consists of three main terminals, pointed out in the map of Figure 5.6: a) Container Terminal, located in the middle of the map, b) Cashin Quays comprising 4 wharves, located at the right side of the map and c) the Oil Terminal, located at the left side of the map. The circled areas under the names W1, W2, W3 are the sites inspected by our reconnaissance team.

The soil profile at the Port typically consists of a superficial layer of soft clay but mostly silty sand, overlying the bedrock. The thickness of this layer, thus the depth to bedrock, begins from a few meters close to the hills and reaches 90 m at the edge of the quays close to the open sea.

The terminals of varying age and type of construction. While all wharves are founded on piles, piles may be made from timber, reinforced concrete, prestressed concrete and steel. The majority of piles are vertical, however there are also inclined ones. Most of the piles are skin friction piles, as they do not reach the bedrock.

The port sustained damage during the Darfield Earthquake in September (PGA equal to 0.33g), but the overall performance was considered to be satisfactory. In general, the predominant effects of the September shaking event were limited settlement and lateral movement of the wharves up to 30 cm (Cubrinovsky et al., 2010).

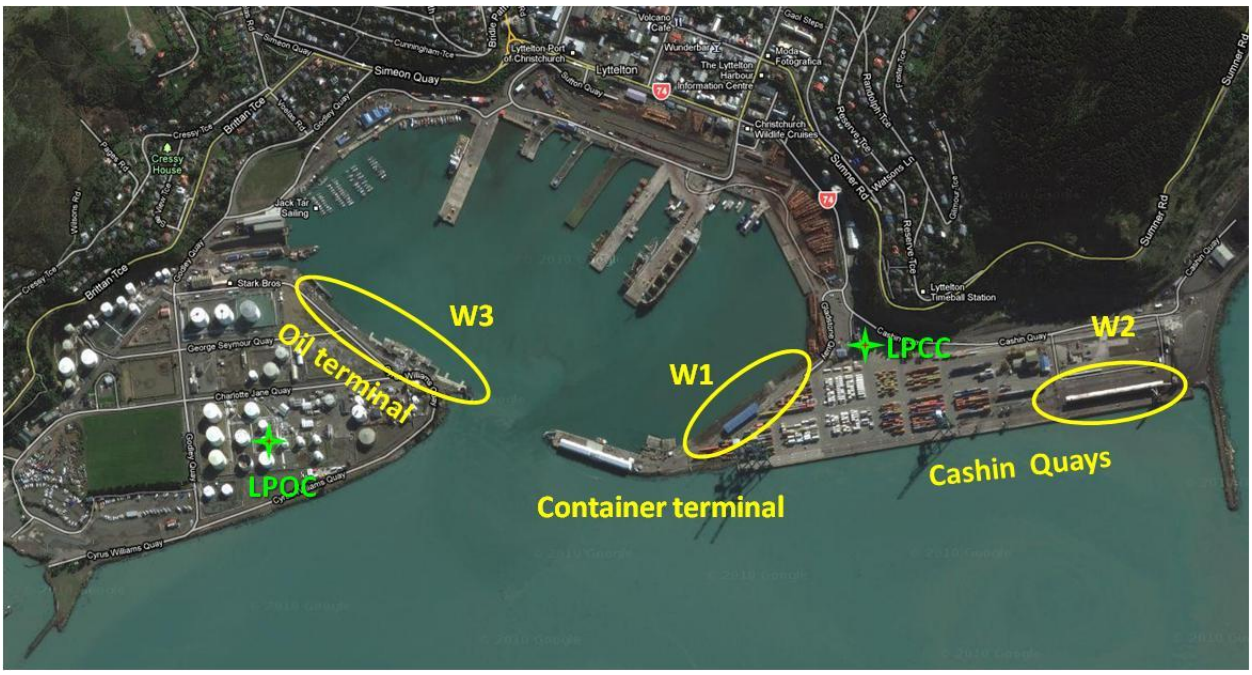

Figure 5.6. Map of Lyttelton Port of Christchurch (site S5 in the map of Figure 5.1). The inspected sites are pointed in the yellow circle. LPCC and LPOC are seismic stations where the accelerations time histories were recorded.

5.2.2. Visit to Lyttelton Port Company.

On the 8th of April 2011, we met Mr. Neil McLennan, Engineering Manager of Lyttelton Port Company, at the office buildings facilities of the company (Figures 5.7 and 5.8). The company is situated at the central upper part of the map in Figure 5.6.

Figure 5.7. Visit to Lyttelton Port Company.

Figure 5.8. View of Lyttelton Port from the office building facilities of Lyttelton Port Company.

Mr. McLennan initially gave us information relative to the history of the construction of the port and later he commented on the performance of the port during the two sequent shaking events of September 2010 and February 2011 . The Container and the OIl Terminal were built in 1870, while the Cashin Quays were built later in 1960. The foundation of Cashin Quays is mostly on steel piles filled with concrete. There are also prestressed concrete piles. The piles reached the 85% of their capacity limit during Darfield 2010.

Cashin Quays were mostly affected by the Christchurch February earthquake, as well. The maximum permanent lateral deformation occurred in one of the Cashin Quays and was measured more than 50 cm. This is the total displacement from both events. O' Rourke et al. (2010) state that the maximum measured displacement at the Cashin Quays was 18 cm after September earthquake. One can deduce that the induced lateral movement during Christchurch earthquake was in the order of 30 cm or more.

Specifically speaking there are mainly two typical pile configurations for Cashin Quays: i) TYPE A, piles founded on rock, and ii) TYPE B, skin friction piles (Figures 5.9 and ???). Obviously, the ones sustained the greater lateral deformation are those of TYPE B, i.e. Quay 2. One can observe that the soil surrounding the piles is very prone to liquefaction and subsequent lateral spreading.

Mr. McLennan let us know that Lyttelton Port Company ran validation dynamic analyses, using LPCC/Darfield record as the input motion. Analyses were consistent with the measurements in the field. Nowadays, these validation numerical tools are going to be used in the strengthening process of the port and also in the design needed for expansion of the port to the east.

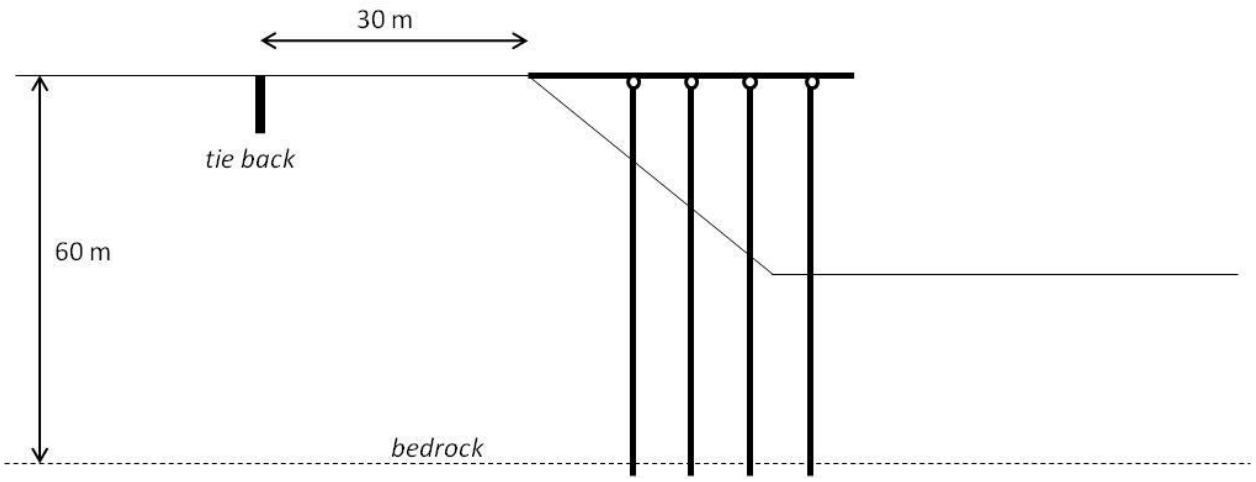

Figure 5.9. TYPE A pile configuration of Cashin Quays: piles founded on bedrock.

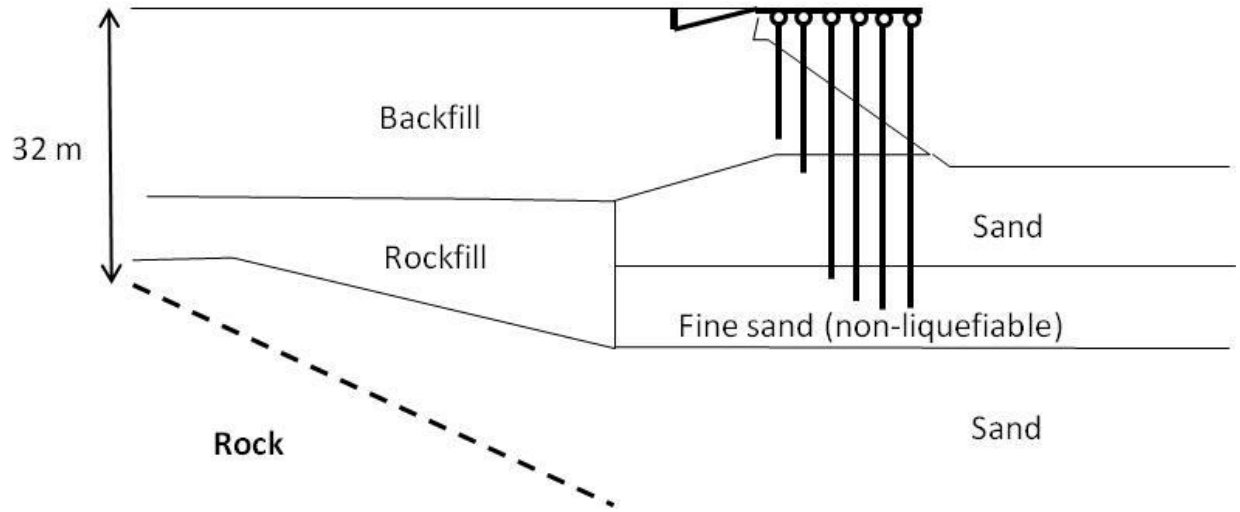

Figure 5.10. TYPE B pile configuration of Cashin Quays: skin-friction piles.

5.2.3. Recorded ground motions

Apart from the LPCC outcrop recorded motion, shown in Chapter 2, there is another station in Lyttelton Port , LPOC, closer to the Oil Terminal, pointed on map of Figure 5.6. The LPOC seismic station was installed under initiative of Professor John Berrill after the Darfield Earthquake. LPOC records, depicted in Figures 5.11 and 5.12 concentrate all the typical characteristics of motions recorded in liquefies sites, such as large period cycles combined with acceleration cut-

off after a threshold value is reached. Despite the moderate maximum PGA value of 0.33g the spectra indicate significant amplification for a broad range of periods up to 2.5 sec (Figure 5.13). Moreover, the comparison of dimensionless acceleration spectra between LPCC (outcrop) and LPOC (on top of liquefied soil) clearly demonstrates the role of soil in filtering the motion characteristics (Figure 5.14).

Liquefaction was evident on the site of the Oil Terminal. The tanks settled uniformly, not sustaining any damage. Lateral spreading of the ground was measured more than 1.5 m

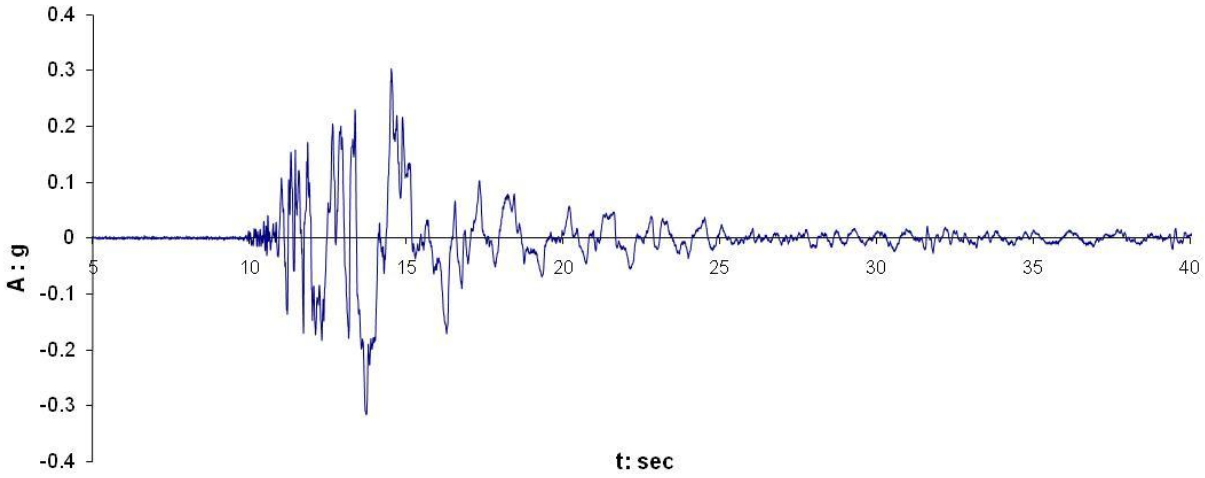

Figure 5.11. Acceleration time history in horizontal direction, x, recorded at LPOC station.

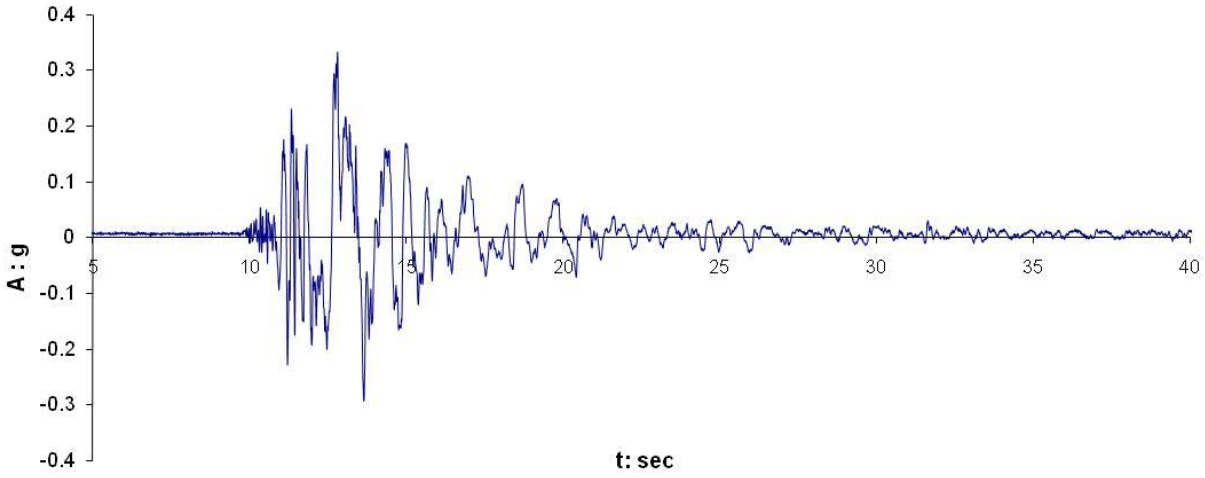

5.12. Acceleration time history in horizontal direction, y, recorded at LPOC station.

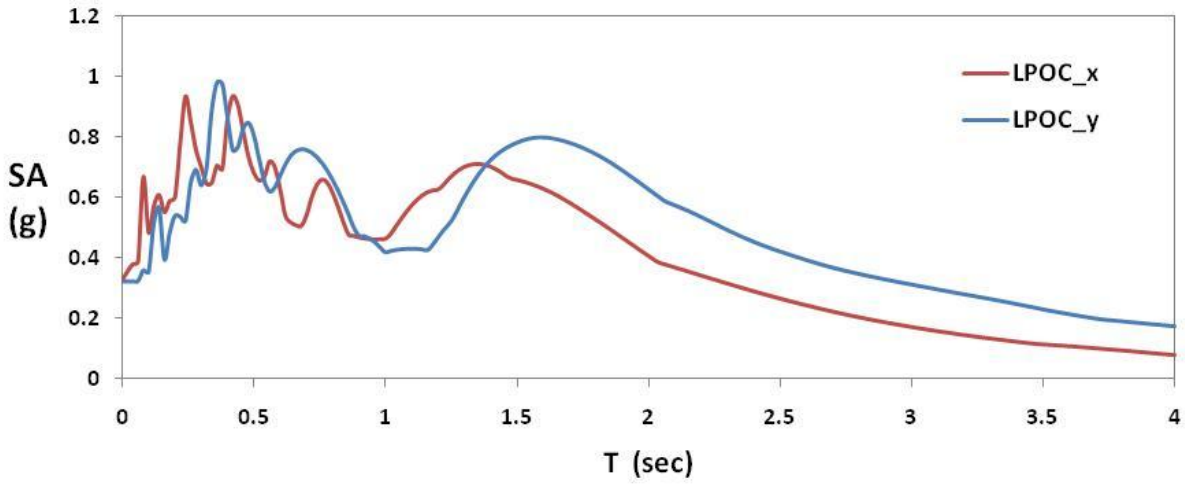

5.13. Acceleration spectra in x-y directions of ground motions recorded at LPOC station.

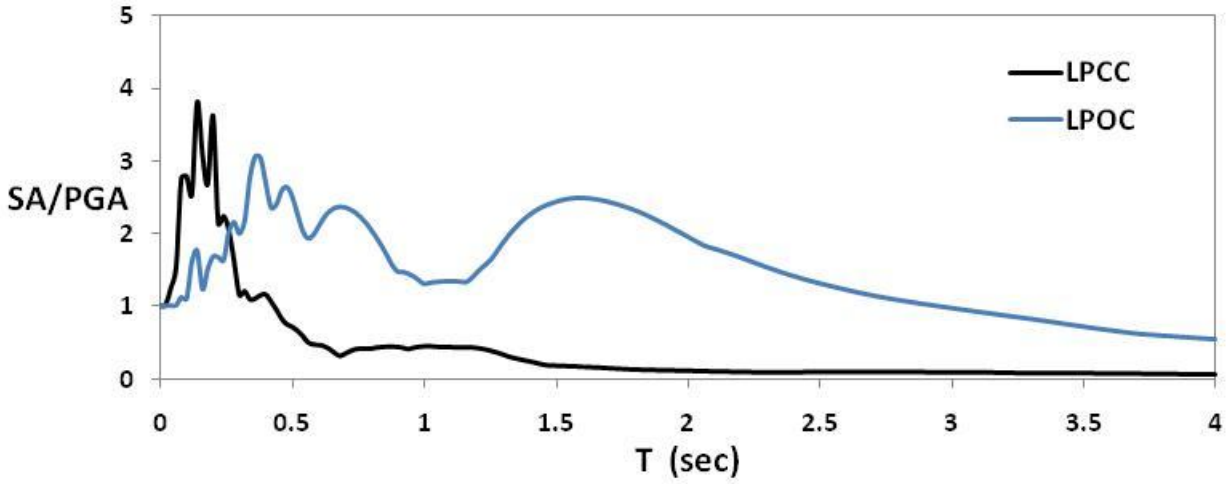

5.14. Comparison of dimensionless acceleration spectra between LPCC (outcrop) and LPOC (on top of liquefied soil).

5.2.4. Inspection of Lyttelton Port wharves

5.2.4.1. Container terminal

The Container terminal is founded on vertical timber piles of diameters ranging from 50 to 80 cm. Inspection was performed in the wharf, illustrated in the circled area under the name W1 in the map of Figure 5.6. Settlement in the order of 1 m and lateral outward movement up to 1.5 m occurred during Christchurch earthquake. Separation of the wharves from the backfill, cracks in the asphalt pavement and failure at the top of the piles were evident.

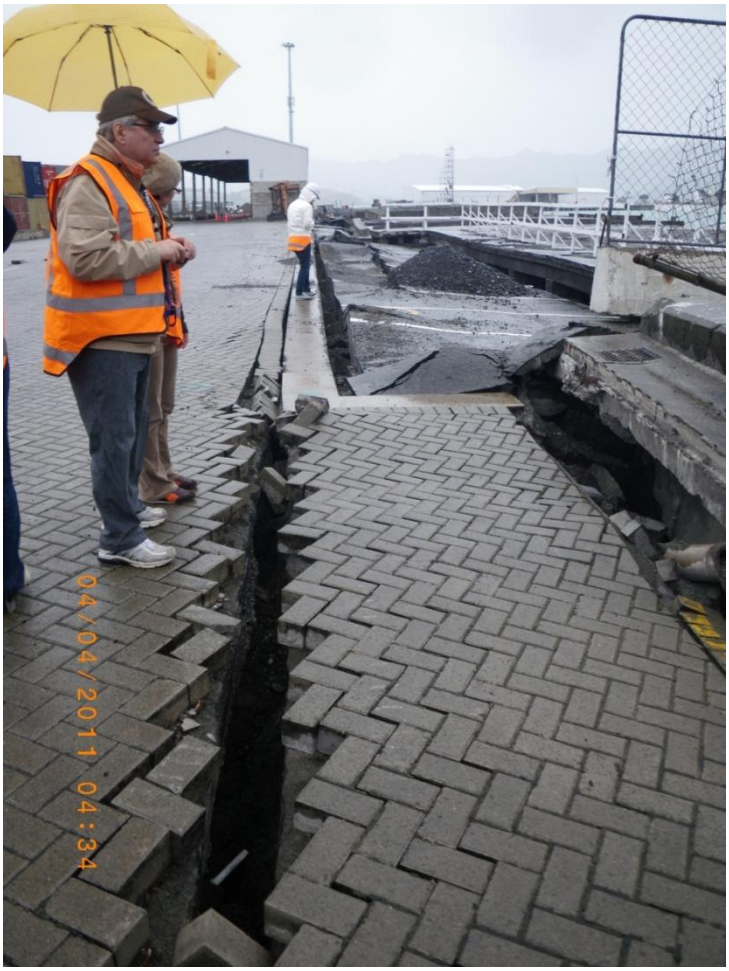

Figure 5.15. Huge cracks in the pavement in the order of 50 cm due to outward lateral movement of the quay (site W2 pointed in the map of Figure 5.6).

Figure 5.16. Cracks in the pavement due to lateral spreading continue to develop several meters behind the quay (site W2 pointed in the map of Figure 5.6).

Figure 5.17. Damage of the container terminal quay (site W2 pointed in the map of Figure 5.6): a) Crack opening and distortion of the asphalt connecting the terminal with the wharves, b) Plastic hinging at the top of a timber pile of 50 cm diameter, c) Relative movement of the deck to the pile, d) Separation of the wharf to the backfill due to 1 m settlement of the backfill and outward movement of the wharf up to 50 cm.

5.2.4.2. Cashin Quays

Inspection was performed in one of Cashin Quays, illustrated in the circled area under the name W2 in the map of Figure 5.6.

Figure 5.18. Large uniform settlement under the heady load of the structure. Cracks in the asphalt due to heaving of the ground at right side of the steel structure (site W2 in the map of Figure 5.6)

Figure 5.19. Detachment of the slabs of the platform due to differential settlement (site W2 in the map of Figure 5.6). Now the slabs have been removed from their initial place.

5.2.4.3. Oil Terminal

Inspection was performed in the wharves, illustrated in the circled area under the name W3 in the map of Figure 5.6. Large settlement of the backfill and fuel pipe line deformation were the most characteristic observations in this field.

Figure 5.20. Settlement of the backfill caused detachment of the wooden beams from the pile heads (site W3 in the map of Figure 5.6).

Figure 5.21. One typical pile configuration (site W3 in the map of Figure 5.6). The timber piles have cracked at the top.

Figure 5.22. Another typical pile configuration (site W3 in the map of Figure 5.6). The concrete piles performed quite well.

Figure 5.23. Large settlement of the backfill (site W3 in the map of Figure 5.6).

Figure 5.24. Settlement of the backfill in the order of 1 m (site W3 in the map of Figure 5.6).

Figure 5.25. a) Cracks in the inclined asphalt due to lateral spreading, b) Ejected sand appeared on the surface indicating that liquefaction has occurred (site W3 in the map of Figure 5.6).

Figure 5.26. Comparison of the damage of site W3 in the map of Figure 5.6 between Darfield and Christchurch earthquakes. The yellow and red circles are the common point of references in all photos. Photo from Darfield earthquake can be found in Cubrinovsky et al. (2010).

Figure 5.27. Comparison of the fuel pipe line deformation (site W3 in the map of Figure 5.6) between Darfield and Christchurch earthquakes. After Darfield earthquake, temporary wooden support was used to accommodate settlement under fuel line (Cubrinovsky et al., 2010). After Christchurch earthquake, the supports are still there and they have settled together with the fuel line.

Comparison between the Darfield 2010 and Christchurch 2011 shaking events has showed that most of the settlement and lateral spreading in the Oil Terminal has occurred in the first earthquake. Additional ground deformation did develop during Christchurch earthquake but it was only a percentage of the initial one.

REFERENCES

ATC-40 (1996) Seismic Evaluation and Retrofit of Concrete Buildings, Report No. ATC-402, Applied Technology Council, Redwood City, California.

Bal, İE, Crowley, H, Pinho, R, Gülay, G (2007) Structural characteristics of Turkish building stock in Northern Marmara region for loss assessment applications, ROSE Research Report 2007/03, IUSS Press, Pavia, Italy.

Blair E. (2010) Equivalent linearization of the existing 3D frame-wall structures for displacement-based assessment, MSc Thesis, IUSS Rose School, Pavia, Italy.

Ben-ill, J. B., R. O. Davis, and I. F. McCahon (1993). Christchurch seismic hazard pilot study, Bull. New Zealand Natl. Soc. Earthquake Eng. 26, 14-27.

Bothara, JK, Mander JB, Dhakal, RP, Klare, RK, Maniyar, MM (2007) "Seismic performance and financial risk of masonry houses", *ISET Journal of Earthquake Technology*, 44(3-4):421-444.

Bradley, B.A., M. Cubrinovski, R.P. Dhakal, and G.A. MacRae (2010). Probabilistic seismic performance and loss assessment of a bridge-foundation-soil system, Soil Dynamics and Earthquake Engineering 30 395-411.

Brown L.J., and J.H. Weeber (1992). Geology of the Christchurch urban area: Scale 1:25,000. Institute of Geological & Nuclear Sciences, Geological Map 1, New Zealand.

Brown, LJ and Weeber, JH (1994), 'Hydrogeological implications of geology at the boundary of Banks Peninsula volcanic rock aquifers and Canterbury Plains fluvial gravel aquifersNew Zealand Journal of Geology and Geophysics, Vol. 37: 181-193

Cubrinovski, M., R. Green, J. Allen, S. Ashford, E. Bowman, B. Bradley, B. Cox, T. Hutchinson, E. Kavazanjian, R. Orense, M. Pender, M. Quigley, T. Wilson, and L. Wotherspoon (2010). Geotechnical reconnaissance of the 2010 Darfield (New Zealand) earthquake, Bulletin of the New Zealand Society for Earthquake Engineering, 43 243-320.

Cubrinovski, M, McCahon, I. (2011) "Foundations on Deep Alluvial Soils", Technical Report Prepared for the Canterbury Earthquakes Royal Commission.

Elder, D. McG., I. F. McCahon, and M. D. Yetton (1991). The earthquake hazard in Christchurch: a detailed evaluation, Research Report to EQC, Soils and Foundations Ltd., Christchurch, New Zealand, 131.

Eidinger, J., A. Tang, and Thomas O'Rourke (2010). Technical Council on Lifeline Earthquake Engineering (TCLEE), Report of the 4 September 2010 Mw 7.1 Canterbury (Darfield), New Zealand Earthquake, American Society of Civil Engineers.

Gülkan, P and Sözen, M (1974) "Inelastic response of reinforced concrete structures to earthquake motions", *ACI Journal*, 71 (12): 604-610.

Hancox, G. and Perrin, N. (2011),Report on Landslide Reconnaissance Flight on 24 February 2011 following the Mw 6.3 Christchurch Earthquake of 22 February 2011, GNS SCIENCE Immediate Report.

Idriss, IM, Boulanger, RW (2006) "Semi-empirical procedures for evaluating liquefaction potential during earthquake", Journal of Soil Dynamics and Earthquake Engineering, 26:115-130.

Ingham, J and Griffith, M (2010) Performance of unreinforced masonry buildings during the 2010 Darfield (Christchurch, NZ) earthquake. Report, NZSEE Library, N.Zealand.

Kam, WY, Akguzel, U, Pampanin, S (2011) 4 Weeks on: Preliminary reconnaissance report from the Christchurch 22 Feb 2011 6.3Mw Earthquake. Report, NZSEE Library, N.Zealand.

NZS 1170.5 (2004). Structural design actions, Standards New Zealand, Wellington, NZ.

Seed, HB, Idriss, IM (1971) "Simplified procedure for evaluating soil liquefactio potential", Journal of the Soil Mechanics and Foundations Division, ASCE, 97(SM9):1249-73.

Shibata, A, and Sözen, M (1976) "Substitute structure method for seismic design in reinforced concrete", *ASCE Journal of the Structural Division*, 102(ST1):1-8.

Smyrou, E., Tasiopoulou, P., Bal, I.E., Gazetas, G. and Vintzileou, E. (2011) "Ground Motions Versus Geotechnical and Structural Damage in the Christchurch February 2011 Earthquake," Seismological Research Letters, **82**(6).

Smyrou, E., Tasiopoulou, P., Bal, I.E., Gazetas, G. and Vintzileou, E. (2011) "Structural and Geotechnical Aspects of the Christchurch and Darfield Earthquakes in N.Zealand", 7th National Turkish Conference on Earthquake Engineering (7UDMK), Istanbul, Turkey.

Tonkin & Taylor Ltd (2011) Geotechnical factual reports. available at http://canterbury.eqc.govt.nz

Toshinawa, T., J. J. Taber, and J. B. Berrill (1997). Distribution of ground-motion intensity inferred from questionnaire survey, earthquake recordings, and microtremor measurements: a case study in Christchurch, New Zealand, during the 1994 Arthurs Pass Earthquake, Bulletin of the Seismological Society of America, 87 356-369.

Uma, SR, Bothara, J, Jury, R, King, A. (2008) "Performance Assessment of Existing Building in New Zealand", *Proceedings of the NZSEE Conference*, Wairakei, N.Zealand, 11-13 April, 45.

Vuran, E, Bal, İE, Crowley, H, Pinho, R (2008) "Determination of Equivalent SDOF Characteristics of 3D Dual Structures", *Proceedings of the 14WCEE*, Beijing, China, 8-12 October, S15-031.

Youd, T.L., and B.L. Carter (2005). Influence on soil softening and liquefaction on spectral acceleration, Journal of Geotechnical and Geoenvironmental Engineering, ASCE, 131(7) 811–825.

Our team at the premises of the fire brigade.

Scott and Nick, our escorts during our expedition.